

PAPER • OPEN ACCESS

Aqueous Two-Phase Separation (ATPS) Methods for Oleic acid extraction from Neem leaves

To cite this article: Shubham Gawade *et al* 2022 *IOP Conf. Ser.: Mater. Sci. Eng.* **1224** 012016

View the [article online](#) for updates and enhancements.

You may also like

- [Neoteric Media as Tools for Process Intensification](#)
C C Beh, R Mammucari and N R Foster
- [Liquid-liquid extraction of Pt\(IV\) from hydrochloric acid solutions using PPG 425 – NaCl – H₂O system](#)
I V Zinov'eva
- [Metallic and semiconducting carbon nanotubes separation using an aqueous two-phase separation technique: a review](#)
Malcolm S Y Tang, Eng-Poh Ng, Joon Ching Juan et al.

Aqueous Two-Phase Separation (ATPS) Methods for Oleic acid extraction from Neem leaves

Shubham Gawade, Sandeep P. Shewale and Amravati Gode

School of Chemical Engineering, MIT Academy of Engineering, Alandi (D), Pune, India-412105

Corresponding author's e-mail address: agode@mitaoe.ac.in

Abstract. The aqueous two-phase separation system (ATPS) signifies an environmentally responsible approach for the extraction of bioactive compounds from a plants basis, as it is a liquid-liquid fractionation technique centred on the inconsistency of two aqueous solutions. In this investigation, various experimental parameters are optimized as the speed of agitation (200, 300 400 and 500 rpm) and solvent ratio (1:1, 2:3 and 3:2) with 20 % (w/w) of Ammonium Sulphate (AMS) salt composition and 30 % (w/w) of Polyethelyene Glycol (PEG). The obtained extract contains alkaloids, flavonoids, tannins, glycosides, acids and total phenolic compounds (TPC). The extracted Oleic acid by the ATPS method was measured with gallic acid equivalent (GAE) of TPC extracted from neem leaves powder. The determined concentration of oleic acid in the practice of TPC is 8.033 mg of GAE/g from the optimized experimental parameter. The optimized results can be cast off for a commercial process on an industrialized scale. Also, the mathematical modelling investigation was done to intent the critical impeller speed (Njs) with the Zwittering model. The identified model calculates the essential speed of agitation (rpm) for maximum extraction yield.

Keywords: Oleic acid, Total phenolic compounds (TPC), Aqueous Two-Phase Separation System (ATPS), Gallic Acid Equivalent (GAE), Critical Impeller Speed (Njs).

1. Introduction

Herbs are used for flavouring, food, medicine, or perfume from ancient times. Culinary use naturally differentiates herbs are implying the leafy green portions of spice also a product from a different part of the plant containing seeds, roots, bark, and fruits. Furthermore, medicinal contents available in the plant's parts are used for the production of some pharmaceutical products such as aspirin, colchicine, ephedrine, morphine, physostigmine, pilocarpine, quinidine, reserpine and vincristine, etc [1-2]. The approach of isolating the bioactive components from the medicinal plants and used for the manufacturing of some pharmaceutical products are becoming prominent. Generally, organic solvents such as methanol, ethanol and diethyl ether are usually helped for extracting the bioactive compounds as of plant basis by the outmoded extraction arrangements. These solvents are relatively expensive,



needs distinctive processing conditions and most importantly disposal of the solvents is a major concern as they are not environmental responsive [3].

Conventional extraction processes are time-consuming and need more solvent for carrying out an operation, also after extraction, the added cost of purification and solvents recovery makes the process uneconomical.

Whereas, ATPS two-stage extraction is developing as a successful and flexible green system for the downstream handling of biomolecules. Fluid two-stage frameworks are low unpredictability frameworks with high adaptability [4]. That is, an expansive assortment might be acquired utilizing substances that pursue the Green Chemistry guideline on ecotoxicity, biodegradability, bioaccumulation and constancy, limiting waste and amplifying yields. Furthermore, they conform to the guideline of changeover of naturally safe structures to permit work under air weight. Since the 1970s numerous classified and out examinations have announced the filtration of proteins and other biologic materials utilizing ATPS, and numerous specialists have considered different operations of ATPS for the extraction and cleaning of organic products [5]. However, the utilization of such frameworks for the recuperation of phenolic mixes from plant materials is extremely constrained. In addition, there is broad writing about the thermodynamic properties of ATPS be that as it may, to the best of our insight, their application to crude unpurified examples has been very constrained [6].

Subsequently, the late nineteenth-century fluid two-phase extraction has been identified to the entire world. Aqueous two-phase can be framed through an extensive diversity of characteristics or else engineered water-solvent polymers& salt blends [7]. Watery two-phase extraction is developed for protected, sparing partition and cleaning of biomolecules, for example, proteins and catalyst extraction. Fluid extraction has numerous favourable circumstances; it is biocompatible, has low interfacial surface pressure among stages and it has high water content, the procedure can incorporate and the ability for strengthening [8-9].

Likewise, the level of corruption for biomolecules is low. In any case, two-polymer and polymer-based salt frameworks have developed quickly and a considerable measure of effort has been placed keen on concentrate this strategy utilizing these sorts of aqueous two-phase separation systems (ATPS). Aqueous two-phase extraction is known as an operative, adaptable and significant developing green method for the subsequential treating of biomolecules. This strategy has points of interest completed traditional extraction systems similar to, simplicity of scaling-up, condition benevolent, minimal effort, fit for nonstop activity and is effective for some sorts of trials exceptionally for the fixation and refinement of biomolecules. The utilization of partiality in ATPS can affect the developed recuperation earnings and developed refinement bends of bio consistent items such as it is an essential phase recuperation strategy [10]. Water as the foremost constituent of together stages in ATPS practices a moderate setting for bioactive molecules to distinct and polymers steady to the assembly and biotic doings through further liquid-liquid extraction approaches could impairment natural goods since of the development circumstances and biological solvents such method reduces the purity of active ingredient present in the extract.

There are two fundamental sorts of ATPS: polymer-polymer and polymer-salt frameworks. The mind-boggling expense of some shaping stage polymers (e.g dextran) limits the use of these frameworks, just legitimized when the expense of the result of intrigue is extensive. Consequently, the choice of the more temperate polymer-salt frameworks is profoundly suggested [10-11].

The novelty of the proposed work is that during the extraction itself two different layers of aqueous solution and salt is obtained, which can help further to reduce the cost of separating components. Also, the systems can be designed by partying a diversity of components in water and two-polymer and polymer-salt systems have developed quickly. The said work majorly focuses on the extraction of oleic acid from neem leaves to powder using ATPS (water + polymer + salt) based on PEG and ammonium sulphate. The aim is to optimize various experimental parameters (time, ATPS composition, particle size) for the removal of Oleic acid from neem leaves powder and its additional practices as natural antioxidants.

2. Material and Methods

The Neem powder was obtained from Hari Parshuram Aushdhalya, Pune., Polyethelyene Glycol (PEG) was procured from SRL Chemicals Pvt Ltd, Mumbai. Folin Ciocalteu's reagent was procured from Qualigens Fine Chemicals, Mumbai. Ammonium Sulphate (AMS) was procured from S.D. Fine Chemicals Pvt Ltd, Mumbai.

2.1. Batch extraction

Batch extractions are a modest method for the extraction of bioactive compounds. The stages in this method are equipped with a 50 ml glass reactor with a four-bladed glass turbine impeller and the combination to be divided is supplementary. Subsequently collaborating, phase parting is proficient each by resolving below gravity. The stages are disconnected and investigated to improve the alienated constituents of the preliminary mixture. The object product would be focused at any of the stages and the pollutants in the additional form. In various cases, reclamation and attentiveness of the product that produces beyond 90% can be attained with a particular extraction stage.

One particular phase removal does not give adequate retrieval, recurrent extractions can be supported obtainable in a sequence of communicating and parting components [12]. The fluid dividers into two stages, each covering added 80% liquid. When basic biomolecules are supplementary to these combinations, biomolecules and cell wreckages are dividers among the stages; by choosing suitable circumstances, cell remains can be limited to one stage as the object bioactive molecule barriers. The segregating of biomolecules among segments mostly be contingent on the equilibrium connection of the arrangement. The partition coefficient is demarcated as [12-13].

$$K = \frac{C_{AT}}{C_{AB}}$$

Where C_{AT} is the equilibrium attentiveness of constituent A in the upper phase and C_{AB} is the equilibrium adsorption of A in the lesser phase. If constituent A helps the greater stage the worth of K will be better. In numerous aqueous arrangements, K is continual finished with an extensive collection of deliberations, as long as the molecular possessions of the stages are not transformed. The theoretic yield in the topmost stage, Y_T , can be premeditated relative to the capacity ratio of the stages, R (up to volume / below volume), and the partition coefficient K of the object molecule as follows [12-13]:

$$Y_T = \frac{V_T C_{AT}}{V_O C_O} = \frac{V_t C_{AT}}{V_t C_{AT} + V_B C_{AB}} = \frac{1}{1 + [\frac{1}{KR}]}$$

Similarly, the theoretic yield in the bottommost stage, Y_B is known by,

$$Y_B = \frac{1}{1 + [\frac{1}{KR}]}$$

Consequently, by changing anyone like K or R we can effortlessly upsurge or reduction the profit of the object particle [14]. Additional constraint recycled to describe two-phase partitioning is the concentration factor, δ_c , distinct as the ratio of produce attentiveness in the favoured stage to the original product attentiveness.

$$\delta_{C,T} = \frac{C_{AT}}{C_{Ao}} \quad (\text{Product partitions to the higher phase})$$

$$\delta_{C,B} = \frac{C_{AB}}{C_{Ao}} \quad (\text{Product partitions to the lower phase})$$

2.2. Determination of the binodal

By settlement, the constituent mainly in the lower layer is represented as abscissa and the predominant element in the upper stage is represented as ordered. The three systems are explained realistically.

2.2.1 Turbidometric titration

In the tubing, with suitable backup solutions, formulate systems through different configurations of recognized weight. Note the added size due to titration, for example, if 5 g methods are organized, use 10 ml tubes. As an example, shows the systems for different systems that can use PEG-phosphate and PEG-dextran, and the essential designs. This can be replicated in a worksheet to permit easy intention. Note down the mass of the tube and titration drop by drop, with suitable dilution till the scheme is zeroed, i.e., a stage is formed.

This can be done through the scheme is continuously mixing or accumulation a droplet, collaborating, adding a second drop and continues the same process. To confirm that it has formed a single-stage system, the schemes must be centrifuged (for example 1000-2000 g, 5 min). Record the concluding mass of the tube and estimate the mass of the additional dilution just before the formation of a phase. Since the number of graduate systems is relative to the total of points in the binodal, superior precision is obtained with a superior number of schemes [15].

2.2.2 Cloud point method

Balance 5 g of a standard solution of constituent X into a 25 ml narrowed flask. Then add drop by drop, a reserve solution of the Y component up to the principal indication of turbidity, which is the cloud point. Note the weight of the Y component necessary for the mixture to become cloudy. This provides the first point in the binodal. Also, add a known weight of diluent lower the cloud point and duplication as indicated [15-16].

2.2.3 Determination of the Tie line

Measuring the connection line for polymeric schemes comprising an optically active composite, for example, PEG-dextran, PEG-Ficoll and ethylene oxide-propylene as well as oxide-Reppal PES 100.

2.2.3.1 Polymeric Methods Comprehending One Optically Active Polymer

Formulate a standard curve for the lively constituent, in the variety of 0 to 10% (p / v), i.e. inside the linear series, through the identical sections arrange a second standard curve for the refractive measure of the index. If the scheme is arranged in a shield, the average curves for the clean constituents must be completed with a similar safeguard, since the salts similarly subsidize the refractive index. Get ready the phased scheme for investigation, assembly sure that the phase components mix well; let the phases separate.

To ensure complete separation, centrifuge at low speed (for example 1000-2000 g, 5 min). The system proportions should be appropriate to permit deduction of at least 5 g upper and lower stage for phase concentration investigation and an additional quantity for density extents. Distinct the higher and subordinate stages building certain not to origin stage relations. Make the suitable dilutions, for example, watery 5 g of phase with the suitable solvent to 25 ml in a volumetric container. Extend the visual revolution for every stage and estimate the individual concentrations. The concentration of another constituent is resolute by determining the refractive index of the developed and subordinate stage and deducting the influence of the refractive index acquired from the optically lively constituent [17].

2.2.3.2 Polymer-Salt Systems

Formulate a standard curve aimed at salt conductivity within the linear series (in% w / v). Arrange the stage schemes as indicated above and eliminate 5 g of samples of the higher too subordinate phases and

diluted with liquid and lyophilized, then note the dehydrated weight. Eliminate an additional section from the higher and subordinate stage, diluted with water and extent the conductivity of every stage. Estimate the salt absorption and deduct the mass involvement of the dehydrated mass of the section [16-18].

3. Results and Discussion

In this investigation, various experimental parameters were optimized such as speed of agitation (200 rpm, 300 rpm, 400 rpm & 500 rpm) and solvent ratio (1:1, 2:3 and 3:2). Extract samples were pipette out at specific time intervals like every 15 min and further standard Folin–Ciocalteu's method was used for analysis purposes. The obtained outcomes indicated that the TPC concentration of TPC in the extraction stage at a specific time. By changing the parameters speed of agitation and solvent ratio in the batch reactor at different times the results were optimized and used for further study.

3.1 Speed of agitation

About 5 g of powder of neem leaves was weighted and fed to 50 ml of batch reactor along with AMS salt (20 %w/w) and 50 ml of PEG (30 %w/w) at a temperature of 30°C till the extraction rate was a steady-state. The maximum speed of agitation produces high turbulence in the batch reactor and increases the rate of mass transfer [11]. The results of various experiments were performed for multiple agitation speeds is shown in figure 3.1 The experimental results shows that the concentration of TPC at 200 rpm significantly low as compared to 500 rpm, but there could be a marginal difference of TPC concentration of 400 and 500 rpm, speed of agitation., therefore for the further study, speed of agitation (400 rpm) was used. The circulation of TPC compounds from the neem leaves powder in the solvents could expand with the accumulative agitation speed. An added rise in the agitation speed has no substantial effect on final extraction yield; it clues that external mass transfer fighting is inconsequential at 400 rpm

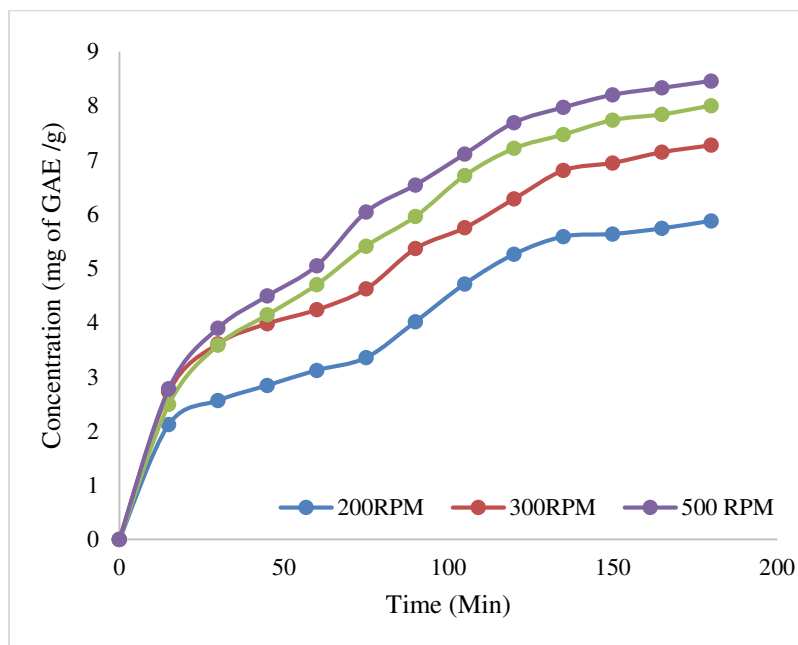


Fig. 3.1 Concentration of TPC obtained from Batch at temp 30°C speed of agitation 200, 300, 400 & 500 rpm)

3.2 Effect of Solvent Ratio (AMS: PEG)

The TPC concentration values in the extract were considered for changed extraction times at different solvent ratios (1:1, 2:3 & 3:2) and the same is shown in Figure 3.2. About 5 g of powder of neem leaves

was weighted and fed to 50 ml of batch reactor along with AMS salt (20 %w/w) and 50 ml of PEG (30 %w/w) at a temperature of 30°C till the extraction rate was a steady-state. There was an increase in TPC concentration and experiential for solvent ratio 01:01. A substantial quantity of solvent favours an additional concentration gradient and cuts diffusional resistance that rises the rate of extraction rate. There was a rise in TPC concentration, for the solvent ratio of 1:1 to 3:2. A substantial quantity of solvent tends to the added concentration gradient and drops diffusional resistance that rises the rate of extraction [11].

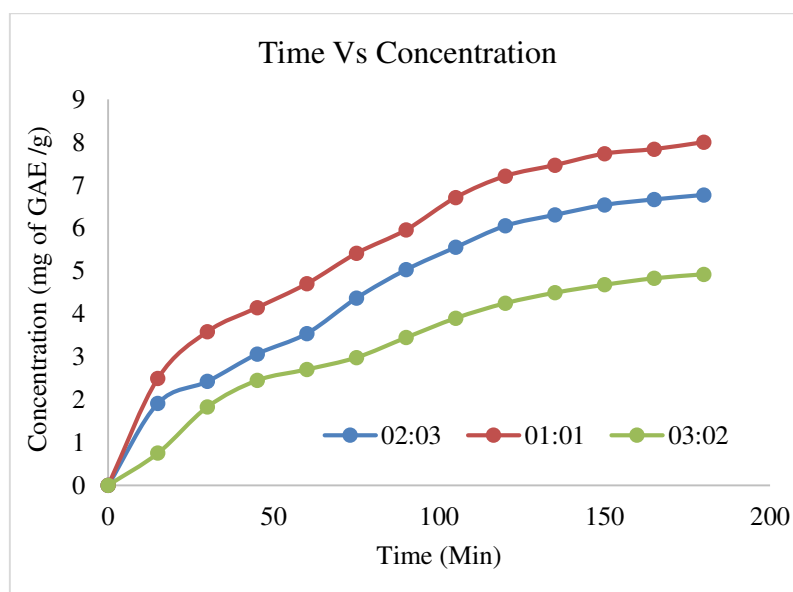


Fig.3.2 Effect of Solvent Ratio (AMS: PEG)

4. Conclusion

The investigation of the ATPS method was beneficial for the sub sequential treating of biomolecules. Also, the experimental parameters were optimized such as speed of agitation and solvent ration and the optimized parameters as 400 rpm and 01:02 solvent ration respectively with AMS salt (20 % w/w) & PEG (30 % w/w). The obtained extract also contains alkaloids, flavonoids, tannins, glycosides, acids and total phenolic compounds (TPC). The extracted Oleic acid by ATPS technique was measured with gallic acid equivalent (GAE) of TPC extracted from neem leaves powder. The determined concentration of oleic acid in the practice of TPC is 8.033 mg of GAE/g from the optimized experimental parameter. The optimized results can be used for a commercial process on an industrial scale.

References

- [1] Alasalvar C, Karamac M, Amarowicz R, Shahidi F, 2006. Antioxidant and antiradical activities in extracts of hazelnut kernel (*Corylus avellana* L.) and hazelnut green leafy cover. *J Agric Food Chem* 54: 4826-4832.
- [2] Babitskaia V, Shcherba V, Lkonnikova N, 2000. Melanin complex of the fungus *Inonotus obliquus*. *Prikl Biokhim Mikrobiol* 36(4): 439-444.
- [3] Dallora N, Klemz J, Filho P, 2007. Partitioning of model proteins in aqueous two-phase systems containing polyethylene glycol and ammonium carbamate. *Biochem Eng J* 34(1): 92-97.
- [4] Karakatsanis A, Liakopoulou M, 2007. Comparison of PEG/ fractionated dextran and PEG/industrial grade dextran aqueous two-phase systems for the enzymic hydrolysis of starch. *Eng* 80(4): 1213-1217.
- [5] Alencar L.V.T.D., Passos L.M.S., Martins M.A.R., Barreto I.M.A., Soares C.M.F., Lima A.S., Souza R.L., 2020. The complete process for the selective recovery of textile dyes using an

aqueous two-phase system. *Sep. Purif. Technol.* 253: <https://doi.org/10.1016/j.seppur.2020.117502>.

- [6] Ying H, Diyun C, Shuqi C, Minhua S, Yongheng C, Yixiong P, Gutha Y, 2021. A green method for recovery of thallium and uranium from wastewater using polyethylene glycol and ammonium sulfate based on the aqueous two-phase system. *J. Clean. Prod.* 297: <https://doi.org/10.1016/j.jclepro.2021.126452>.
- [7] Leitner M, Vandelle E, Gaupels F, Bellin D, Delledonne M, 2009. NO signals in the haze: Nitric oxide signalling in plant defence. *Curr Opin Plant Biol* 12(4): 451-458.
- [8] Liu SP, Zong ZM, Wei Q, Wei XY, 2010. Study on organic compounds in aqueous two phase system phase forming and distribution. *Chem Ind Times* 24(12): 21-24.
- [9] Ahareh AS, Gholamreza P, Javad RS, Shahla S, Naghmeh H, 2020. Separation of erythromycin using aqueous two-phase system based on acetonitrile and carbohydrates. *Fluid Phase Equilib.* 505: <https://doi.org/10.1016/j.fluid.2019.112360>
- [10] Perla JV, Salvador VG, Iran AT, Yolanda SM, Leticia GC, Artemio PL, Diana GR, 2020. Separation of bioactive compounds from epicarp of 'Hass' avocado fruit through aqueous two-phase systems. *Food Bioprod. Process.* 123:238-250.
- [11] Sandeep Shewale & Virendra K. Rathod (2018) Extraction of total phenolic content from *Azadirachta indica* or (neem) leaves: Kinetics study, Preparative Biochemistry & Biotechnology, 48:4, 312-320, DOI: 10.1080/10826068.2018.1431784
- [12] Singh SB, Jayasuriya H, Dewey R, Polishook JD, Dombrowski AW, Zink DL, Guan Z, Collado J, Platas G, Pelaez F, Felock PJ, Hazuda DJ, 2003. Isolation, structure, and HIV-1 integrase inhibitory activity of structurally diverse fungal metabolites. *J Ind Microbiol Biotechnol* 30(12): 721-731.
- [13] Srinivas ND, Barhate RS, Raghavarao KSMS, 2002. Aqueous two-phase extraction in combination with ultrafiltration for down-stream processing of *Ipomoea peroxidase*. *J Food Eng* 54(1): 1-6.
- [14] Uma DB, Ho CW, Wan Aida WM, 2010. Optimization of extraction parameters of total phenolic compounds from Henna (*Lawsonia inermis*) leaves. *Sains Malaysiana* 39(1): 119-128.
- [15] Wang SY, Wu JH, Cheng SS, Lo CP, Chang HN, Shyur LF, Chang ST, 2004. Antioxidant activity of extracts from *Calocedrus formosana* leaf, bark, and heartwood. *J Wood Sci* 50: 422-426.
- [16] Zhao YX, Miao KJ, Zhang MM, Wei ZW, Zheng WF, 2009. Effects of nitric oxide on production of antioxidant phenolic compounds in *Phaeoporus obliquus*. *Mycosystema* 28(5): 750-754.
- [17] Zheng WF, Zhao YX, Zhang MM, Wei ZW, Miao KJ, Sun WG, 2009. Oxidative stress response of *Inonotus obliquus* induced by hydrogen peroxide. *Med Mycol* 47: 814-823.
- [18] Zheng WF, Miao KJ, Liu YB, Zhao YX, Zhang MM, Pan SY, Dai YC, 2010. Chemical diversity of biologically active metabolites in the sclerotia of *Inonotus obliquus* and submerged culture strategies for up-regulating their production. *Appl Microbiol Biotechnol* 87(4): 1237-1254.

Simulation of M-ary QAM and M-ary PSK Modulation Techniques Using MATLAB GUI

Pranjal Dwivedi^a, Alok Ranjan^a, Ashish Srivastava^{a*}

^a*Department of Electronics & Telecommunication, MIT Academy of Engineering, Pune, India*

Abstract

The world has seen a transformation due to the recent pandemic. The field of education is drastically affected by it. There is a need to move from classroom teaching to online teaching, and the biggest hurdle is to impart practical knowledge. This paper attempts to study the concepts like M-ary Phase shift keying (PSK) and M-ary Quadrature amplitude modulation (QAM), used in modern-day communication systems, using a simulation platform. For this purpose, simulation using a graphical user interface (GUI) is proposed to study various M-ary PSK and M-ary QAM types. MATLAB is used to implement the GUI. The modulation, transmission, demodulation, and recovery of a signal implemented through the GUI will help learners understand the concepts better. Moreover, the constellation diagrams for M-ary PSKs and M-ary QAMs can be examined using the developed GUI.

Keywords- *Phase Shift Keying (PSK), Quadrature Amplitude Modulation (QAM), Constellation diagram, Graphical User Interface (GUI)*

© 2021 – Authors.

1. Introduction

The field of digital communication is growing and evolving rapidly, modulation techniques and their enhancements have become important. The digital modulation techniques must be tested and analyzed using the latest mathematical simulation platforms for improvements and effectiveness. With the development of communication techniques, the demand for reliable and fast data transmission has increased, which is also a reason for the simulation and analysis of these modulation techniques. Now that we know about increasing the data rate by changing the envelope, phase, and frequency of the carrier signal, different digital modulation schemes based on keying techniques are used to implement digital communication systems. These modulation schemes map the baseband data into more than four possible carrier signals because the degrees of freedom are two, i.e., phase and amplitude. In M-ary signaling, two or more bits are grouped, and symbols have some energy associated with them, known as symbol energy. The number of signals that can be generated is given by $M=2^m$, where m is an integer indicating the number of bits. Different modulation types like amplitude shift keying,

* Corresponding author.

E-mail address: aksrivastava@entc.mitaoe.ac.in

frequency-shift keying, and phase-shift keying exist depending on whether the amplitude, phase, or frequency is changed. The modulation technique is called Quadrature Amplitude Modulation (QAM) when the amplitude and phase are varied.

These days communication systems are studied through the simulation environment Sadinov et al., 2017. Implementation and calculation of the BER of M-PSK and M-QAM can be done using the signal space approach Lu et al., 1999. Laboratory sessions can be conducted in three ways, first, the live hands-on sessions, second, through simulation, and third remote laboratories Nickerson et al., 2006. Conducting laboratory sessions for engineering education needs a careful lookout, with detailed dos and don'ts Krivickas et al., 2007. A different approach needs to have opted for teaching-learning in distance learning mode Tomei, 2010. Digital communication experiments can have a wide range of concepts from basics to complex like jamming Wickert, 2011. MATLAB is used as the simulation platform and is a suitable platform for explaining wireless communication concepts to undergraduate students Zheng et al., 2007. Simulink being graphical, this programming environment gives good visualization of the results Hirst et al., 2013. The advanced applications of digital communication can be designed using MATLAB Yuting et al., 2010. The GUI can be converted to a mobile application for ease of access. Also, GUI will help in increasing learning efficiency. Interactive learning software can improve the learning experience of the students Naim et al., 2016. The programming approach can help the learners to understand software engineering Douglas 2005. The further sections elaborate on the concerning theory and methodology that were undertaken to implement the idea presented in the paper. The second section describes the considered modulation technique along with the role of noise in the communication system. The third section deals with the discussion and interpretations of the developed GUI. The conclusion drawn through the implementation and execution of is the presented idea is elaborated in the fourth section.

2. The Modulation Techniques

The section describes the theory behind the considered modulation technique and methodology opted to implement the GUIs. It is essential to emphasize the importance of M-ary encoding and the modulation techniques. The section concludes with a brief description of noise in the communication system in general and developed GUI in particular.

2.1. *M*-ary Encoding

To represent a signal using more than two bits, we use the word *M*-ary. The term *M* defines the number of bits being used to transmit one symbol, and it also gives an insight into the combinations and energy levels. *M*-ary encoding plays a critical role in digital modulation and communication. It improves the SNR, increases power and bandwidth efficiency in a modulation scheme. Different *M*-ary encoding is used in the digital world. Due to the features mentioned above, the encoding techniques are known with specific names. For instance, a 2-ary Phase Shift Keying modulation (2-PSK) is known as Binary Phase Shift Keying. Similarly, 4-PSK is known as Quadrature Phase Shift Keying.

In these modulation techniques, two or more bits are considered together to form a symbol, and the symbols $S_1(t)$, $S_2(t)$, ..., $S_m(t)$ are transmitted during the symbol period T . The possible number of signals depends on the value of *M*.

These modulation techniques find attractive application in the band-limited channels because of their higher bandwidth efficiency at the expense of power efficiency. There are certain drawbacks of these modulation techniques, like, poor error performance because of the minimal separation between the signals. Another

important point that needs to be taken into consideration is the bit rate and baud rate. Different modulation techniques result in different baud rates, which vary the bandwidth requirement of the signals.

As the value of M goes on increasing for a particular modulation scheme, the number of bits transmitted per symbol also increases, the resulting combination of bits forming a signal increases and, in turn, increasing the constellation points in a constellation diagram. With the rise in the constellation points, there tends to be some inter symbol interference (ISI) between the points. This results in distortion and corruption of the transmitted signal as the decision boundary of one symbol start interfering with the other symbols' boundary.

2.2. BPSK

It is a two-phase modulation. A binary message with 0 and 1 is represented by two different phase states, i.e., 0° and 180° for 0 and 1, respectively. For generating a BPSK signal, a basis function is chosen. Once we get the basis function, any vector present in the signal space can be represented as a linear combination of this function. In BPSK the modulation is done by varying the phase of the basis function depending on the message bits. The phase states of the carrier signal can be represented as follows:

$$S_1(t) = A_c \cos 2\pi f_c t, \quad 0 \leq t \leq T_b \text{ for binary 1} \quad (1)$$

$$S_0(t) = A_c \cos(2\pi f_c t \pm \pi), \quad 0 \leq t \leq T_b \text{ for binary 0} \quad (2)$$

Here A_c represents the amplitude of the sinusoidal signal, f_c is the carrier frequency calculated in Hz, t is the instantaneous time in seconds, and T_b is the bit period in seconds. The signals S_0 and S_1 denote the modulated signal when information 0 and 1 are transmitted, respectively.

The BPSK transmitter can be implemented using the nonreturn to zero (NRZ) polar coding method and multiplying the output by a reference oscillator running at carrier frequency f_c . In this case, it is convenient to choose the oversampling factor as the ratio of sampling frequency (f_s) and the carrier frequency (f_c).

2.3. QPSK

In this modulation technique, two information bits that are combined as one symbol are modulated. The modulator is required to select one of the four possible carrier phase shift states. A QPSK signal with a symbol duration T is defined as:

$$S(t) = A_c \cos(2\pi f_c t + \theta_n), \quad 0 \leq t \leq T \text{ for } n = 1, 2, 3, 4 \quad (3)$$

and the signal phase is defined as:

$$\theta_n = (2n - 1)\pi/4, \quad (4)$$

Therefore, the possible phase outcomes are $\pi/4$, $3\pi/4$, $5\pi/4$ and $7\pi/4$. Equation [4] above requires two orthogonal basis functions, which are in-phase and quadrature signaling points.

For the generation of a QPSK signal, a splitter is used to separate the odd and even bits from the generated information bits. The odd bits and even bits are converted to NRZ polar at the same time. It is to be noted here that the BPSK modulation requires a symbol duration same as that of bit duration, but when QPSK is used, the

symbol duration becomes twice as that of bit duration. Hence, QPSK sends a message at a rate that is twice as compared to the BPSK.

2.4. *M*-ary QAM

Quadrature amplitude modulation is a modulation technique that encodes the information or message signal with the carrier signal by varying the carrier signal's amplitude and phase. The carrier signal is subdivided into two signals which are 90° out of phase from each other. These signals are termed In-phase and Quadrature phase signals. Since both the amplitude and phase are constantly varied, the signal envelope is not constant and has a higher bandwidth efficiency than other *M*-ary signaling schemes with the same power consumption. Suppose M_1 and M_2 represent the number of possible values of amplitudes and phases, respectively. The total number of bits per symbol transmitted is the combination of amplitude and phase modulation and is given by $\log_2(M_1M_2)$.

Constellation diagram is used for graphical representation of the envelope of the state of the symbol and is considered an essential tool in analyzing the performance of QAM. The x-axis and the y-axis of the diagram represent the in-phase and the quadrature-phase components of the modulated signal, respectively. The separation between the signals in the constellation diagram tells us about the difference between the modulation schemes and how the receiver distinguishes them.

To measure the modulation schemes' performance, one needs to calculate the bit error rate (BER) while assuming that the systems contain additive white Gaussian noise (AWGN).

2.5. Noise

Noise is the unwanted electrical signal that is present in almost every electrical system. It interferes with the signal and leads to improper or distorted production and reception of the transmitted signal. Due to this, interference generates specific errors in the signal analysis and affects the sensitivity of receivers.

The noise is present in almost all communication systems and is the primary disturbance in those systems. AWGN has typically zero mean. The deviation of the received signals with noise increases with an increase in the variance. This noise is used to model any communication systems where the noise interferences are kept in check.

3. Results and Discussions

A Graphical User Interface Development Environment (GUIDE) can be used to create custom applications and user interfaces. A GUI can be made by dragging and dropping components. GUIDE generates two files, one contains layout information, and the other has implementation code. The simulation of discussed modulation techniques through GUIs was developed comprising a random signal, converting it into integer representation, modulation using inbuilt MATLAB functions, adding noise, simulation of the channel, demodulation using the inbuilt MATLAB function.

The GUI can also take desired inputs from the user and simulate the modulation and demodulation to show the results. Different parameters can be studied and analyzed through the developed GUI. Used parameters paved the way to compare the modulation techniques. The GUI of the modulation techniques along with constellation diagram was developed with the help of 'push button', 'box' and 'axes' widgets in MATLAB.

Various modulation techniques, including BPSK, QPSK, and QAM, can be learned using the options available on the GUI, as seen in Figure 1.

Figure 1 shows in-phase, and quad-phase components of the signal are depicted separately along with the combined modulated signal. From this figure, different phases can be observed at the message transitions from 0 to 1 or 1 to 0. Similarly, we can obtain BPSK, 8-PSK, and 16-PSK modulated signals by clicking on the corresponding push button on the GUI. On clicking the “Navigate to QAM” push button, the other GUI for QAM will open. In the second GUI, options for 4, 8, 16, and 64 QAM are provided. The learner can click on the desired technique to be studied. For example, on clicking the push button for 8-QAM, the results of this will pop up, as shown in Figure 2. A message signal is shown in the digital format (in terms of bits). The number of symbols is represented in terms of discrete signals in which there are M number of distinct amplitude levels. The symbols are separated by fixed symbol duration. Modulated signals in analog form can also be seen in the figure. In the same GUI for 8-QAM, the constellation diagram is also depicted. The reference constellation is adjusted to the desired constellation. Eight yellow points represent the transmitted symbol. The distance between each point and origin is different, which specifies the change in amplitude. Similarly, each point is located at a different location and specifies the phase change. With the help of the constellation diagram, the learner can easily find out the Euclidian distance for a particular modulation scheme.

Through Figure 3, the 16-QAM can be studied, and it gives the learner a better insight for understanding the modulated signal and the constellation diagram. The different information signal in digital format is considered as an input for the 16-QAM. Here also one can observe sixteen different amplitude levels in symbol representation in discrete form. Continuous, modulated signal can also be seen in Figure 3.

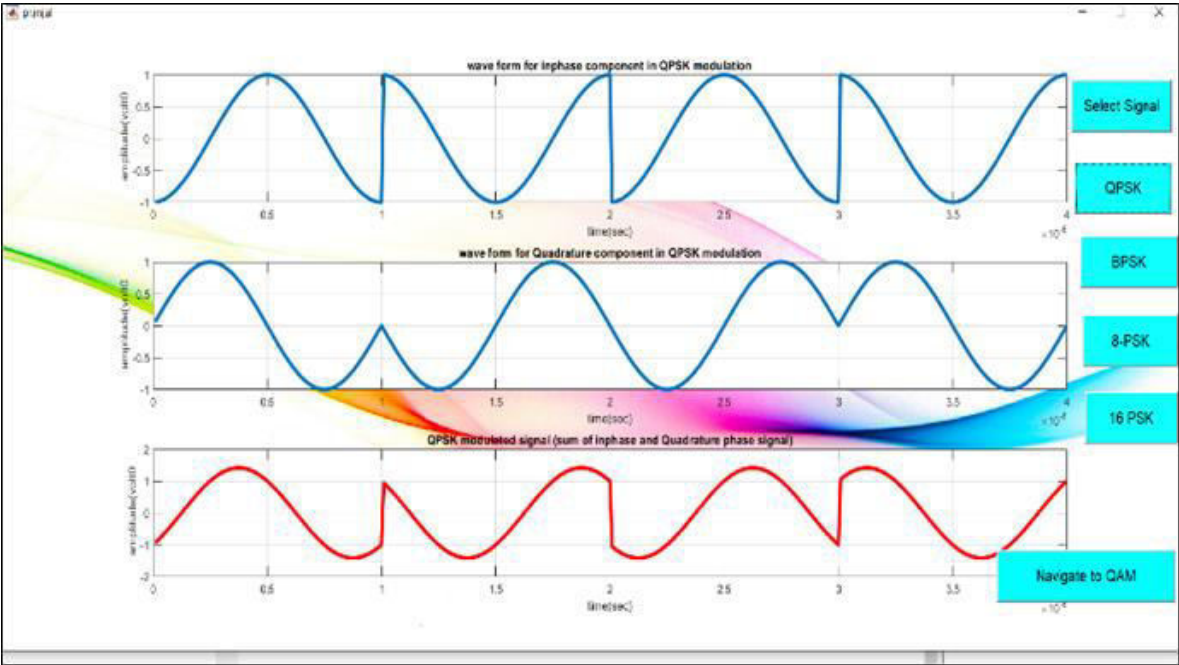


Fig. 1. In-phase, Quad-phase, and Modulated QPSK Signal

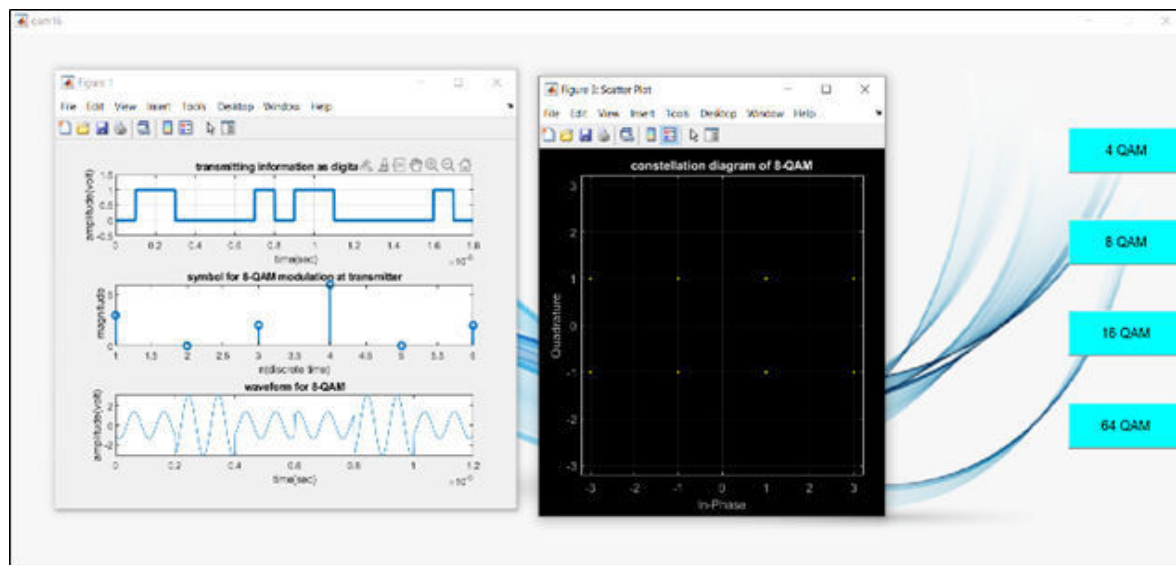


Fig. 2. 8-QAM Modulated Signal with Constellation Diagram

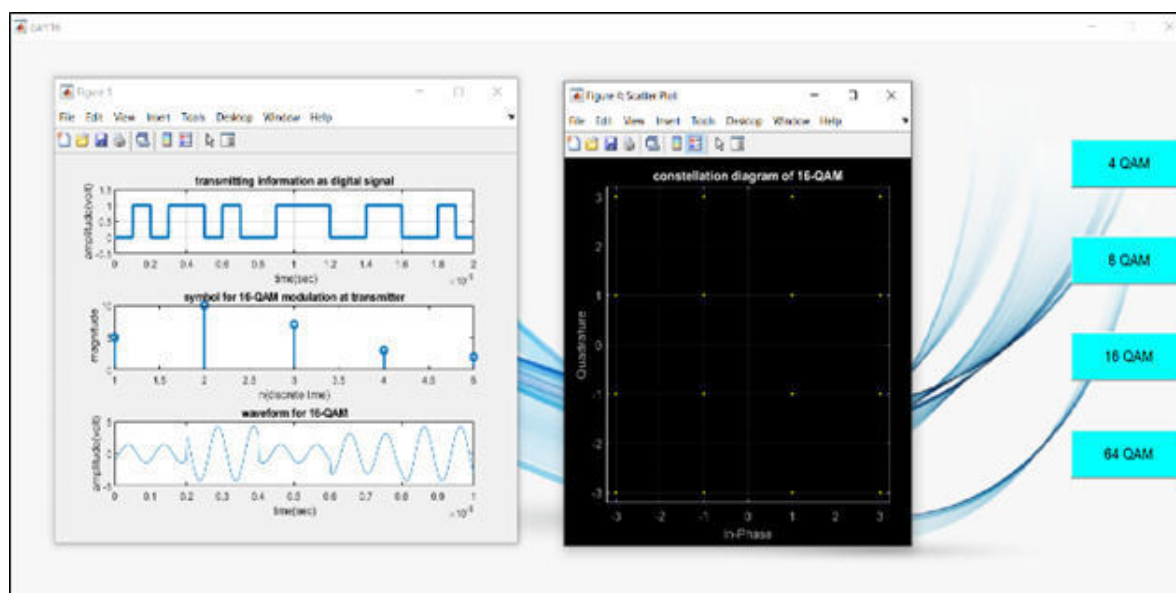


Fig. 3. 8-QAM Modulated Signal with Constellation Diagram

4. Conclusions

The paper elaborates the M-ary modulation techniques using MATLAB environment. The motivation for the paper's central theme was employed from the fact that practical teaching has been very difficult in pandemic situations and will raise an alarming situation if something is not done. Teaching-learning through the use of the developed GUI will efficiently help the students to visualize and understand different modulation schemes. The modulations considered are phase shift keying variants (BPSK, QPSK, 8-PSK, 16-PSK) and Quadrature Amplitude Modulation (4-QAM, 8-QAM, 16-QAM, 64-QAM). The developed GUIs will provide a better learning experience to the learner. The results show different stages of modulation of the message signal. The constellation diagram of the received signal after passing through the channel in the presence of noise can also be observed. With the increase in modulation order, Euclidian distance decreases; thus bit error rate increases. The lower value of modulation has disadvantages such as transmission problems, lesser bandwidth efficiency, and lesser power efficiency. The theoretical concepts of digital modulation techniques can be taught to a learner using the developed GUI for an improved learning experience without compromising on practical aspects in online or distance learning mode.

References

- S. M. Sadinov, May 22- 26, 2017, "Simulation Study of M-ARY QAM Modulation Techniques using Matlab/Simulink." MIPRO 2017, Opatija, Croatia
- Jianhua Lu, K. B. Letaief, Justin C-I Chuang, and Ming L. Liou, 2nd February 1999, "M-PSK and M-QAM BER Computation Using Signal-Space Concepts", IEEE Transactions On Communications, Vol. 47, No.
- J. Ma and J. Nickerson, pp. 1-24, 2006, "Hands-On, Simulated, and Remote Laboratories: A Comparative Literature Review," Journal of ACM Computing Surveys, vol. 38, no. 3.
- R. Krivickas and J. Krivickas, 2007, "Laboratory Instruction in Engineering Education," Global Journal of Engineering Education, vol. 11, no. 2, pp. 191-196.
- Lawrence A. Tomei, 2010, Designing Instruction for the Traditional, Adult, and Distance Learner: A New Engine for Technology-Based Teaching, Information Science Reference, New York, USA.
- M. Wickert, 2011 IEEE, 2011, "Digital Communication with Jamming Experiments for a Signal Processing First Course," Digital Signal Processing Workshop and IEEE Signal Processing Education Workshop (DSP/SPE), pp.101-106.
- J. Z. Zhang, R.D. Adams & K. Burbank, 2007 UICEE, "Using MATLAB to Improve Learning Effectiveness and Quality in an Undergraduate Course on Wireless Communications and Systems," Global J. of Engng. Educ., Vol.11, No.1, Australia, pp. 45-54.
- Brice A. Hirst and Yahong R. Zheng, 2013, "Utilization of MATLAB Simulink Exercises for an Undergraduate Communications Course," Proceedings of the 2013 American Society for Engineering Education Annual Conference & Exposition, American Society for Engineering Education.
- D. Yuting and F Lijun, 2010, "The Simulation Design of MATLAB applied to the Mode Technology of Digital Communication System," Third International Symposium on Information Science and Engineering, IEEE Computer Society, pp.438-441.
- Naim, Nani Fadzlina, et al. "Interactive Learning Software for Engineering Subjects Based on MATLAB-GUI." Journal of Telecommunication, Electronic and Computer Engineering (JTEC) 8.6 (2016): 77-81.
- Douglas Bell, 2005., Software Engineering for Students: A Programming Approach. 4th Edition, Pearson Education Limited, Harlow, England.



Pranjal Dwivedi is a student in the Department of Electronics and Telecommunication Engineering, School of Electrical Engineering, MIT Academy of Engineering Pune. He had been working in the field of wired and wireless communications as a research enthusiast.



Alok Ranjan is a student in the Department of Electronics and Telecommunication Engineering, School of Electrical Engineering, MIT Academy of Engineering Pune. For the last two years, he has been working in the communication domain and has a firm grip over the simulation platforms and latest technical tools.



Ashish Srivastava is working as an Assistant Professor in the Department of Electronics and Telecommunication Engineering, School of Electrical Engineering, MIT Academy of Engineering Pune. He is a Doctoral candidate in the National Institute of Technology Patna. Ashish's research interest lies in the field of communication engineering.

Robust Control Algorithm for Piezo-electric Energy Scavenging

Shailesh Shinde^{a*}, Ashitosh Chavan^{a†}, Aniket Gundecha^a, Kaliprasad Mahapatro^b

^aMIT Academy of Engineering, Alandi(D), Pune, Maharashtra, INDIA

^bAvantika University, Ujjain, MP, INDIA

Abstract

The paper proposes a robust control algorithm for the piezoelectric energy scavenging in the presence of uncertainties. The nonlinear dynamics makes the piezoelectric actuators unstable and shows substantial uncertainty and disturbances in the output. In this study a closed loop step down DC–DC converter along with the Extended State Observer (ESO) is implemented. This paper proposes step by step design of buck converter and its linear mathematical model. The output of a buck converter is taken as a feedback along with the heuristic implementation of ESO. Extended state observer is designed such that it estimates the state and lumped uncertainties. The proposed algorithm is addressed to maintain the output voltage constant in the piezoelectric energy harvester under the uncertainties. The efficacy of the proposed algorithm is verified using MATLAB Simulink and the result shown in this paper showcase a better voltage regulation in the presence of uncertainties and wide range of dynamic input voltage.

Keywords- *Buck Converter, Extended State Observer (ESO), Piezoelectric Energy Scavenging*

© 2021 – Authors.

1. Introduction

The demand for renewable energy sources is increasing day by day. The process of the conversion of renewable energy into electrical energy is referred to as energy scavenging and it can be utilized in many applications including portable electronics, wireless gadgets and power systems Lu et al., 2010. Energy harvester is used to recharge the battery and the input for the harvester is dynamic, as it is obtained from environmental energy sources such as sunlight, wind, etc. Lu et al., 2010. Different energy harvesting methodologies are available such as piezoelectric Ayrikyan et al., 2017, wind Wu et al., 2013, thermoelectric Hu et al., 2020 and solar Carvalho and Paulino, 2010. Because of better liberal vibration accessibility and good harvesting material property, piezoelectric energy harvesting based method is selected Ayrikyan et al., 2017.

In piezoelectric approach, due to unstable vibration status the output voltage is also changing Grace et al., 2011. In order to scavenge as much energy as possible, a run-time adaptive mechanism is required to track the output voltage with the vibration of piezoelectric element Chao et al., 2007. Energy scavenging systems provide constant output voltage with the growing application of DC–DC converter Gundecha et al., 2016,

* Corresponding author.

E-mail address: srshinde@entc.maepune.ac.in

† Corresponding author.

E-mail address: adchavan@mitaoe.ac.in.

Nguyen et al., 2021. The piezoelectric sensors are used to stimulate the development of specific converters to operate such actuators Bellmund et al., 2007. Different switching converter topologies have been employed to drive such actuators, buck Lakshmi and Raj, 2014, boost Gundecha et al., 2016, and buck-boost Lefeuvre et al., 2007.

The voltage in the output cannot be considered as constant and it should be controlled by different strategies. A variety of controlling strategies like PID controller Djmel et al., 2019, fuzzy logic Ardhenta et al., 2020, and sliding mode control Utomo et al., 2020 are available to control the power converter. The effects of uncertainties and disturbance in control are estimated by introducing some observing methods like disturbance observer (DO), State and disturbance observer (SDO) Chavan et al., 2019, Discrete Kalman Filter and High Gain Observers Ali et al., 2019, H_∞ Wang et al., 2020, Luenberger Observer Wang and Li, 2020. Extended state observer (ESO) Han, 2009 is a better observing technique that can estimate both state as well as disturbance with less plant information Li et al., 2011. The ESO is used to estimate the present uncertainty and disturbance in order to minimize the effect in the output Bin et al., 2014. ESO has been widely applied in various areas like motion control systems Mahapatro et al., 2019, robot control systems Ma et al., 2020 and vibrations Shi et al., 2021.

Based on the literature, most commonly used control algorithms and the observers are listed in Table 1.

Table 1. Literature on control algorithms & observers

Control Algorithms	Observers	
PID Control	Disturbance Observer (DO)	State & Disturbance Observer (SDO)
Sliding Mode Control (SMC)	High Gain Observers	Discrete Kalman Filter Observers
Fuzzy Logic Control	H_∞ Observer	

The rest of the paper is organized as follows: Section 2 introduces piezoelectric energy scavenging system. Section 3 describes the operation of a DC–DC buck converter. Section 4 gives the mathematical modelling of DC–DC buck converter. Section 5 explains the concept of control design. The results are shown with related discussion in section 6. The paper is concluded in section 7.

2. Piezoelectric Energy Scavenging

Piezoelectric materials are used for energy scavenging to convert mechanical strain into an electrical form due to their small size and the piezoelectric effect. The equivalent circuit of a vibrating piezoelectric element can be modeled as a source of sinusoid current $i_p(t)$ parallel to its C_p electrode capacitor.

AC–DC rectifier is required as the output of piezoelectric material is an AC signal. The magnitude of the polarization current I_p depends on the level of mechanical excitation of the piezoelectric element, frequency of mechanical vibration and hence the rectifier voltage may not be constant Ottman et al., 2003. The ability to achieve and maintain constant output voltage is accomplished by placing a DC–DC step-down converter between the rectifier and the electronic load as shown in Fig.1. A DC–DC step-down converter is known as buck converter. A buck converter is placed between the rectifier and the electronic load. The control approach used an extended state observer (ESO) for estimating state as well as lumped disturbance. This strategy gives constant and regulated output voltage by using ESO in the presence of certain uncertainties.

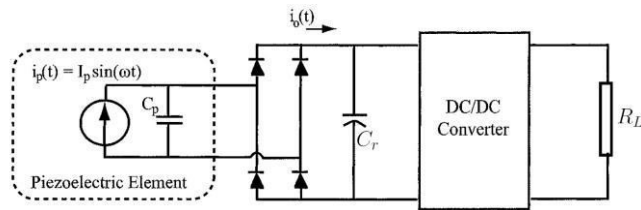


Fig. 1. Energy harvesting circuitry

The DC component of the output current and the rectifier capacitor voltage give the power of the piezoelectric element Ottman et al., 2003 are shown as;

$$\dot{i}_0(t) = \frac{2I_p}{\pi} - \frac{2V_r \omega C_p}{\pi} \quad P(t) = \frac{2V_r}{\pi} (I_p - V_r \omega C_p)$$

Where V_r is the rectifier capacitor voltage and ω is the resonating frequency.

The controller of the converter is designed to achieve and maintain the constant output voltage in presence of the uncertainties. The output obtained from the piezoelectric sensor is characterized and studied for selection of proper voltage levels for further interface. The frequency of vibration plays an important role in the generation of the corresponding electrical voltage Ottman et al., 2003, Vulture. The characteristics of a piezoelectric sensor when operated in different conditions are shown in Table 2. The tip mass range is considered from 0 gram to 7.8 gram and their corresponding variation in frequency, AC voltage and rectified DC voltage is stated in Table I. The system efficiency depends on the rectification output in conjunction with the DC-DC converter. A step down converter is used to maintain the constant output voltage.

Table 2. Characteristics of piezoelectric sensor

Tip Mass (gram)	Frequency (Hz)	Open Ckt. Vtg (rms)	Rectified O/P (V _{dc})	Tip Mass (gram)	Frequency (Hz)	Open Ckt. Vtg (rms)	Rectified O/P (V _{dc})
0	120	3.2	3.11	2.4	75	6.5	7.7
0	120	4.4	4.8	2.4	75	7.5	9.17
0	120	5.5	6.3	2.4	75	11.5	14.81
0	120	10.1	12.84	7.8	50	10.3	13.12
2.4	75	4.7	5.22	7.8	50	15.4	20.31

3. Buck Converter

Buck converter is referred to as step down converter. In a buck converter, an unregulated DC input voltage is converted to a regulated low DC output voltage. A typical buck converter is shown in Fig 2. The buck converter comprises a power MOSFET Ramirez et al., 2006 used as a controllable switch Q with two states $\mu = 0$ and $\mu = 1$, a diode D , an inductor L , and a filter capacitor. The buck converter is connected to a DC source which is rectified from piezoelectric output of voltage E that provides a regulated DC voltage V_o to the load resistor R .

When the MOSFET Q is ON, the diode D is reversed biased and the input current, I_L flows through the inductor L and resistor R . When the MOSFET Q is OFF, the diode D gets conducted and the inductor current flows through the inductor, capacitor and resistor.

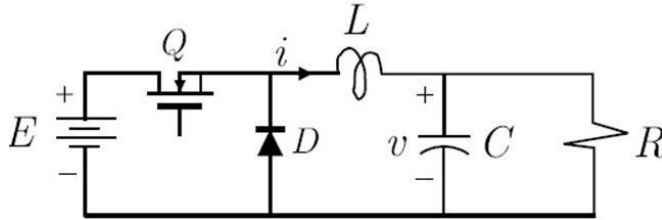


Fig. 2. Circuit diagram of buck converter

Therefore the output voltage depends on the input voltage, duty cycle and it is always less than the input voltage. The inductor value depends upon the frequency, load and ripple current, input and output voltages Lakshmi and Raja, 2014. Designing a good performance buck converter, the inductor ripple current should lie between 10% to 20% of the output current. The output voltage ripple is the most important criterion for selecting the capacitors.

The output voltage, value of inductance and capacitor are given as;

$$V_0 = E \times d \quad L = \frac{(E - V_{out}) \times d}{f_s \times \Delta I_L} \quad C = \frac{I_L}{8 \times f_s \times \Delta V_{out}}$$

Where d is the duty cycle.

4. Modeling of Buck Converter

Consider the ideal configuration as shown in Fig. 2, to describe the dynamics of DC-DC buck converter. The mathematical modeling of a DC-DC buck converter is based on the controlling action of switch Wang et al., 2015.

When the switch is ON (i.e. at $\mu = 1$), the equation is obtained by applying Kirchhoff's laws to the circuit shown in Fig. 2.

$$\frac{di_L}{dt} = \frac{E - V_0}{L} \quad (1)$$

$$\frac{dV_0}{dt} = \frac{i_L}{C} - \frac{V_0}{RC} \quad (2)$$

Where i_L is the inductor current and V_0 is the output voltage.

When the switch is OFF (i.e. at $\mu = 0$), the equation is obtained by applying Kirchhoff's laws to the circuit shown in Fig. 2.

$$\frac{di_L}{dt} = \frac{-V_0}{L} \quad (3)$$

$$\frac{dV_0}{dt} = \frac{i_L}{C} - \frac{V_0}{RC}$$

Then combining equation (1), (2), (3), (4) and when $\mu \in [0, 1]$, the average model can be written as;

$$\frac{di_L}{dt} = \frac{\mu E - V_0}{L} \quad (5)$$

$$\frac{dV_0}{dt} = \frac{i_L}{C} - \frac{V_0}{RC} \quad (6)$$

In practice, the load resistance may vary and the assumed nominal value of R is R_0 .

Let $z_1 = (V_0 - V_{ref})$ and $z_2 = \left(\frac{i_L}{C}\right) - \left(\frac{V_0}{R_0 C}\right)$ be the state variables, hence the model is rewritten as;

$$\dot{z}_1 = \frac{i_L}{C} - \frac{V_0}{RC} + \varphi_1(t) \quad (7)$$

Where $\varphi_1(t) = -\frac{V_0}{RC} + \frac{V_0}{R_0 C}$ is the mismatched disturbance.

Therefore;

$$\dot{z}_2 = \frac{\mu E - V_0}{LC} - \frac{1}{R_0 C} \left(\frac{i_L}{C} - \frac{V_0}{RC} \right) \quad (8)$$

It can be simplified as;

$$\dot{z}_2 = \frac{\mu E - V_{ref}}{LC} - \frac{z_1}{LC} - \frac{1}{R_0 C} \left(\frac{V_0}{R_0 C} - \frac{V_0}{RC} \right) \quad (9)$$

Denoting; $u = \frac{\mu E - V_{ref}}{LC}$ and $\varphi_2(t) = -\frac{1}{R_0 C} \left(\frac{V_0}{R_0 C} - \frac{V_0}{RC} \right)$

The model can be simplified using equation (7) and (9) as;

$$\dot{z}_1 = z_2 + \varphi_1(t) \quad (10)$$

$$\dot{z}_2 = u - \frac{z_1}{LC} - \frac{z_2}{R_0 C} + \varphi_2(t) \quad (11)$$

5. Control Design

A robust control for variable load in a DC-DC buck converter is designed in this section with a piezoelectric energy scavenging system. The ESO is used to estimate two states as well as disturbance Han, 2009. A proposed control configuration is shown in Fig. 3.

Consider the mismatched disturbance estimation of $\varphi_1(t)$, based on the ESO technique is designed as;

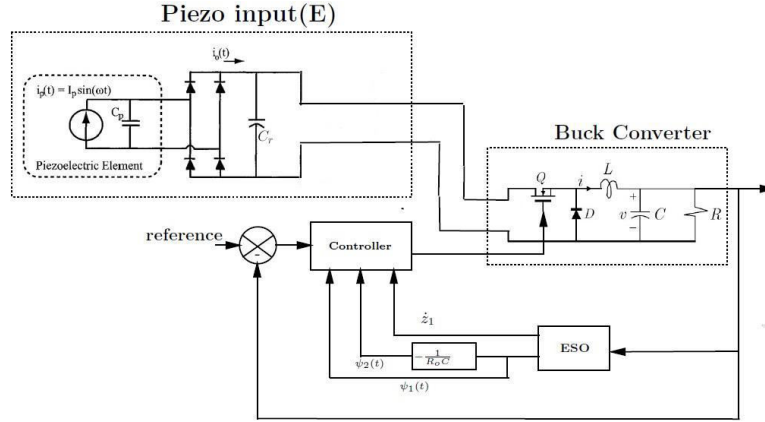


Fig. 3. Proposed control configuration

$$\hat{z}_1 = \hat{z}_2 + z_2 - \beta_1(\hat{z}_1 - z_1) \quad (12)$$

$$\hat{z}_2 = -\beta_3(\hat{z}_1 - z_1) \quad (13)$$

Where, $z_1 = \hat{z}_1$, $z_2 = \hat{\varphi}_1(t)$ and $\beta_1 > 0$, $\beta_2 > 0$.

From the equation (7), (8), (9) and (10) the relationship between φ_1 and φ_2 is given by;

$$\hat{\varphi}_2(t) = -\frac{1}{R_0 C} \hat{\varphi}_1(t) \quad (14)$$

In a buck converter, ESO is employed to observe and estimate the disturbance φ_i of a plant and which is based on control input and plant output. The proposed ESO-based system under mismatched disturbance is designed in Gundecha et al., 2016, Mahpatro et al., 2015 as;

$$u = \left[\frac{z_1}{LC} + \frac{z_2}{R_0 C} - \hat{\varphi}_2 - k_1 \hat{z}_1 - k_2 (z_2 + \hat{\varphi}_1) \right] \quad (15)$$

6. Results and Discussion

The proposed algorithm has been tested for voltage tracking in a buck converter with piezoelectric energy scavenging system. The responses of variable output load resistance and dynamic changes in input voltage are tested on the propose algorithm.

The proposed work is used to control and analyse the effect of dynamic variation in piezoelectric input. From Ottman et al., 2003 the trajectory as shown in Fig. 4(a) is designed. For variable input voltage E , the

load resistance is changed from 200Ω to 150Ω . From Fig. 4(b), it is observed that the controller design in equation (11) estimates the changes in the state and adjusts the duty cycle for getting output voltage at $4.5V$.

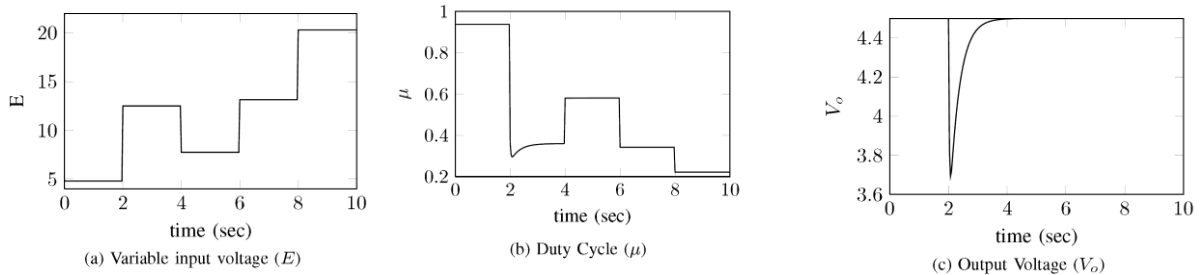


Fig. 4. Dynamic variation in piezoelectric input

Case 1: Variable Load Resistance (R_L)

The buck converter is evaluated under variable load resistance conditions for tracking the reference voltage. The input voltage is considered as, $E = 8V$, reference voltage as, $V_{ref} = 4.5V$. The tracking and estimation performance for 180Ω resistance is shown in Fig. 5. The duty cycle (μ) and the controlled output are shown in Fig. 5(c), 5(d). The results are tested for different R_L range from 140Ω to 240Ω . The cumulative results for *Case 1* are illustrated in Table 3.

Table 3. Performance result for variable load resistance

R_L (Ω)	μ (V_{ms})	Tracking Error ($z_1 = V_{ref} - V_o$)	Estimation Error ($e = z_1 - \hat{z}_1$)	R_L (Ω)	μ (V_{ms})	Tracking Error ($z_1 = V_{ref} - V_o$)	Estimation Error ($e = z_1 - \hat{z}_1$)
180	0.5466	0	0.0026	230	0.5861	0	0.0051
200	0.5777	0	0.0031	240	0.5962	0	0.0076

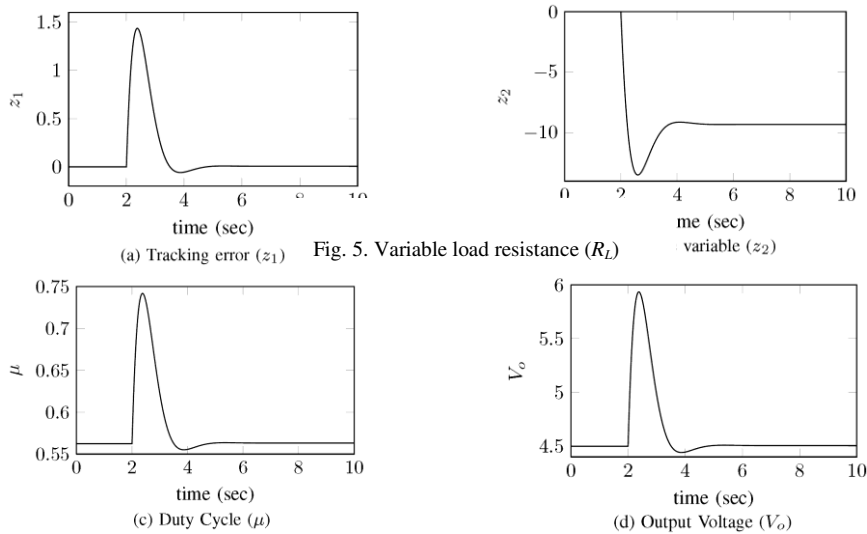


Fig. 5. Variable load resistance (R_L)

Case 2: Variable Input Voltage (E)

The estimation and tracking performance for an input voltage is tested for different E range from 8V to 16V. The results are illustrated in Table 4.

Table 4. Performance result for variable input voltage

E (V)	μ (V_{rms})	Tracking Error ($z_1 = V_{ref} - V_0$)	Estimation Error ($e = z_1 - \hat{z}_1$)	E (V)	μ (V_{rms})	Tracking Error ($z_1 = V_{ref} - V_0$)	Estimation Error ($e = z_1 - \hat{z}_1$)
8	0.5548	0	0.0013	12	0.3698	0	0.0013
10	0.4438	0	0.0013	14	0.3170	0	0.0013

Case 3: Variable Reference Voltage (V_{ref})

The reference voltage is varied from 3.8V to 5.8V and the load resistance $R_L = 200$ with the input voltage $E = 8V$. The proposed controller is suitable to regulate the required output voltage. The results for variable reference varied from 3.8V to 5.8V are shown in Table 5.

Table 5. Performance result for variable reference voltage

V_{ref} (V)	μ (V_{rms})	Tracking Error ($z_1 = V_{ref} - V_0$)	Estimation Error ($e = z_1 - \hat{z}_1$)	V_{ref} (V)	μ (V_{rms})	Tracking Error ($z_1 = V_{ref} - V_0$)	Estimation Error ($e = z_1 - \hat{z}_1$)
3.8	0.4685	0	0.0011	4.5	0.5548	0	0.0013
4.0	0.4931	0	0.0012	5.8	0.7150	0	0.0017

The proposed work shows the robust voltage tracking of buck converters for piezoelectric energy harvesting and the results are verified in simulation. The different cases of the piezoelectric energy scavenging are considered and obtain better voltage tracking results with various dynamic constants. The effects of disturbances are compensated by ESO, caused by load and input uncertainties.

7. Conclusions

The paper proposed a robust control approach for DC–DC buck converter for scavenging electrical energy from a mechanically excited piezoelectric element. The disturbances caused by variation in load and input are compensated by using ESO. A good disturbance rejection against input and load resistance variation is obtained with better voltage tracking performance and state estimation. A robust control strategy with application to piezoelectric energy scavenging for uncertain dynamics is confirmed.

References

- [1] J. Lu, S. Liu, Q. Wu, and Q. Qiu, 2010. "Accurate modeling and prediction of energy availability in energy harvesting real-time embedded systems," in International Green Computing Conference. Chicago: IEEE, pp. 469–476.
- [2] Ayrikyan, A. Kastner, N. H. Khansur, S. Yasui, M. Itoh and K. G. Webber, 2017. "Lead-Free Multilayer Piezoceramic Composites: Effect of Cosintering on Electromechanical Properties," in IEEE Transactions on Ultrasonics, Ferroelectrics, and Frequency Control, vol. 64, no. 7, pp. 1127–1134, doi: 10.1109/TUFFC.2017.2701882.
- [3] Y. Wu, W. Liu, and Y. Zhu, 2013. "Design of a wind energy harvesting wireless sensor node," in International Conference on Information Science and Technology (ICIST). Yangzhou: IEEE, pp. 1494–1497.
- [4] Z. Hu, E. Mu and Z. Wu, 2020. "MEMS thermoelectric power chip for large scale thermal energy harvesting," 2020 IEEE 8th Electronics System-Integration Technology Conference (ESTC), pp. 1-6, doi: 10.1109/ESTC48849.2020.9229864.
- [5] C. Carvalho and N. Paulino, 2010. "A mosfet only, step-up dc-dc micro power converter, for solar energy harvesting applications," in 17th International Conference on Mixed Design of Integrated Circuits and Systems (MIXDES). Warsaw: IEEE, pp. 499–504.
- [6] E. Grace, D. Rajan, and A. clarence asis, 2011. "Performance evaluation of different rectifiers for piezo-electric energy harvesting applications," in International Conference on Recent Advancements in Electrical, Electronics and Control Engineering. IEEE, pp. 248–252.
- [7] L. Chao, C.-Y. Tsui, and W.-H. Ki, 2007. "Vibration energy scavenging and management for ultra-low power applications," in Low Power Electronics and Design (ISLPED). Portland: IEEE, pp. 316–321.
- [8] D. Gundecha, V. Gohokar, K. A. Mahapatro, and P. V. Suryawanshi, 2016. "Control of DC–DC converter in presence of uncertain dynamics," in Intelligent Systems Technologies and Applications, vol. 384. Springer, pp. 315–326.
- [9] S. H. Nguyen, H. Richardson and R. Amirtharajah, 2021. "A Bias-Flip Interface and Dual-Input DC-DC Converter for Piezoelectric and RF Energy Harvesting," International Symposium on Circuits and Systems (ISCAS), pp. 1-5, doi 10.1109/ISCAS51556.2021.9401590.
- [10] O. Gomis-Bellmunt, D. Montesinos-Miracle, S. Galceran-Arellano, and A. Sudri-Andreu, 2007. "A buck-boost bidirectional converter to drive piezoelectric actuators," in Power Electronics and Applications. Aalborg: IEEE, pp. 1–7.
- [11] S. Lakshmi and T. S. R. Raja, 2014. "Design and implementation of an observer controller for a buck converter," Turkish Journal of Electrical Engineering & Computer Sciences, pp. 562–572.
- [12] E. Lefeuvre, D. Audigie, C. Richard, and D. Guyomar, 2007. "Buck-boost converter for sensorless power optimization of piezoelectric energy harvester," in Power Electronics, vol. 22. IEEE, pp. 2018–2025.
- [13] O. Djamel, G. Dhaouadi, S. Youcef and M. Mahmoud, 2019. "Hardware Implementation of Digital PID Controller for DCDC Boost Converter," International Conference on Power Electronics and their Applications (ICPEA), pp. 1-4, doi: 10.1109/ICPEA1.2019.8911129.
- [14] L. Ardhenta, M. R. Ansyari, R. K. Subroto and R. N. Hasanah, 2020. "DC Voltage Regulator using Buck-Boost Converter Based PID-Fuzzy Control," Electrical Power, Electronics, Communications, Controls and Informatics Seminar (EECCIS), pp. 117-121, doi: 10.1109/EECCIS49483.2020.9263425.
- [15] T. Utomo, G. T. A. Wedangga and L. Ardhenta, 2020. "Sliding Mode Control based on Power Information of Boost Converter for Voltage Regulator," 2020 10th Electrical Power, Electronics, Communications, Controls and Informatics Seminar (EECCIS), pp. 37-42, doi: 10.1109/EECCIS49483.2020.9263442.
- [16] D. Chavan, A. D. Gundecha, K. A. Mahapatro, and P. V. Suryawanshi, 2019. "State and disturbance observer for robust motion control," in International Conference on Recent Trends on Electronics, Information, Communication & Technology. IEEE, pp. 1252–1256.
- [17] D. Ali, M. Asim, F. Wallam, Z. Qazi, A. Abbas and Y. Naudhani, 2019. "Experimental Testing of Observers Comprising Discrete Kalman Filter and High-Gain Observers," International Conference on Computing, Mathematics and Engineering Technologies (iCoMET), pp. 1-5, doi: 10.1109/ICOMET.2019.8673453.
- [18] G. Wang, M. Chadli and S. Mammar, 2020. "H_∞ memory observer design for vehicle suspension state estimation and unknown road reconstruction," Mediterranean Conference on Control and Automation (MED), pp.479-483, doi: 10.1109/MED48518.2020.9183121.
- [19] P. Wang, N. Li, X. Sun and C. Wang, 2020. "Deadbeat Predictive Current Control for PMSM Based on Improved Luenberger Observer," Chinese Control Conference (CCC), pp. 2373-2377, doi: 10.23919/CCC50068.2020.9189403.
- [20] J. Han, "From pid to active disturbance rejection control," in Industrial Electronics, vol. 56. Beijing: IEEE, 2009, pp. 900–906.
- [21] W. Bin, Y. Jun, W. Junxiao, and L. Shihua, 2014. "Extended state observer based control for DC–DC buck converters subject to mismatched disturbances," in Chinese Control Conference. Nanjing: IEEE, pp. 8080–8085.
- [22] S. Li and Z. Liu, 2009. "Adaptive speed control for permanent-magnet synchronous motor system with variations of load inertia," in Industrial Electronics, vol. 56. Nanjing: IEEE, pp. 3050–3059.

- [23] K. A. Mahapatro, A. D. Gundecha, A. D. Chavan, and P. V. Suryawanshi, 2019. "Disturbance rejection in motion control based on equivalent input disturbance approach with experimental validation," in International Conference on Recent Trends on Electronics, Information, Communication & Technology. IEEE, pp. 1247–1251.
- [24] Z. Ma, Y. Xiao, P. Wang and Y. Zhao, 2020. "Linear-Extended-State- Observer Based Pinning Control of Nonlinear Multi-Robots System," in IEEE Access, vol. 8, pp. 144522-144528, doi: 10.1109/ACCESS. 2020.3014399.
- [25] W. Shi, K. Liu and W. Zhao, 2021. "Active Vibration Isolation of a Maglev Inertially Stabilized Platform Based on an Improved Linear Extended State Observer," in IEEE Access, vol. 9, pp. 743-751, doi: 10.1109/ACCESS.2020.3046886.
- [26] G. K. Ottman, H. F. Hofmann, and G. A. Lesieutre, 2003. "Optimized piezoelectric energy harvesting circuit using Step-Down converter in discontinuous conduction mode," in IEEE Transactions on Power Electronics, vol. 18. IEEE, pp. 696–703.
- [27] Vulture, Piezoelectric Energy Harvestors, MIDE.
- [28] H. Sira-Ramirez and R. Silva-Ortigoza, 2006. Control Design Techniques in Power Electronics Devices. Springer-Verlag London limited.
- [29] J. Wang, S. Li, JunYang, BinWu, and Q. Li, 2015. "Extended state observer based sliding mode control for PWM-based DC–DC buck power converter systems with mismatched disturbances," in IET Control Theory and Applications, vol. 9. China: IET, pp. 579–586.



Shailesh S Shinde is Master's student in the Department of Electronics at MIT Academy of Engineering, Alandi (D), Pune, India. His research interests cover Uncertainty and Disturbance Estimation, Hybrid Renewable Energy Sources, Energy Scavenging.



Ashitosh Dilip Chavan is an Assistant Professor in the Department of Electronics and Telecommunication at MIT Academy of Engineering, Alandi (D), Pune, India. His thrust research interests cover robust control, sliding mode control (SMC) for dynamical systems, active disturbance rejection control (ADRC) for linear and nonlinear systems, uncertainty and disturbance estimation, observer designs, control law design of motion control and application in automotive domain. He is author and co-author of different research studies of journals, conference proceedings.



Dr. Aniket D. Gundecha is an Assistant Professor in the Department of Electronics and Telecommunication at MIT Academy of Engineering, Alandi (D), Pune, India. His research interests cover Uncertainty and Disturbance Estimation, Observer Designs, Active Disturbance Rejection Control for Linear and Nonlinear Systems, Hybrid Renewable Energy Sources, Energy Scavenging, Embedded Control Design for Control Systems. He has various publications in journals, conferences and book chapters of national and international repute.



Kaliprasad A Mahapatro is an Assistant Professor at Avantika University, Ujjain, MP. He is a researcher and academician with interest in Control System Design. Being a passionate researcher, Kaliprasad has published several papers in high indexed journal and conferences like IEEE, Springer etc. His primary research areas include, sliding mode control, active disturbance rejection control for linear and nonlinear systems, PID Control design and applications, control law design of energy scavenging from renewable energy sources.

Conferences > 2021 International Conference... ?

Signature Recognition Models: Performance Comparison

Publisher: IEEE [Cite This](#) PDF

Atharva Gadre ; Pradyumna Pund ; Gouri Ajmire ; Shubhangi Kale All Authors

16
Full
Text Views




Alerts

Manage Content Alerts

Add to Citation Alerts

More Like This


- A Novel Approach for Handwriting Recognition in Malayalam Manuscripts using Contour Detection and Convolutional Neural Nets
2018 International Conference on Advances in Computing, Communications and Informatics (ICACCI)
Published: 2018
- Rumour Detection Based on Graph Convolutional Neural Net
IEEE Access
Published: 2021
- Show More

Abstract	<div> Download PDF</div> <p>Abstract:In recent times Signature Verification has become an act of absolute necessity in the area of biometric verification. Unlike other verification problems, every small deta... View more</p> <p>► Metadata</p> <p>Abstract:</p> <p>In recent times Signature Verification has become an act of absolute necessity in the area of biometric verification. Unlike other verification problems, every small detail between genuine and forged signatures needs to be observed because a skilled forgery can only differ by only some specific kind of features of the real signature. The task of verifying signatures has become even harder in writing independent scenarios. In this paper, with the help of Siamese Network, VGG16 model and DEEP CNN models we have modeled a system that will verify signatures offline. Siamese networks use two images as input with shared weights, which can be trained to learn the features of both the images to find out the similarity between them. This is done by passing sets of similar and dissimilar images to the network so that it can learn to reduce the loss and Euclidean distance between similar images and increase it in dissimilar images. As for VGG 16, it is a pre-trained 16-layer model that is based on CNN, these 16 layers consist of max layer, pooling layers, and many more. CNN is simply a convolutional neural network on which both Siamese and VGG models are based. The performance analysis shows the VGG16 to have best accuracy about 85-90%, Siamese shows 65-70% and CNN shows 65-70% and the Siamese network to have the highest speed in identification.</p>
Document Sections	
I. Introduction	
II. Proposed Systems and Methodology	
III. Dataset	
IV. Pre-Processing	
V. Result (Performance Analysis)	
Show Full Outline	
Authors	
Figures	
References	
Keywords	
Metrics	



Smart Trends in Computing and Communications pp 619–627

Apriori Algorithm with Dynamic Parameter Selection and Pruning of Misleading Rules

[Aditya Veer](#) , [Mohit Gurav](#), [Shreyansh Dange](#), [Shubham Chandgude](#) & [Vaishali Wangikar](#)

Conference paper | [First Online: 26 October 2021](#)

287 Accesses

Part of the [Lecture Notes in Networks and Systems](#) book series (LNNS, volume 286)

Abstract

In the field of knowledge discovery in databases (KDD), the effectiveness of association rules is important. Association rules are a technique of data mining, wherein we identify the relationship between one item to another. For mining, the association rules Apriori algorithm is widely used. The idea of the Apriori algorithm is to find the frequent sets from a transactional database. Through the frequent sets, association rules are obtained, and these rules must satisfy the minimum confidence threshold. This paper presents an improved method for deciding an optimum



Advanced Data Mining Tools and Methods for Social Computing

Hybrid Computational Intelligence for Pattern Analysis

2022, Pages 107-125

Chapter 6 - A machine learning approach to aid paralysis patients using EMG signals

Manisha Choudhary ^a, Monika Lokhande ^a, Rushikesh Borse ^a, Avinash Bhute ^b

Show more ▾

Outline | Share | Cite

<https://doi.org/10.1016/B978-0-32-385708-6.00013-8>

[Get rights and content](#)

Abstract

This work focuses on hand movement classification from electromyography (EMG) signals using machine learning algorithms. The use of EMG signals for the human–human interface to move a paralyzed person is discussed. EMG signals are generated when the electric potential of the muscles changes after receiving signals from the brain due to the contraction or expansion of muscles. EMG signals were collected by connecting electrodes to a person's arm and they were recorded using the BYB Spike Recorder App. Features were extracted from these signals and a dataset was obtained using these features. Hand movement of the person using this dataset was classified using various algorithms like k-nearest neighbor (KNN), support vector machine, naive Bayes, and decision tree. All algorithms offered a promising accuracy of around 90%, except KNN, whose accuracy was 60%. Thus, they can be used to control movements of people with disabilities by a human–human interface.

[<](#) Previous

Next [>](#)

Keywords

EMG signals; Feature extraction; Machine learning; Human–human interface

[Recommended articles](#)

Cited by (0)

Copyright © 2022 Elsevier Inc. All rights reserved.



Copyright © 2022 Elsevier B.V. or its licensors or contributors.
ScienceDirect® is a registered trademark of Elsevier B.V.

RELX™

PAPER • OPEN ACCESS

Aqueous Two-Phase Separation (ATPS) Methods for Oleic acid extraction from Neem leaves

To cite this article: Shubham Gawade *et al* 2022 *IOP Conf. Ser.: Mater. Sci. Eng.* **1224** 012016

View the [article online](#) for updates and enhancements.

You may also like

- [Neoteric Media as Tools for Process Intensification](#)
C C Beh, R Mammucari and N R Foster
- [Liquid-liquid extraction of Pt\(IV\) from hydrochloric acid solutions using PPG 425 – NaCl – H₂O system](#)
I V Zinov'eva
- [Metallic and semiconducting carbon nanotubes separation using an aqueous two-phase separation technique: a review](#)
Malcolm S Y Tang, Eng-Poh Ng, Joon Ching Juan et al.

Aqueous Two-Phase Separation (ATPS) Methods for Oleic acid extraction from Neem leaves

Shubham Gawade, Sandeep P. Shewale and Amravati Gode

School of Chemical Engineering, MIT Academy of Engineering, Alandi (D), Pune, India-412105

Corresponding author's e-mail address: agode@mitaoe.ac.in

Abstract. The aqueous two-phase separation system (ATPS) signifies an environmentally responsible approach for the extraction of bioactive compounds from a plants basis, as it is a liquid-liquid fractionation technique centred on the inconsistency of two aqueous solutions. In this investigation, various experimental parameters are optimized as the speed of agitation (200, 300 400 and 500 rpm) and solvent ratio (1:1, 2:3 and 3:2) with 20 % (w/w) of Ammonium Sulphate (AMS) salt composition and 30 % (w/w) of Polyethelyene Glycol (PEG). The obtained extract contains alkaloids, flavonoids, tannins, glycosides, acids and total phenolic compounds (TPC). The extracted Oleic acid by the ATPS method was measured with gallic acid equivalent (GAE) of TPC extracted from neem leaves powder. The determined concentration of oleic acid in the practice of TPC is 8.033 mg of GAE/g from the optimized experimental parameter. The optimized results can be cast off for a commercial process on an industrialized scale. Also, the mathematical modelling investigation was done to intent the critical impeller speed (Njs) with the Zwittering model. The identified model calculates the essential speed of agitation (rpm) for maximum extraction yield.

Keywords: Oleic acid, Total phenolic compounds (TPC), Aqueous Two-Phase Separation System (ATPS), Gallic Acid Equivalent (GAE), Critical Impeller Speed (Njs).

1. Introduction

Herbs are used for flavouring, food, medicine, or perfume from ancient times. Culinary use naturally differentiates herbs are implying the leafy green portions of spice also a product from a different part of the plant containing seeds, roots, bark, and fruits. Furthermore, medicinal contents available in the plant's parts are used for the production of some pharmaceutical products such as aspirin, colchicine, ephedrine, morphine, physostigmine, pilocarpine, quinidine, reserpine and vincristine, etc [1-2]. The approach of isolating the bioactive components from the medicinal plants and used for the manufacturing of some pharmaceutical products are becoming prominent. Generally, organic solvents such as methanol, ethanol and diethyl ether are usually helped for extracting the bioactive compounds as of plant basis by the outmoded extraction arrangements. These solvents are relatively expensive,



needs distinctive processing conditions and most importantly disposal of the solvents is a major concern as they are not environmental responsive [3].

Conventional extraction processes are time-consuming and need more solvent for carrying out an operation, also after extraction, the added cost of purification and solvents recovery makes the process uneconomical.

Whereas, ATPS two-stage extraction is developing as a successful and flexible green system for the downstream handling of biomolecules. Fluid two-stage frameworks are low unpredictability frameworks with high adaptability [4]. That is, an expansive assortment might be acquired utilizing substances that pursue the Green Chemistry guideline on ecotoxicity, biodegradability, bioaccumulation and constancy, limiting waste and amplifying yields. Furthermore, they conform to the guideline of changeover of naturally safe structures to permit work under air weight. Since the 1970s numerous classified and out examinations have announced the filtration of proteins and other biologic materials utilizing ATPS, and numerous specialists have considered different operations of ATPS for the extraction and cleaning of organic products [5]. However, the utilization of such frameworks for the recuperation of phenolic mixes from plant materials is extremely constrained. In addition, there is broad writing about the thermodynamic properties of ATPS be that as it may, to the best of our insight, their application to crude unpurified examples has been very constrained [6].

Subsequently, the late nineteenth-century fluid two-phase extraction has been identified to the entire world. Aqueous two-phase can be framed through an extensive diversity of characteristics or else engineered water-solvent polymers& salt blends [7]. Watery two-phase extraction is developed for protected, sparing partition and cleaning of biomolecules, for example, proteins and catalyst extraction. Fluid extraction has numerous favourable circumstances; it is biocompatible, has low interfacial surface pressure among stages and it has high water content, the procedure can incorporate and the ability for strengthening [8-9].

Likewise, the level of corruption for biomolecules is low. In any case, two-polymer and polymer-based salt frameworks have developed quickly and a considerable measure of effort has been placed keen on concentrate this strategy utilizing these sorts of aqueous two-phase separation systems (ATPS). Aqueous two-phase extraction is known as an operative, adaptable and significant developing green method for the subsequential treating of biomolecules. This strategy has points of interest completed traditional extraction systems similar to, simplicity of scaling-up, condition benevolent, minimal effort, fit for nonstop activity and is effective for some sorts of trials exceptionally for the fixation and refinement of biomolecules. The utilization of partiality in ATPS can affect the developed recuperation earnings and developed refinement bends of bio consistent items such as it is an essential phase recuperation strategy [10]. Water as the foremost constituent of together stages in ATPS practices a moderate setting for bioactive molecules to distinct and polymers steady to the assembly and biotic doings through further liquid-liquid extraction approaches could impairment natural goods since of the development circumstances and biological solvents such method reduces the purity of active ingredient present in the extract.

There are two fundamental sorts of ATPS: polymer-polymer and polymer-salt frameworks. The mind-boggling expense of some shaping stage polymers (e.g dextran) limits the use of these frameworks, just legitimized when the expense of the result of intrigue is extensive. Consequently, the choice of the more temperate polymer-salt frameworks is profoundly suggested [10-11].

The novelty of the proposed work is that during the extraction itself two different layers of aqueous solution and salt is obtained, which can help further to reduce the cost of separating components. Also, the systems can be designed by partying a diversity of components in water and two-polymer and polymer-salt systems have developed quickly. The said work majorly focuses on the extraction of oleic acid from neem leaves to powder using ATPS (water + polymer + salt) based on PEG and ammonium sulphate. The aim is to optimize various experimental parameters (time, ATPS composition, particle size) for the removal of Oleic acid from neem leaves powder and its additional practices as natural antioxidants.

2. Material and Methods

The Neem powder was obtained from Hari Parshuram Aushdhalya, Pune., Polyethelyene Glycol (PEG) was procured from SRL Chemicals Pvt Ltd, Mumbai. Folin Ciocalteu's reagent was procured from Qualigens Fine Chemicals, Mumbai. Ammonium Sulphate (AMS) was procured from S.D. Fine Chemicals Pvt Ltd, Mumbai.

2.1. Batch extraction

Batch extractions are a modest method for the extraction of bioactive compounds. The stages in this method are equipped with a 50 ml glass reactor with a four-bladed glass turbine impeller and the combination to be divided is supplementary. Subsequently collaborating, phase parting is proficient each by resolving below gravity. The stages are disconnected and investigated to improve the alienated constituents of the preliminary mixture. The object product would be focused at any of the stages and the pollutants in the additional form. In various cases, reclamation and attentiveness of the product that produces beyond 90% can be attained with a particular extraction stage.

One particular phase removal does not give adequate retrieval, recurrent extractions can be supported obtainable in a sequence of communicating and parting components [12]. The fluid dividers into two stages, each covering added 80% liquid. When basic biomolecules are supplementary to these combinations, biomolecules and cell wreckages are dividers among the stages; by choosing suitable circumstances, cell remains can be limited to one stage as the object bioactive molecule barriers. The segregating of biomolecules among segments mostly be contingent on the equilibrium connection of the arrangement. The partition coefficient is demarcated as [12-13].

$$K = \frac{C_{AT}}{C_{AB}}$$

Where C_{AT} is the equilibrium attentiveness of constituent A in the upper phase and C_{AB} is the equilibrium adsorption of A in the lesser phase. If constituent A helps the greater stage the worth of K will be better. In numerous aqueous arrangements, K is continual finished with an extensive collection of deliberations, as long as the molecular possessions of the stages are not transformed. The theoretic yield in the topmost stage, Y_T , can be premeditated relative to the capacity ratio of the stages, R (up to volume / below volume), and the partition coefficient K of the object molecule as follows [12-13]:

$$Y_T = \frac{V_T C_{AT}}{V_O C_O} = \frac{V_t C_{AT}}{V_t C_{AT} + V_B C_{AB}} = \frac{1}{1 + [\frac{1}{KR}]}$$

Similarly, the theoretic yield in the bottommost stage, Y_B is known by,

$$Y_B = \frac{1}{1 + [\frac{1}{KR}]}$$

Consequently, by changing anyone like K or R we can effortlessly upsurge or reduction the profit of the object particle [14]. Additional constraint recycled to describe two-phase partitioning is the concentration factor, δ_c , distinct as the ratio of produce attentiveness in the favoured stage to the original product attentiveness.

$$\delta_{C,T} = \frac{C_{AT}}{C_{Ao}} \quad (\text{Product partitions to the higher phase})$$

$$\delta_{C,B} = \frac{C_{AB}}{C_{Ao}} \quad (\text{Product partitions to the lower phase})$$

2.2. Determination of the binodal

By settlement, the constituent mainly in the lower layer is represented as abscissa and the predominant element in the upper stage is represented as ordered. The three systems are explained realistically.

2.2.1 Turbidometric titration

In the tubing, with suitable backup solutions, formulate systems through different configurations of recognized weight. Note the added size due to titration, for example, if 5 g methods are organized, use 10 ml tubes. As an example, shows the systems for different systems that can use PEG-phosphate and PEG-dextran, and the essential designs. This can be replicated in a worksheet to permit easy intention. Note down the mass of the tube and titration drop by drop, with suitable dilution till the scheme is zeroed, i.e., a stage is formed.

This can be done through the scheme is continuously mixing or accumulation a droplet, collaborating, adding a second drop and continues the same process. To confirm that it has formed a single-stage system, the schemes must be centrifuged (for example 1000-2000 g, 5 min). Record the concluding mass of the tube and estimate the mass of the additional dilution just before the formation of a phase. Since the number of graduate systems is relative to the total of points in the binodal, superior precision is obtained with a superior number of schemes [15].

2.2.2 Cloud point method

Balance 5 g of a standard solution of constituent X into a 25 ml narrowed flask. Then add drop by drop, a reserve solution of the Y component up to the principal indication of turbidity, which is the cloud point. Note the weight of the Y component necessary for the mixture to become cloudy. This provides the first point in the binodal. Also, add a known weight of diluent lower the cloud point and duplication as indicated [15-16].

2.2.3 Determination of the Tie line

Measuring the connection line for polymeric schemes comprising an optically active composite, for example, PEG-dextran, PEG-Ficoll and ethylene oxide-propylene as well as oxide-Reppal PES 100.

2.2.3.1 Polymeric Methods Comprehending One Optically Active Polymer

Formulate a standard curve for the lively constituent, in the variety of 0 to 10% (p / v), i.e. inside the linear series, through the identical sections arrange a second standard curve for the refractive measure of the index. If the scheme is arranged in a shield, the average curves for the clean constituents must be completed with a similar safeguard, since the salts similarly subsidize the refractive index. Get ready the phased scheme for investigation, assembly sure that the phase components mix well; let the phases separate.

To ensure complete separation, centrifuge at low speed (for example 1000-2000 g, 5 min). The system proportions should be appropriate to permit deduction of at least 5 g upper and lower stage for phase concentration investigation and an additional quantity for density extents. Distinct the higher and subordinate stages building certain not to origin stage relations. Make the suitable dilutions, for example, watery 5 g of phase with the suitable solvent to 25 ml in a volumetric container. Extend the visual revolution for every stage and estimate the individual concentrations. The concentration of another constituent is resolute by determining the refractive index of the developed and subordinate stage and deducting the influence of the refractive index acquired from the optically lively constituent [17].

2.2.3.2 Polymer-Salt Systems

Formulate a standard curve aimed at salt conductivity within the linear series (in% w / v). Arrange the stage schemes as indicated above and eliminate 5 g of samples of the higher too subordinate phases and

diluted with liquid and lyophilized, then note the dehydrated weight. Eliminate an additional section from the higher and subordinate stage, diluted with water and extent the conductivity of every stage. Estimate the salt absorption and deduct the mass involvement of the dehydrated mass of the section [16-18].

3. Results and Discussion

In this investigation, various experimental parameters were optimized such as speed of agitation (200 rpm, 300 rpm, 400 rpm & 500 rpm) and solvent ratio (1:1, 2:3 and 3:2). Extract samples were pipette out at specific time intervals like every 15 min and further standard Folin–Ciocalteu's method was used for analysis purposes. The obtained outcomes indicated that the TPC concentration of TPC in the extraction stage at a specific time. By changing the parameters speed of agitation and solvent ratio in the batch reactor at different times the results were optimized and used for further study.

3.1 Speed of agitation

About 5 g of powder of neem leaves was weighted and fed to 50 ml of batch reactor along with AMS salt (20 %w/w) and 50 ml of PEG (30 %w/w) at a temperature of 30°C till the extraction rate was a steady-state. The maximum speed of agitation produces high turbulence in the batch reactor and increases the rate of mass transfer [11]. The results of various experiments were performed for multiple agitation speeds is shown in figure 3.1 The experimental results shows that the concentration of TPC at 200 rpm significantly low as compared to 500 rpm, but there could be a marginal difference of TPC concentration of 400 and 500 rpm, speed of agitation., therefore for the further study, speed of agitation (400 rpm) was used. The circulation of TPC compounds from the neem leaves powder in the solvents could expand with the accumulative agitation speed. An added rise in the agitation speed has no substantial effect on final extraction yield; it clues that external mass transfer fighting is inconsequential at 400 rpm

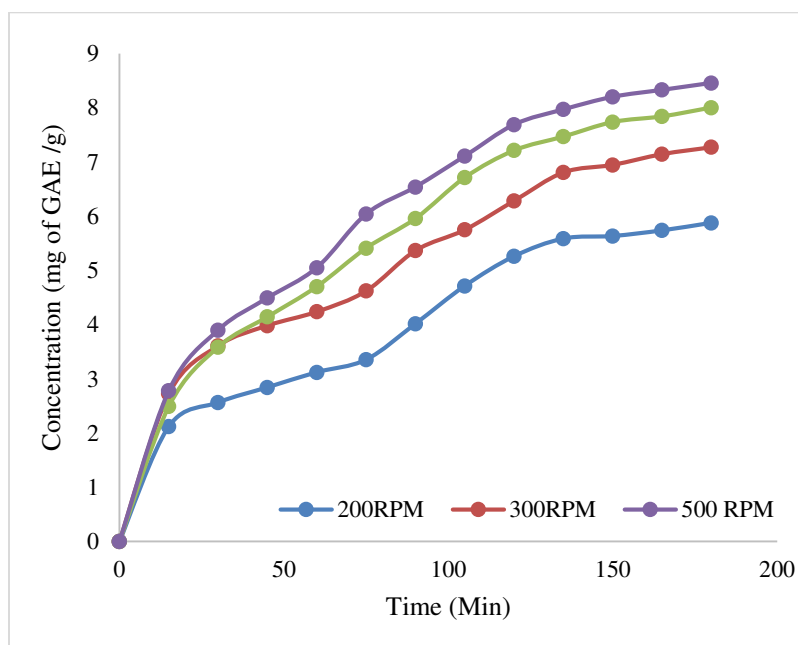


Fig. 3.1 Concentration of TPC obtained from Batch at temp 30°C speed of agitation 200, 300, 400 & 500 rpm)

3.2 Effect of Solvent Ratio (AMS: PEG)

The TPC concentration values in the extract were considered for changed extraction times at different solvent ratios (1:1, 2:3 & 3:2) and the same is shown in Figure 3.2. About 5 g of powder of neem leaves

was weighted and fed to 50 ml of batch reactor along with AMS salt (20 %w/w) and 50 ml of PEG (30 %w/w) at a temperature of 30°C till the extraction rate was a steady-state. There was an increase in TPC concentration and experiential for solvent ratio 01:01. A substantial quantity of solvent favours an additional concentration gradient and cuts diffusional resistance that rises the rate of extraction rate. There was a rise in TPC concentration, for the solvent ratio of 1:1 to 3:2. A substantial quantity of solvent tends to the added concentration gradient and drops diffusional resistance that rises the rate of extraction [11].

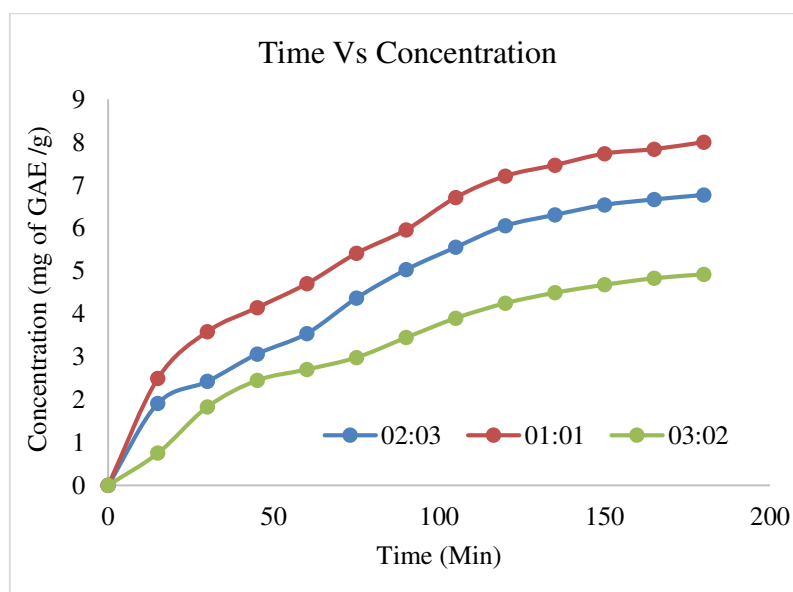


Fig.3.2 Effect of Solvent Ratio (AMS: PEG)

4. Conclusion

The investigation of the ATPS method was beneficial for the sub sequential treating of biomolecules. Also, the experimental parameters were optimized such as speed of agitation and solvent ration and the optimized parameters as 400 rpm and 01:02 solvent ration respectively with AMS salt (20 % w/w) & PEG (30 % w/w). The obtained extract also contains alkaloids, flavonoids, tannins, glycosides, acids and total phenolic compounds (TPC). The extracted Oleic acid by ATPS technique was measured with gallic acid equivalent (GAE) of TPC extracted from neem leaves powder. The determined concentration of oleic acid in the practice of TPC is 8.033 mg of GAE/g from the optimized experimental parameter. The optimized results can be used for a commercial process on an industrial scale.

References

- [1] Alasalvar C, Karamac M, Amarowicz R, Shahidi F, 2006. Antioxidant and antiradical activities in extracts of hazelnut kernel (*Corylus avellana* L.) and hazelnut green leafy cover. *J Agric Food Chem* 54: 4826-4832.
- [2] Babitskaia V, Shcherba V, Lkonnikova N, 2000. Melanin complex of the fungus *Inonotus obliquus*. *Prikl Biokhim Mikrobiol* 36(4): 439-444.
- [3] Dallora N, Klemz J, Filho P, 2007. Partitioning of model proteins in aqueous two-phase systems containing polyethylene glycol and ammonium carbamate. *Biochem Eng J* 34(1): 92-97.
- [4] Karakatsanis A, Liakopoulou M, 2007. Comparison of PEG/ fractionated dextran and PEG/industrial grade dextran aqueous two-phase systems for the enzymic hydrolysis of starch. *Eng* 80(4): 1213-1217.
- [5] Alencar L.V.T.D., Passos L.M.S., Martins M.A.R., Barreto I.M.A., Soares C.M.F., Lima A.S., Souza R.L., 2020. The complete process for the selective recovery of textile dyes using an

aqueous two-phase system. *Sep. Purif. Technol.* 253: <https://doi.org/10.1016/j.seppur.2020.117502>.

- [6] Ying H, Diyun C, Shuqi C, Minhua S, Yongheng C, Yixiong P, Gutha Y, 2021. A green method for recovery of thallium and uranium from wastewater using polyethylene glycol and ammonium sulfate based on the aqueous two-phase system. *J. Clean. Prod.* 297: <https://doi.org/10.1016/j.jclepro.2021.126452>.
- [7] Leitner M, Vandelle E, Gaupels F, Bellin D, Delledonne M, 2009. NO signals in the haze: Nitric oxide signalling in plant defence. *Curr Opin Plant Biol* 12(4): 451-458.
- [8] Liu SP, Zong ZM, Wei Q, Wei XY, 2010. Study on organic compounds in aqueous two phase system phase forming and distribution. *Chem Ind Times* 24(12): 21-24.
- [9] Ahareh AS, Gholamreza P, Javad RS, Shahla S, Naghmeh H, 2020. Separation of erythromycin using aqueous two-phase system based on acetonitrile and carbohydrates. *Fluid Phase Equilib.* 505: <https://doi.org/10.1016/j.fluid.2019.112360>
- [10] Perla JV, Salvador VG, Iran AT, Yolanda SM, Leticia GC, Artemio PL, Diana GR, 2020. Separation of bioactive compounds from epicarp of 'Hass' avocado fruit through aqueous two-phase systems. *Food Bioprod. Process.* 123:238-250.
- [11] Sandeep Shewale & Virendra K. Rathod (2018) Extraction of total phenolic content from *Azadirachta indica* or (neem) leaves: Kinetics study, Preparative Biochemistry & Biotechnology, 48:4, 312-320, DOI: 10.1080/10826068.2018.1431784
- [12] Singh SB, Jayasuriya H, Dewey R, Polishook JD, Dombrowski AW, Zink DL, Guan Z, Collado J, Platas G, Pelaez F, Felock PJ, Hazuda DJ, 2003. Isolation, structure, and HIV-1 integrase inhibitory activity of structurally diverse fungal metabolites. *J Ind Microbiol Biotechnol* 30(12): 721-731.
- [13] Srinivas ND, Barhate RS, Raghavarao KSMS, 2002. Aqueous two-phase extraction in combination with ultrafiltration for down-stream processing of *Ipomoea peroxidase*. *J Food Eng* 54(1): 1-6.
- [14] Uma DB, Ho CW, Wan Aida WM, 2010. Optimization of extraction parameters of total phenolic compounds from Henna (*Lawsonia inermis*) leaves. *Sains Malaysiana* 39(1): 119-128.
- [15] Wang SY, Wu JH, Cheng SS, Lo CP, Chang HN, Shyur LF, Chang ST, 2004. Antioxidant activity of extracts from *Calocedrus formosana* leaf, bark, and heartwood. *J Wood Sci* 50: 422-426.
- [16] Zhao YX, Miao KJ, Zhang MM, Wei ZW, Zheng WF, 2009. Effects of nitric oxide on production of antioxidant phenolic compounds in *Phaeoporus obliquus*. *Mycosystema* 28(5): 750-754.
- [17] Zheng WF, Zhao YX, Zhang MM, Wei ZW, Miao KJ, Sun WG, 2009. Oxidative stress response of *Inonotus obliquus* induced by hydrogen peroxide. *Med Mycol* 47: 814-823.
- [18] Zheng WF, Miao KJ, Liu YB, Zhao YX, Zhang MM, Pan SY, Dai YC, 2010. Chemical diversity of biologically active metabolites in the sclerotia of *Inonotus obliquus* and submerged culture strategies for up-regulating their production. *Appl Microbiol Biotechnol* 87(4): 1237-1254.



Gavin Publishers is an international open access journal publisher peer reviewed articles.

AIP

Conference Proceedings

HOME

BROWSE

MORE ▼

[Home](#) > [AIP Conference Proceedings](#) > [Volume 2417, Issue 1](#) > [10.1063/5.0072779](#)

< PREV

NEXT >



No Access

Published Online: 19 October 2021

CFD analysis of exhaust pipe of a diesel engine

AIP Conference Proceedings **2417**, 060002 (2021); <https://doi.org/10.1063/5.0072779>Pawankumar Yadav^{a)} and Pramod Kothmire^{b)}[View Affiliations](#)[View Contributors](#)

Topics ▼

ABSTRACT



PDF



E-READER

PAPER • OPEN ACCESS

Rectangular and Square Cross-Sections Microchannel Heat Sink CFD Simulation and Analytical Validation Using Liquid Water & Water-Aluminium Oxide Nanofluid as a Cooling Medium

To cite this article: Saurabh Narayan Pawar *et al* 2021 *IOP Conf. Ser.: Mater. Sci. Eng.* **1145** 012093

View the [article online](#) for updates and enhancements.

You may also like

- [Mono and hybrid nanofluid based heat sink technologies - A review](#)
A Chandravadhana, V NandaKumar and K Venkatramanan
- [Role of 1,2-benzisothiazolin-3-one \(BIT\) in the Improvement of Barrier CMP Performance with Alkaline Slurry](#)
Tengda Ma, Baimei Tan, Yuling Liu et al.
- [CFD Simulation and Analytical Validation of Rectangular and Square microchannel heat sink with liquid water as cooling medium](#)
Saurabh Narayan Pawar and Nilesh Balkishanji Totla

Retraction

Retraction: Rectangular and Square Cross-Sections Microchannel Heat Sink CFD Simulation and Analytical Validation Using Liquid Water & Water-Aluminium Oxide Nanofluid as a Cooling Medium (*IOP Conf. Ser.: Mater. Sci. Eng.* **1145 012093)**

Published 23 February 2022

This article (and all articles in the proceedings volume relating to the same conference) has been retracted by IOP Publishing following an extensive investigation in line with the COPE guidelines. This investigation has uncovered evidence of systematic manipulation of the publication process and considerable citation manipulation.

IOP Publishing respectfully requests that readers consider all work within this volume potentially unreliable, as the volume has not been through a credible peer review process.

IOP Publishing regrets that our usual quality checks did not identify these issues before publication, and have since put additional measures in place to try to prevent these issues from reoccurring. IOP Publishing wishes to credit anonymous whistleblowers and the [Problematic Paper Screener](#) [1] for bringing some of the above issues to our attention, prompting us to investigate further.

[1] Cabanac G, Labbé C and Magazinov A 2021 arXiv:[2107.06751v1](#)

Retraction published: 23 February 2022



Content from this work may be used under the terms of the [Creative Commons Attribution 3.0 licence](#). Any further distribution of this work must maintain attribution to the author(s) and the title of the work, journal citation and DOI.

Published under licence by IOP Publishing Ltd

Rectangular and Square Cross-Sections Microchannel Heat Sink CFD Simulation and Analytical Validation Using Liquid Water & Water-Aluminium Oxide Nanofluid as a Cooling Medium

Saurabh Narayan Pawar¹ Jugal Shrinivas Makam¹ Nilesh Balkishanji Totla²

¹Student, MIT Academy of Engineering, Pune, India.

²Sr Assistant Professor, MIT Academy of Engineering, Pune, India.

¹snpawar@mitaoe.ac.in ²jsmakam@mitaoe.ac.in, ³nbtotla@mech.maepune.ac.in

Abstract. In this study, cooling performance of copper material based microchannel heat sink was investigated using two different approaches which are CFD and Analytical. Microchannel heat sink with two different cross-sectional geometries of rectangular and square was considered for the present study. In the present work CFD simulation is carried out using two different cooling fluids which are liquid water and water- Al_2O_3 nanofluid. Nanofluid volume fraction of 0.3% was used for present study. Re number in between 200-1000 was used for the present study. For CFD simulation purpose heat sink of dimension of $25.4\text{mm} \times 25.4\text{mm} \times 2.384\text{mm}$ is considered in the study. Boundary condition of constant heat flux is assumed by providing heat flux at constant rate at bottom of the assembly. To compare between square and rectangular cross section microchannel heat sink, the hydraulic diameter is kept same in both the cases and CFD simulation was conducted. With using water- Al_2O_3 nanofluid as the working fluid the rectangular cross section is showing better performance in terms of cooling as compare to the square cross section. Drop in pressure results in rectangular section calculated using water Al_2O_3 nanofluid using both CFD and Analytical approach are in good agreement with difference of 13.4%

Keywords: Computational fluid dynamics, Heat transfer, Microchannel heat sink, ICEM-Fluent CFD.

1. Introduction

In this modern era, use of smaller and compact devices has been increased tremendously. Modern computers that uses smaller electronic devices is the best example of it. Along with using this device, the problem of dissipation of heat has been increased also as if it is not removed then it might damage the component. Many researchers have presented their work regarding effective heat transfer and faster cooling of these devices so as to protect these devices using microchannels and minichannels. Microchannel and minichannel heat sink study has been carried out in various literature using different working fluids and different geometries for investigating the cooling performance and enhancing the heat transfer rate. [1] presented thermodynamic investigation results in circular tube for fully developed turbulent forced convection with water- Al_2O_3 nanofluid using entropy generation minimization method. Volume fraction of nanofluid in range of 0% to 6% was used and Reynolds number ranging from 5000 to 180000 were used. Using velocity and temperature fields obtained during CFD analysis the entropy



generation rates were numerically determined. It has been proved that at each Reynolds number there is a cross sectional area which is optimum for which there is minimum entropy generation in tube and as with increase in Reynolds number the optimal area of cross section increases. [2] investigated nanofluid application on the system of parabolic trough collector. Using Al_2O_3 /synthetic oil nanofluid and using Finite Element Method the multifield coupling simulation of PTC system was implemented for performance investigation. The Al_2O_3 particle concentration effects on PTC system were also studied. Good agreement was observed between experimental data and numerical results. Using Al_2O_3 /synthetic nanofluid there is a great reduction in absorber maximum temperature and temperature gradient. [3] explored effects of various aspects which include heat source/sink location, number of tubes, average Nusselt number, Rayleigh number, volume concentration. By employing Finite Volume based control volume technique, governing equations are numerically solved. In the studied cavity, considerable enhancement in heat transfer was observed using nanofluids. [4] presented numerical study results of parabolic trough solar collector of high concentration ratio on the thermodynamic and thermal performance. In this study, 80° rim angle and 113 concentration ratio parabolic trough system was used. The thermal physical properties temperature dependency have been considered for both copper nanoparticles and base fluid. The combination of CFD and Monte-Carlo ray tracing procedures was used in numerical analysis. [5] numerically investigated different microstructures microchannels with forced convection heat transfer. In microstructural grooves vortices will appear. Using Nusselt number the microchannel geometries influence on performance of heat transfer was evaluated. The highest heat transfer performance was possessed by microstructure with V shaped groove.

[6] investigated numerically forced convection heat transfer of laminar flow in corrugated channel of trapezoidal section using copper water nanofluid. The Reynolds number ranging between 100 to 700 and volume fraction of nanoparticles in range of 0% to 5% was considered. The geometrical parameter effects like corrugated channel wavelength and amplitude have been presented. It was observed that with increasing volume fraction of nanoparticles the average Nusselt number increases with increase in pressure drop. [7] studied microchannel and minichannel using single phase liquid flow. Microscale liquid flow fundamental issue was addressed by author and relation for single phase liquid flow pressure drop calculations were given. Researchers in [8] conducted investigation experimentally and explored conventional sized channel based classical correlation validity for predicting single phase flow thermal behaviour in rectangular microchannel. Width of microchannels considered ranged between $194\mu m$ to $534\mu m$. Deionized water was used for analysis with Reynolds number ranging from 300 to 3500. Classical and continuum approach based numerical predictions and experimental data were found to be in good agreement with showing 5% of average deviation. [9] used three nanofluid types namely carbon nanotubes-Ga, copper-Ga, diamond-Ga and carried out natural convection investigation of enhancement of heat transfer and generation of the entropy in cavity which is differentially heated. In this volume fraction of nanofluids is in between 0.01 to 0.15. Model of two-phase mixture is used for simulation of the nanofluid flow. Results showed that with Grashof number increment local entropy generation, heat transfer and convective intensity increases. [10] studied numerically heat transfer and analysis of fluid flow in channel having blocks at bottom wall. Nanofluid is used in this study. Channel inlet temperature of fluids are taken less than walls. Using control volume approach the governing equations are solved numerically. Results concluded that by using blocks on hot walls and using nanoparticles there is enhancement in channel heat transfer. By simulation, upto 60% enhancement in channel heat transfer is shown due to nanoparticles and blocks.

[11] investigated experimentally Foam/NEPCM composite heat transfer with phase change with foam porosity effect consideration. 47° Wall temperature reduction is provided which is maximum by Foam/NEPCM composite as compared to pure NEPCM. [12] employed CFD approach and studied serpentine tube heat exchanger for thermo hydraulic performance extensive exploration. The volume flow rates in the range of 1L/min to 5L/min was used. The Al_2O_3 /water based nanofluid influence was broadly studied on thermo hydraulic performance using 1%, 3% and 5% nanoparticles concentrations. Higher performance of heat transfer was provided as compared to other cases using low to high serpentine tube. At the expense of pressure drop which is negligible the higher coefficient of heat transfer

was provided using nanoparticles which are highly concentrated. [13] showed that by swirl flows, vortices and thermal boundary layer subsequent breaking the heat exchanger thermal efficiency is augmented by vortex generator. For this numerical study which is 3D validated vortex generator of triangular winglet type is selected. Working fluids which are air, water and nanofluids of two different types are analyzed with vortex generator which is non-central. [14] showed that less important role is played by O_2 and SO_2 in water and MEA losses than evaporation. For capturing CO_2 ionic liquids at room temperature are proposed potential candidates recently. IL to MEA aqueous solution addition reduced MEA and water losses. [15] stated that in many industrial applications the essential tool is surface cooling. In enhancement of heat transfer the important factor is area of the wetted surface utilization effectively. The vortex generator surface texture effects on vortex dynamics and heat transfer are studied, with pressure drop which is minimal the surface temperature found to reduce by vortex stretching. [16] have presented their work in microchannel heat sink using microchannel with rectangular and square cross section keeping the hydraulic diameter same in both of the cross sections. Liquid water was used as a cooling medium. As comparing with microchannel with square cross section, the better cooling performance was shown by rectangular cross section. In the present study, microchannel heat sink with rectangular and square cross section are considered and studied using two different types of fluid which are liquid water and water- Al_2O_3 nanofluid of 0.3% volume fraction. Using CFD approach both the cross sections are compared using both of the cooling fluids.

2. Physical Model & CFD Simulation

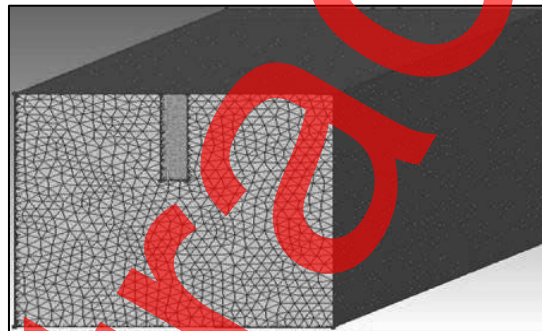


Figure 1. Rectangular microchannel heat sink model with meshing

CFD is a tool which is used to solve many engineering problems which involves fluid flow and heat transfer. CFD stands for Computational Fluid Dynamics. To get the heat sink machining was done on square block of copper with dimensions of 25.4 length, 25.4mm width and 70mm height. Now the dimension of rectangular section are considered to be 25.4mm length (L), 25.4mm width (W) and 2.384mm height (H) for CFD analysis in the present study. The rectangular section dimensions are same as that in [8]. There are N=10 straight parallel rectangular cross section microchannels in microchannel heat sink block same as that used in [8], but in the present study for CFD work, one rectangular cross section was considered and analysis was conducted as shown in Figure 1. The results obtained by CFD analysis of the rectangular and square heat sink was studied by using same hydraulic diameter in both the cases. The cooling fluids used in both the cases were liquid water and water- Al_2O_3 nanofluid of 0.3% volume fraction. The results of both the cross sections were compared using two cooling fluids mentioned. Re number was considered from 200 to 1000 for both of the cross sections.

Table 1. Dimensions of Rectangular and Square cross sections

Microchannel Dimensions	D_h	Height	Width
Rectangular	0.318 mm	$H_r=0.884$ mm	$W_r=0.194$ mm
Square	0.318 mm	$H_s=0.318$ mm	$W_s=0.318$ mm

The dimensions and notations used in table 1. Are same as those which were used in [16]. As shown in Figure 1. The fluid flows from inlet to outlet through the rectangular cross section microchannel. Constant heat flux was provided at bottom of the heat sink so that heated assembly temperature was brought down by cooling fluid by increment in temperature of cooling fluid from inlet to outlet. Using ICEM-CFD module the meshing of the assembly was done. Using GSF of 6 and tetra/mixed mesh type meshing was done. GSF stands for global scale factor. Fluent_V6 output solver and ANSYS solver was used. Keeping mesh density same the solid and fluid zones were meshed. The ICEM output was used and then using fluent software further analysis was done. It used navier stokes equation to solve the problem related to heat transfer and fluid flow. While analysis viscous laminar flow was selected and energy equation was kept on. Copper was selected as solid material.

3. Boundary conditions and assumptions:

1. Single phase laminar flow was used.
2. Working fluid and solid properties were treated as constant.
3. Three dimensional steady state fluid flow was considered.
4. Velocity values of 0.8149m/s, 1.6298m/s, 2.444m/s, 3.2596m/s, 4.0745m/s were obtained for Reynolds number of 200, 400, 600, 800, 1000 respectively using water- Al_2O_3 nanofluid of 0.3% volume fraction.
5. Outlet pressure was considered to be 0 Pa gauge with pressure outlet condition.
6. 450000 W/m^2 heat flux was provided at bottom.
7. Insulation was considered at assembly top surface.

The further analysis was done using CFD post processing section.

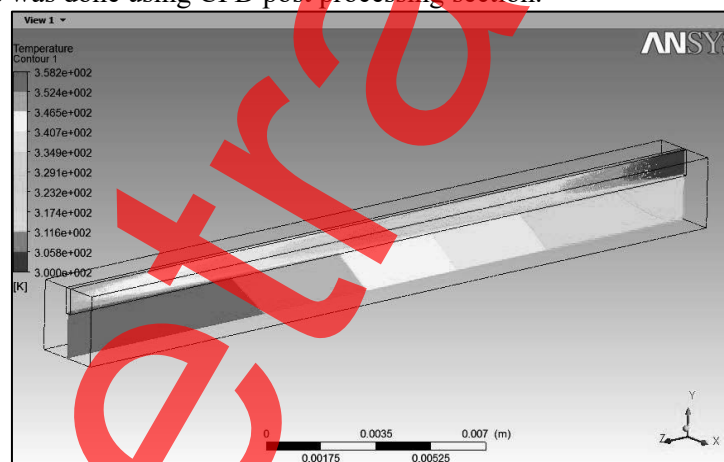


Figure 2. Temperature variation in rectangular cross section microchannel at 200 Reynolds number using water Al_2O_3 nanofluid of 0.3% volume fraction

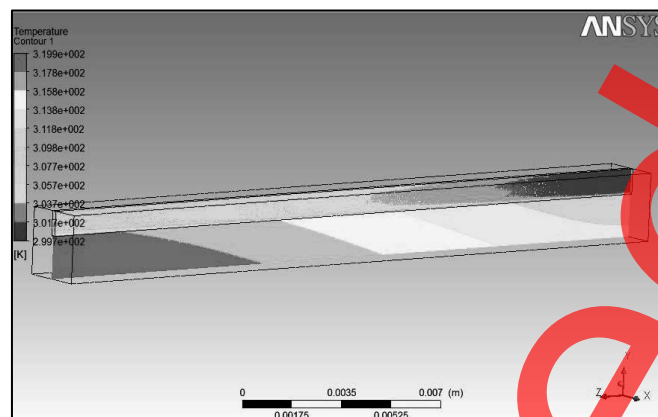


Figure 3. Temperature variation in rectangular cross section microchannel at 1000 Reynolds number using water- Al_2O_3 nanofluid of 0.3% volume fraction

Figure 2 and Figure 3. Represent temperature variation in rectangular cross section microchannel. As heat flux at constant rate was supplied at bottom of the assembly the assembly gets heated which is cooled by the working fluid flowing from inlet to outlet through the rectangular microchannel.

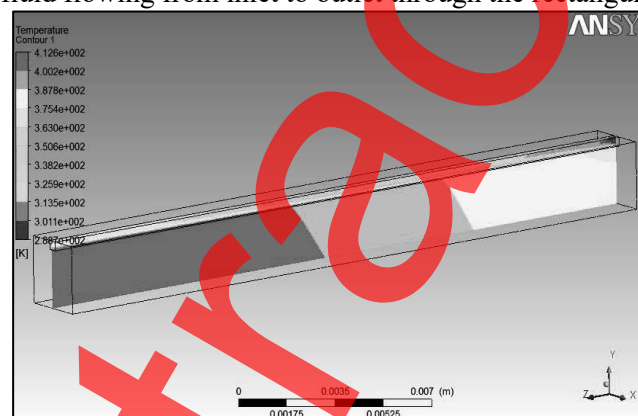


Figure 4. Temperature variation in square cross section microchannel at 200 Reynolds number using water Al_2O_3 nanofluid of 0.3% volume fraction

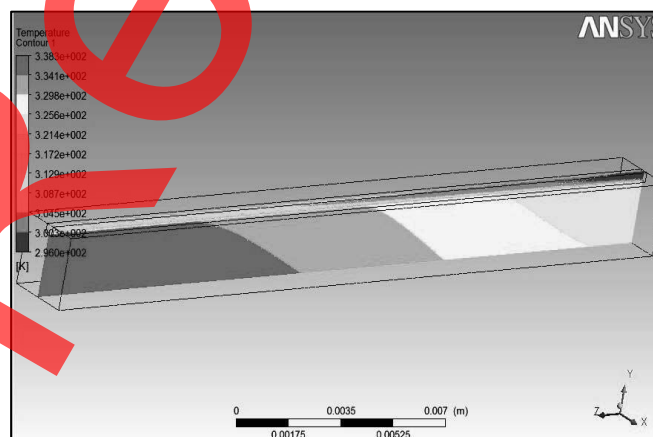


Figure 5. Temperature variation in square cross section microchannel at 200 Reynolds number using water- Al_2O_3 nanofluid of 0.3% volume fraction

Figure 4 and Figure 5. Represent the temperature variation in the square cross section microchannel. Fluid temperature increases as flows from inlet to outlet by absorbing heat from the heated assembly and it cools down the heated assembly.

4. Data Reduction from CFD Results

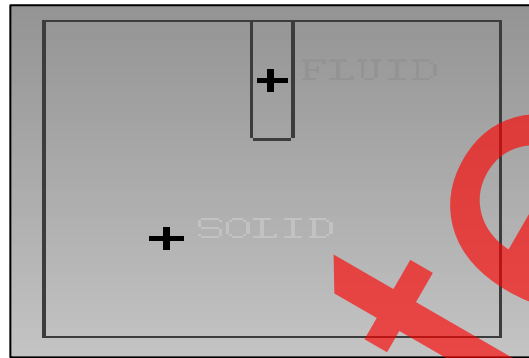


Figure 6. Rectangular microchannel heat sink front view

The Figure 6 was taken from [16]. Heat transfer takes place from the heated assembly to the cooling fluid by forced convection as fluid is flowing with certain velocity. For conduction CFD analysis, 2 zones were created namely solid and fluid zone. Lines were created in the assembly, 3 in fluid and 1 in solid part. From inlet to outlet the 3 lines were created at fluid section, one at top, one at middle and one at bottom.

Temperature difference between fluid inlet and outlet temperatures,

$$(\Delta T)_f = T_{f,o} - T_{f,i} \quad (1)$$

The average temperature of fluid was given as,

$$T_{f,avg} = (T_{f,i} + T_{f,o})/2 \quad (2)$$

Average fluid temperature and average wall temperature difference was given as,

$$(\Delta T) = T_{w,avg} - T_{f,avg} \quad (3)$$

Mass flow of the fluid passing through the microchannel was calculated as,

$$\dot{m} = \rho A_{cs} V \quad (4)$$

The hydraulic diameter is given as,

$$D_h = (4A_{cs})/P \quad (5)$$

The formula for Reynolds number is,

$$Re = (\rho V D_h) / \mu \quad (6)$$

Heat absorbed by the cooling fluid as it flows through the microchannel is given as,

$$Q = \dot{m} C_p (\Delta T)_f \quad (7)$$

And the heat transfer coefficient associated with the above forced convection heat transfer process is given as,

$$Q = h A_s (\Delta T) \quad (8)$$

All Equations from (1)-(8) used are same as those which were used in [16].

5. Results & Discussions

Microchannel with different cross sections was used and between them comparison was conducted using liquid water and water- Al_2O_3 nanofluid of 0.3% volume fraction as a cooling medium. With both of the fluids the rectangular cross section was better with respect to the heat transfer as that of square cross section.

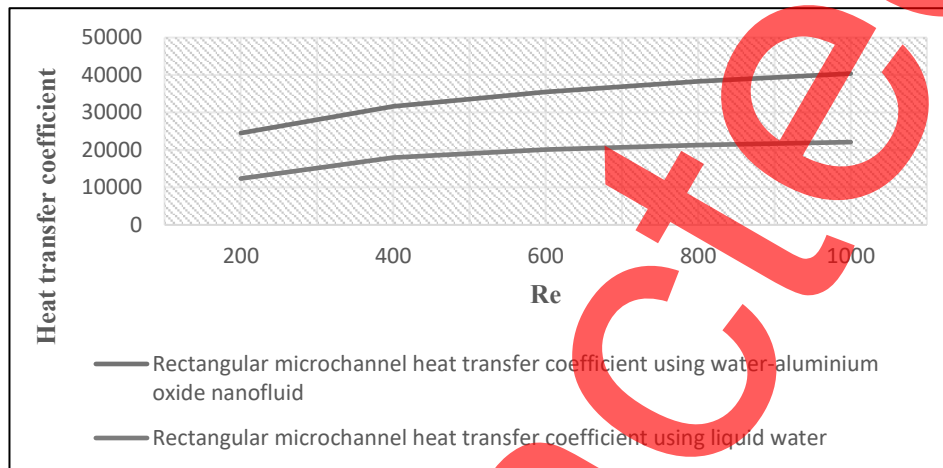


Figure 7. Comparison of heat transfer coefficient in rectangular microchannel using liquid water and water-aluminium oxide nanofluid

As shown in Figure 7. The values of heat transfer coefficient expressed in W/m^2K obtained for rectangular microchannel using nanofluid are higher compared to the values obtained with liquid water. The heat transfer coefficient values for rectangular microchannel using liquid water at Reynolds number of 600, 800 and 1000 are taken from [16]. The percentage increase in heat transfer coefficient using nanofluid in rectangular microchannel was observed to be 49.5%, 43.09%, 43.3%, 44% and 45% for Reynolds number of 200, 400, 600, 800 and 1000 respectively and average percentage increment of 45%.

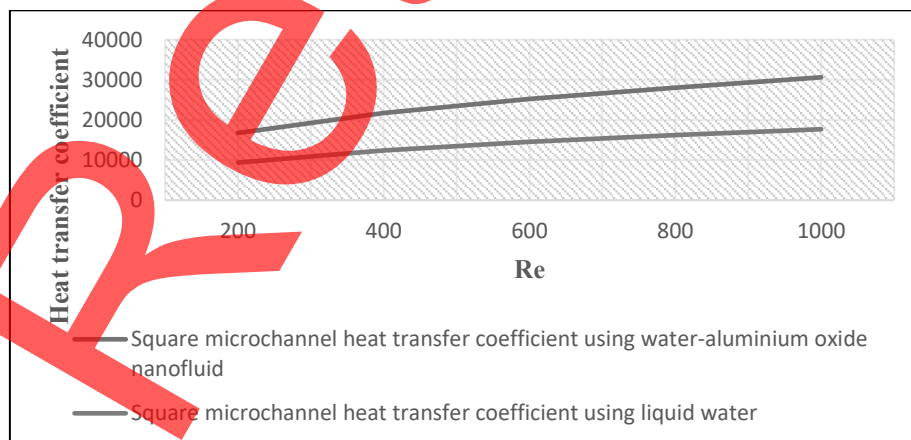


Figure 8. Comparison of heat transfer coefficient in square microchannel using liquid water and water-aluminium oxide nanofluid

As shown in Figure 8. In each case the nanofluid is giving better heat transfer coefficient values expressed in W/m^2K as compared to the liquid water in square cross section microchannel. The heat transfer coefficient values at Reynolds number of 600, 800 and 1000 for square cross section using liquid water are taken from [16]. The percentage increase in heat transfer coefficient values using nanofluids as compare to using water for Reynolds number of 200, 400, 600, 800 and 1000 in square microchannel was observed to be 44%, 42.9%, 42%, 42% and 42% respectively with average percentage increment of 42.5%.

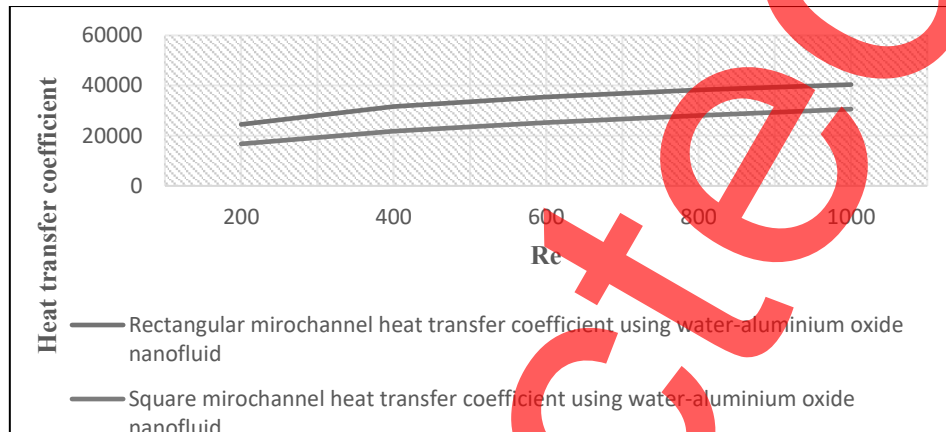


Figure 9. Comparison of heat transfer coefficient in rectangular and square microchannel using water-aluminium oxide nanofluid

From Figure 9. We can conclude that rectangular microchannel is giving better performance as that of square section while using nanofluid as cooling medium. The percentage increase in heat transfer coefficient values expressed in W/m^2K using rectangular microchannel as compared to square using nanofluid as a cooling medium was observed to be 31.6%, 31%, 29%, 26.7% and 24% for the Reynolds number of 200, 400, 600, 800 and 1000 with average percentage increment of 28.4%.

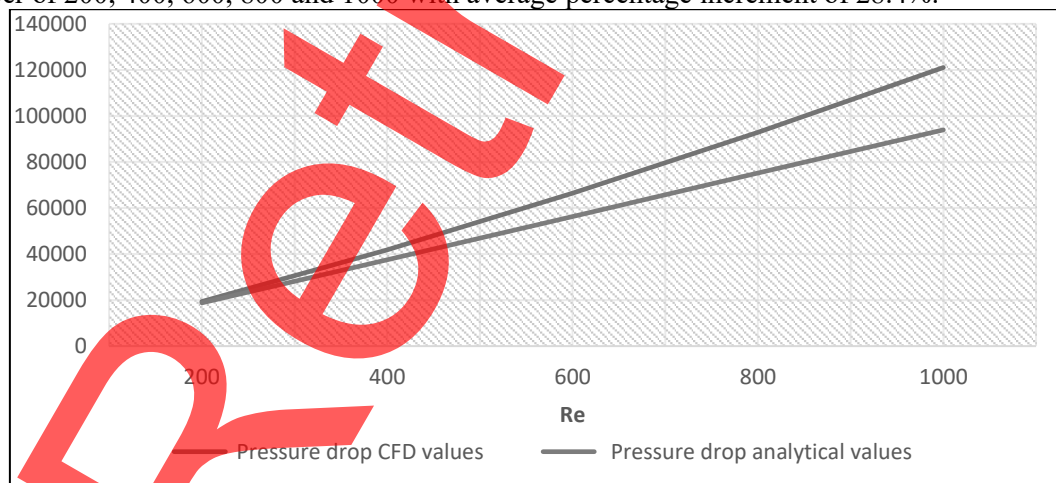


Figure 10. Pressure drop values in rectangular cross section using water-aluminium oxide nanofluid

The values of pressure drop in Pa are expressed in Figure 10. Using CFD and Analytical approach. With the flow pressure drop increases because of the frictional head loss. The analytical values of pressure drop are calculated using formula given in [7]. The percentage variation between the pressure drop values obtained using CFD Analytical approach for Reynolds number of 200, 400, 600, 800 and 1000 was observed to be 3.05%, 10%, 15.2%, 19.12% and 19.9% with average variation of 13.4%.

6. Conclusion

Present study was conducted using liquid water and water- Al_2O_3 nanofluid with 0.3% volume fraction. As compared to liquid water the nanofluid is showing better heat transfer performance. The rectangular is better to use as compared to square cross section microchannel as heat will be effectively removed by rectangular cross section because heat transfer coefficient values obtained are higher for rectangular than square cross section.

1. Average percentage increment in heat transfer coefficient values in rectangular microchannel with water- Al_2O_3 nanofluid as cooling medium as compared to the liquid water was obtained to be 45%.
2. Average percentage increment in heat transfer coefficient values in square microchannel with water- Al_2O_3 nanofluid as cooling medium as compared to the liquid water was obtained to be 42.5%.
3. Average percentage increment in heat transfer coefficient values in rectangular microchannel as compared to the square microchannel with water- Al_2O_3 nanofluid as cooling medium was obtained to be 28.4%.
4. Average pressure drop variation in rectangular microchannel with water- Al_2O_3 nanofluid as cooling medium using analytical and CFD approach was observed to be 13.4%.
So it is better to use rectangular as that of square microchannel and nanofluid as compared to liquid water.

References

- [1] Aggrey Mwesigye, Zhongjie Huan, *Thermodynamic analysis and optimization of fully developed turbulent forced convection in a circular tube with water- Al_2O_3 nanofluid*, International Journal of Heat and Mass Transfer **89** (2015), pp 694-706.
- [2] Yanjuan Wang, Jinliang Xu, Qibin Liu, Yuanyuan Chen, Huan Liu, *Performance analysis of a parabolic trough solar collector using Al_2O_3 /synthetic oil nanofluid*, Applied Thermal Engineering **107** (2016), pp 469-478.
- [3] Yulin Ma, Mojtaba Jamiatia, Alireza Aghaei, Mohammad Sepehrirad, Amin Dezfulizadeh, Masoud Afrand, *Effect of differentially heated tubes on natural convection heat transfer in a space between two adiabatic horizontal concentric cylinders using nano-fluid*, International Journal of Mechanical Sciences **163** (2019), p 105148.
- [4] Aggrey Mwesigye, Zhongjie Huan, Josua P. Meyer, *Thermal performance and entropy generation analysis of a high concentration ratio parabolic trough solar collector with Cu – Therminol® VP-1 nanofluid*, Energy Conversion and Management **120** (2016), pp 449-465.
- [5] Yang Liu, Jing Cui, WeiZhong Li, Ning Zhang, *Effect of Surface Microstructure on Microchannel Heat Transfer Performance*, Journal of Heat Transfer, DECEMBER 2011, **133** / , pp 124501-1.
- [6] M.A. Ahmed, M.Z. Yusoff, N.H. Shuaib, *Effects of geometrical parameters on the flow and heat transfer characteristics in trapezoidal-corrugated channel using nanofluid*, International Communications in Heat and Mass Transfer **42** (2013), pp 69-74.
- [7] Satish G. Kandlikar, *Single-Phase Liquid Flow in Minichannels and Microchannels*, Heat Transfer and Fluid Flow in Minichannels and Microchannels, 2014 Elsevier Ltd.
- [8] Poh-Seng Lee, Suresh V. Garimella, Dong Liu, *Investigation of heat transfer in rectangular microchannels*, International Journal of Heat and Mass Transfer **48** (2005), pp 1688–1704.
- [9] Xiaoming Zhou, Yanni Jiang, Xunfeng Li, Keyong Cheng, Xiulan Huai, Xidong Zhang, Hulin Huang, *Numerical investigation of heat transfer enhancement and entropy generation of natural convection in a cavity containing nano liquid-metal fluid*, International Communications in Heat and Mass Transfer **106** (2019), pp 46-54.

- [10] H. Heidary, M.J. Kermani, *Heat transfer enhancement in a channel with block(s) effect and utilizing Nano-fluid*, International Journal of Thermal Sciences **57** (2012) , pp 163-171.
- [11] W.Q. Li, S.J. Guo, L. Tan, L.L. Liu, W. Ao, *Heat transfer enhancement of nano-encapsulated phase change material (NEPCM) using metal foam for thermal energy storage*, International Journal of Heat and Mass Transfer **166** (2021) , p 120737.
- [12] M. Awais, M. Saad, Hamza Ayaz, M.M. Ehsan, Arafat A. Bhuiyan, *Computational assessment of Nano-particulate (Al_2O_3 /Water) utilization for enhancement of heat transfer with varying straight section lengths in a serpentine tube heat exchanger*, Thermal Science and Engineering Progress **20** (2020) , p 100521.
- [13] Man-Wen Tian, Saleh Khorasani, Hazim Moria, Samira Pourhedayat, Hamed Sadighi Dizaji, *Profit and efficiency boost of triangular vortex-generators by novel techniques*, International Journal of Heat and Mass Transfer **156** (2020) , p 119842.
- [14] H. Anandakumar and K. Umamaheswari, A bio-inspired swarm intelligence technique for social aware cognitive radio handovers, Computers & Electrical Engineering, vol. **71**, pp. 925–937, Oct. 2018. doi:10.1016/j.compeleceng.2017.09.016
- [15] R. Arulmurugan and H. Anandakumar, Early Detection of Lung Cancer Using Wavelet Feature Descriptor and Feed Forward Back Propagation Neural Networks Classifier, Lecture Notes in Computational Vision and Biomechanics, pp. 103–110, 2018. doi:10.1007/978-3-319-71767-8_9.
- [16] Saurabh Narayan Pawar, Nilesh Balkishanji Totla, *CFD Simulation and Analytical Validation of Rectangular and Square microchannel heat sink with liquid water as cooling medium*, 3rd International Congress on Advances in Mechanical Sciences, IOP Conf. Series: Materials Science and Engineering 998 (2020) 012030, IOP Publishing, doi:10.1088/1757-899X/998/1/012030.

2022 | OriginalPaper | Chapter

Reverse Supply Chain Network for Plastic Waste Management

Authors: Rakshit Shetty, Neha Sharma, Vishal A. Bhosale

Published in: Emerging Research in Computing, Information, Communication and Applications

Publisher: Springer Singapore

Login to get access

Show more

Please log in to get access to this content

Log in

Register for free

previous chapter

next chapter

Literature

Metadata





Smart Technologies for Energy, Environment and Sustainable Development, Vol 1 pp 707–723

A Study on Women Police Bullet-Proof Jacket Considering Anthropometry Data, Comfort and Safety in Pune, India

[Chinmayanand Prakash Jagtap](#), [Shilpi Bora](#), [Pranjal Arun Patil](#), [Abhijeet Malge](#) & [Mahesh Goudar](#)

Conference paper | [First Online: 25 February 2022](#)

200 Accesses

Part of the [Springer Proceedings in Energy](#) book series (SPE)

Abstract

An effective study was held with a survey carried out by interacting with a number of lady police about the current Bullet-Proof vest available, which are bullet resistant to a particular threat level. These are not manufactured according to the concern of women. This study helps in figuring out the need for a new bullet-proof vest for women. The survey gave many aspects which need to be changed. The paper flows by briefing today's availability and condition for women's working in various defence sectors. With current scenarios and the changes

2022 | OriginalPaper | Chapter

Improvement in Liquid and Plastic Limit for Black Cotton Soil by Addition of RBI Grade 81

Authors: Prashant Khedkar, Shraddha Shinde, Sakshi Wayal, Bhaskar Wabhitkar

Published in: Smart Technologies for Energy, Environment and Sustainable Development, Vol 1

Publisher: Springer Nature Singapore

Login to get access

Show more

Please log in to get access to this content

Log in

Register for free

previous chapter

next chapter

Literature

Metadata



Smart Technologies for Energy, Environment and Sustainable Development, Vol 1 pp 261–272

Shear Strength Improvement of Black Cotton Soil Reinforced with Waste Plastic Bottle Strips

[Nilesh Shirpurkar](#) , [Dhanraj Saste](#), [Vaibhav Varpe](#) & [Bhaskar Wabhitkar](#)

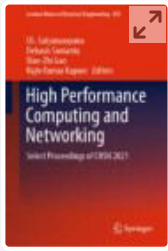
Conference paper | [First Online: 25 February 2022](#)

200 Accesses

Part of the [Springer Proceedings in Energy](#) book series (SPE)

Abstract

India generates an average of 26,000 tons of plastic a day. The plastic processing industry is producing 13.4 MT in 2015 and growing to 22 million tons (MT) a year by 2020 (TOI article 2019) [1]. Black cotton soil has a very low-bearing capacity. Due to its characteristics, it forms a very poor foundation material. Black cotton soil falls under a major constituent of soil in India. The soil undergoes volumetric changes when soil is present on the water table. Increase in water content causes the swelling of the soils and loss of strength. Decrease in moisture content resulting in soil shrinkage. BC



High Performance Computing and Networking, pp 425–436

SquashCord: Video Conferencing Application Using WebRTC

Adhiksha Thorat & Avinash Bhute 

Conference paper | [First Online: 23 March 2022](#)

165 Accesses

Part of the [Lecture Notes in Electrical Engineering](#) book series (LNEE, volume 853)

Abstract

WebRTC is a framework that helps to facilitate real-time communication between browsers. It provides services through application programming interface (API) and allows web applications and sites to exchange video and audio streams in real time. It is an open-source software developed by Google. The research presented in this paper delves into the development of a multi-peer video conferencing application that is developed using technologies like WebRTC, Node.js and Socket.io. WebRTC establishes a peer-to-peer network, and Socket.io (a library in Node.js) acts as a signalling mechanism for exchanging data necessary for establishing this network. The developed application works well on

Conferences > 2021 International Conference... ?

Signature Recognition Models: Performance Comparison

Publisher: IEEE [Cite This](#) PDF

Atharva Gadre ; Pradyumna Pund ; Gouri Ajmire ; Shubhangi Kale All Authors

16
Full
Text Views



Alerts

Manage Content Alerts

Add to Citation Alerts

More Like This

A Novel Approach for Handwriting Recognition in Malayalam Manuscripts using Contour Detection and Convolutional Neural Nets
2018 International Conference on Advances in Computing, Communications and Informatics (ICACCI)
Published: 2018

Rumour Detection Based on Graph Convolutional Neural Net
IEEE Access
Published: 2021


Show More

Abstract	
Document Sections	Download PDF
I. Introduction	Abstract: In recent times Signature Verification has become an act of absolute necessity in the area of biometric verification. Unlike other verification problems, every small deta... View more
II. Proposed Systems and Methodology	
III. Dataset	
IV. Pre-Processing	
V. Result (Performance Analysis)	
Show Full Outline ▾	► Metadata
	Abstract: In recent times Signature Verification has become an act of absolute necessity in the area of biometric verification. Unlike other verification problems, every small detail between genuine and forged signatures needs to be observed because a skilled forgery can only differ by only some specific kind of features of the real signature. The task of verifying signatures has become even harder in writing independent scenarios. In this paper, with the help of Siamese Network, VGG16 model and DEEP CNN models we have modeled a system that will verify signatures offline. Siamese networks use two images as input with shared weights, which can be trained to learn the features of both the images to find out the similarity between them. This is done by passing sets of similar and dissimilar images to the network so that it can learn to reduce the loss and Euclidean distance between similar images and increase it in dissimilar images. As for VGG 16, it is a pre-trained 16-layer model that is based on CNN, these 16 layers consist of max layer, pooling layers, and many more. CNN is simply a convolutional neural network on which both Siamese and VGG models are based. The performance analysis shows the VGG16 to have best accuracy about 85-90%, Siamese shows 65-70% and CNN shows 65-70% and the Siamese network to have the highest speed in identification.
Authors	
Figures	
References	
Keywords	
Metrics	



Techno-Societal 2020 pp 477–487

IoT Enabled Secured Card Less Ration Distribution System

[Shilpa K. Rudrawar](#) , [Kuldeepak Phad](#) & [Prajwal Durugkar](#)

Conference paper | [First Online: 20 May 2021](#)

260 Accesses

Abstract

Proposed paper put light on the automation in distribution of goods by using IOT based ration distribution system which uses the biometric verification and the cloud storage technology. Proposed system looks like an Automated Teller machine (ATM). We can simplify the process by using an interactive approach. Aadhar cards contain details like contact number, residential details, details of bank account and available scheme. Details of customers are stored and maintained as the database in the cloud storage by the government. Here we are storing the customer's data in the cloud using storage technology such as Google Firebase. This database contains the necessary information such as Aadhar details,



Techno-Societal 2020 pp 241–247

Detection of Brain Tumor Using Image Processing and Neural Networks

[Vanshika Dhillon](#) , [Dipti Sakhare](#) & [Shilpa Rudrawar](#)

Conference paper | [First Online: 20 May 2021](#)

260 Accesses

Abstract

Artificial Intelligence (AI) is an umbrella consisting of many small blocks like machine learning, evolution computation, robotics, vision, natural language process and planning, speech processing etc. In the past years AI has developed a lot and given its share to make human life better, easy and compact. The word “technology” is a term which can be defined in many ways. The definition of the word keeps evolving with the continuous development in various fields. Decades ago, it used to take an entire room to accommodate a single computer but now we use the same computer at the ease of our fingertips. With the rapid development in technology mankind’s expectations and needs have also increased. Human race demands accurate results in less time with easier



Recent Advances in Manufacturing Modelling and Optimization pp 231–240

Selection of Passenger Car Using TOPSIS Method

[S. Y. Borole](#) , [P. U. Malu](#) & [A. G. Kamble](#)

Conference paper | [First Online: 22 April 2022](#)

152 Accesses

Part of the [Lecture Notes in Mechanical Engineering](#) book series (LNME)

Abstract

The car is one of the basic needs in today's world for transportation of the passengers, and selection of car is a very crucial task for the customer. The quality of the car varies with respect to the attributes. The customers are in search of a car which is best in attributes. The present work gives the selection procedure for selection of best car using multi-attribute decision-making method viz: technique for order of preference by similarity to ideal solution method based upon different attribute. There are five alternatives and five attributes considered like cost, mileage, safety rating, transmission and brake horsepower for the selection of car and the ranks are obtained. The



Recent Advances in Manufacturing Modelling and Optimization pp 829–842

Project Scheduling Using Linear Programming, CPM and Crashing Time Technique

[Takshay V. Sayre](#), [Keshav Kumar](#), [Divyansh A. Waghmare](#),
[Yash S. Deshpande](#) & [Vishal A. Bhosale](#)

Conference paper | [First Online: 22 April 2022](#)

152 Accesses

Part of the [Lecture Notes in Mechanical Engineering](#) book series (LNME)

Abstract

Project scheduling is a method by which we can shorten the duration of the project or crash the duration of a project at the expense of certain added cost to meet the specified project deadline. The project might lag behind the given schedule for many numbers of reasons, and this situation may call for measures like crashing some activities by appointing extra resources. This crashing of activities is generally done by trial-and-error method which is not very productive and incurs extra costs. The crashing of activity is to be done in such a way that the project should be completed



Recent Advances in Manufacturing Modelling and Optimization pp 739–749

Application of Polymer Composite for Weight Reduction in the Automobile Sector Toward a Sustainable Development

[Anand S. Baldota](#), [Vishal J. Dulange](#), [Shahrukh S. Patel](#) & [Manoj W. Bhalwankar](#) 

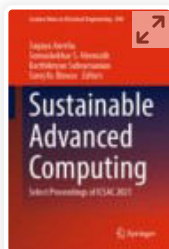
Conference paper | [First Online: 22 April 2022](#)

157 Accesses

Part of the [Lecture Notes in Mechanical Engineering](#) book series (LNME)

Abstract

In recent years, co-relation of sustainable development with the the growth of the industries, these questions have been a hot topic for research. The increasing awareness, greater restrictions on emission control, and its long-term environmental impact have led to an urgent need to develop lightweight and fuel-efficient vehicles in the global automobile industry. Polymer composites due to their lightweight and recyclability have been largely used in the automotive sector. This has led to a constant need to research and develop high-



Sustainable Advanced Computing pp 381–394

Region-Based Stabilized Video Magnification Approach

[Sanket Yadav](#) , [Prajakta Bhalkare](#) & [Usha Verma](#)

Conference paper | [First Online: 31 March 2022](#)

96 Accesses

Part of the [Lecture Notes in Electrical Engineering](#) book series (LNEE, volume 840)

Abstract

Eulerian video magnification (EVM) is used to magnify the imperceptible signals inside the video in the form of color. For this, it requires the jitter-free stable video of the target occupying the major part of the frame. And most of the time, the real-world/real-time videos cannot satisfy the above requirements completely. This is where EVM lacks optimal results. And this thought motivated authors to develop a new region-based stabilized video magnification (RSVM) approach. This preprocesses the input by stabilization of video, then detection–tracking–cropping of ROI, to get the motion-free-modulated input which satisfies requirements of EVM. Further, performance of both methods is

analyzed for different inputs and amplification factor with performance metrics as PSNR, elapsed time, extents of color, and motion magnification. Results reveal that the RSVM approach performs better than EVM to handle motions and also fasten the process.

Keywords

Video stabilization Region of interest

Eulerian video magnification

This is a preview of subscription content, [access via your institution.](#)

▼ Chapter

EUR 24.95

Price excludes VAT (India)

- DOI: 10.1007/978-981-16-9012-9_31
- Chapter length: 14 pages
- Instant PDF download
- Readable on all devices
- Own it forever
- Exclusive offer for individuals only
- Tax calculation will be finalised during checkout

Buy Chapter

> eBook

EUR 128.39

> Hardcover Book

EUR 159.99

[Learn about institutional subscriptions](#)

References

1. Wu H-Y, Rubinstein M, Shih E, Guttag J, Durand F, Freeman W (2012) Eulerian video

magnification for revealing subtle changes in the world. *ACM Trans Graph* 31(4):1–8

2. Liu L, Lu L, Luo J, Zhang J, Chen X (2014) Enhanced Eulerian video magnification. In: 2014 7th international congress on image and signal processing. Dalian, pp 50–54, <https://doi.org/10.1109/CISP.2014.7003748>
-

3. Alzahrani A, Whitehead A (2015) Preprocessing realistic video for contactless heart rate monitoring using video magnification. In: 2015 12th conference on computer and robot vision. Halifax, NS, pp 261–268. <https://doi.org/10.1109/CRV.2015.41>
-

4. Zhang K, Jin X, Wu A (2017) Accelerating Eulerian video magnification using FPGA. In: 2017 19th international conference on advanced communication technology (ICACT). Bongpyeong, pp 554–559, <https://doi.org/10.23919/ICACT.2017.7890151>
-

5. Yu H, Lin H, Zhang E, Li J, Chen G (2017) Region-based euler video amplification algorithm. In: 2017 10th international congress on image and signal processing, BioMedical Engineering and Informatics (CISP-BMEI). Shanghai, pp 1–5, <https://doi.org/10.1109/CISP-BMEI.2017.8302082>
-

6. Wu X, Yang X, Jin J et al (2018) PCA-based magnification method for revealing small signals in video. *SIViP* 12:1293–1299.
<https://doi.org/10.1007/s11760-018-1282-0>
-

7. Al-allaq ZJ, Shahadi HI, Albattat HJ (2019) Powerful and low time phase-based video magnification enhancing technique. In: 2019 4th scientific international conference Najaf (SICN). Al-Najef, Iraq, pp 133–138,
<https://doi.org/10.1109/SICN47020.2019.9019338>
-

8. Moya-Albor E, Brieva J, Ponce H, Martínez-Villaseñor L (2020) A non-contact heart rate estimation method using video magnification and neural networks. *IEEE Instrum Meas Mag* 23(4):56–62.
<https://doi.org/10.1109/MIM.2020.9126072>
-

9. Zhang J, Zhang K, Yang X, Wen C (2020) Heart rate measurement based on video acceleration magnification. In: 2020 Chinese control and decision conference (CCDC). Hefei, China, pp 1179–1182,
<https://doi.org/10.1109/CCDC49329.2020.9164451>
-

10. Zhang Y, Pintea SL, Van Gemert JC (2017) Video acceleration magnification. In: 2017 IEEE conference on computer vision and pattern

recognition (CVPR). Honolulu, HI, pp 502–510,
<https://doi.org/10.1109/CVPR.2017.61>

11. Yadav S, Bhalkare P, Shingde S, Verma U (2020) Performance analysis of video magnification methods. In: 2020 third international conference on smart systems and inventive technology (ICSSIT). Tirunelveli, India, pp 1293–1301,
<https://doi.org/10.1109/ICSSIT48917.2020.9214167>
-

12. Li B, Chen Y, Ren J, Cheng L (2017) A fast video stabilization method based on feature matching and histogram clustering. In: Balas V, Jain L, Zhao X (eds) Information technology and intelligent transportation systems. Advances in intelligent systems and computing, vol 455. Springer, Cham.
https://doi.org/10.1007/978-3-319-38771-0_31
-

13. Viola P, Jones M (2001) Rapid object detection using a boosted cascade of simple features. In: Proceedings of the 2001 IEEE computer society conference on computer vision and pattern recognition. CVPR 2001, Kauai, HI, USA, pp I–I,
<https://doi.org/10.1109/CVPR.2001.990517>
-

14. Tomasi C, Kanade T (1991) Shape and motion from image streams: a factorization method-2. point features in 3D motion. Technical Report

CMU-CS-91–105, Carnegie Mellon University,
Pittsburgh, PA

15. Senigagliesi L, Ricciuti M, Ciattaglia G, Santis AD, Gambi E (2021) Comparison of video and radar contactless heart rate measurements. In: Communications in computer and information science information and communication technologies for ageing well and e-health, pp 96–113. https://doi.org/10.1007/978-3-030-70807-8_6

16. Kassab LY, Law A, Wallace B, Larivière-Chartier J, Goubran R, Knoefel F (2021) Effects of region of interest size on heart rate assessment through video magnification. IEEE Int Symp Med Meas Appl (MeMeA) 2021:1–6. <https://doi.org/10.1109/MeMeA52024.2021.9478596>

17. Sharma P, Kokare PM, Kolekar MH (2019) Performance comparison of KLT and CAMSHIFT algorithms for video object tracking. In: Khare A, Tiwary U, Sethi I, Singh N (eds) Recent trends in communication, computing, and electronics. Lecture notes in electrical engineering, vol 524. Springer, Singapore. https://doi.org/10.1007/978-981-13-2685-1_31

18. Lucas BD, Kanade T (1981) An iterative image

registration technique with an application to stereo vision. In: Proceedings of the 7th international joint conference on artificial intelligence – vol 2 (IJCAI'81). Morgan Kaufmann Publishers Inc., San Francisco, CA, USA, pp 674–679

19. Zhao J, Zhang W, Chai R, Wu H, Chen W (2021) Non-contact physiological parameters detection based on MTCNN and EVM. In: Communications in computer and information science cognitive systems and signal processing, pp 507–516.
https://doi.org/10.1007/978-981-16-2336-3_48
-

20. Coachkriengsak “Steve jobs passion in work,” YouTube, 2 Aug 2011 [Video file]. Available: <https://www.youtube.com/watch?v=PznJqxon4zE>. [Accessed: 15 Jan 2020]
-

Author information

Authors and Affiliations

School of Electrical Engineering, MIT Academy of Engineering, Pune, India

Sanket Yadav, Prajakta Bhalkare & Usha Verma

Corresponding author

Correspondence to [Sanket Yadav](#).

Editor information

Editors and Affiliations

**Department of Computer Science, CHRIST
(Deemed to be University), Bengaluru,
Karnataka, India**

Dr. Sagaya Aurelia

**Department of Mechanical Engineering, Indian
Institute of Technology Madras, Chennai, Tamil
Nadu, India**

Dr. Somashekhar S. Hiremath

**Department of Information Technology,
University of Technology and Applied Science,
Sultanate of Oman, Oman**

Dr. Karthikeyan Subramanian

**Department of Computer Science Engineering,
National Institute of Technology Silchar, Silchar,
Assam, India**

Dr. Saroj Kr. Biswas

Rights and permissions

[Reprints and Permissions](#)

Copyright information

© 2022 The Author(s), under exclusive license to
Springer Nature Singapore Pte Ltd.

About this paper

Cite this paper

Yadav, S., Bhalkare, P., Verma, U. (2022). Region-Based
Stabilized Video Magnification Approach. In: Aurelia, S.,
Hiremath, S.S., Subramanian, K., Biswas, S.K. (eds)

Sustainable Advanced Computing. Lecture Notes in
Electrical Engineering, vol 840. Springer, Singapore.

https://doi.org/10.1007/978-981-16-9012-9_31

[.RIS](#)  [.ENW](#)  [.BIB](#) 

DOI

https://doi.org/10.1007/978-981-16-9012-9_31

Published	Publisher Name	Print ISBN
31 March 2022	Springer, Singapore	978-981-16- 9011-2

Online ISBN	eBook Packages
978-981-16- 9012-9	Intelligent Technologies and Robotics Intelligent Technologies and Robotics (R0)

Not logged in - 43.227.20.34

Not affiliated

SPRINGER NATURE

© 2022 Springer Nature Switzerland AG. Part of [Springer Nature](#).

Conferences > 2022 12th International Confe... ?

Enhancing the Security of Medical Images in Telemedicine Using Region-based Crypto-Watermarking Approach

Publisher: IEEE Cite This PDF

Usha Verma ; Neelam Sharma All Authors

1 Paper Citation


40 Full Text Views

Alerts

View References

Manage Content Alerts

Add to Citation Alerts

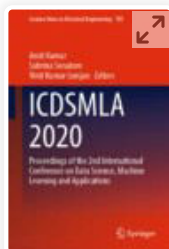
Abstract	 Downl PDF
Document Sections	
I. Introduction	Abstract: Along with maintaining the confidentiality and privacy of patient information, the preservation and authentication of internal physiological features of tissues and organ... View more
II. Related Work In Literature	
III. Methodology	► Metadata
IV. Implementation and Results	Abstract: Along with maintaining the confidentiality and privacy of patient information, the preservation and authentication of internal physiological features of tissues and organs present in any type of medical images is equally important while transmitting medical images in Telemedicine. To achieve it, this paper presents a region-based approach for Medical Image by integrating cryptography in the digital watermarking. To preserve the internal physiological features, medical image is separated into two regions – Region of Interest (ROI) and Not-a-Region of Interest (NROI). ROI contains the important internal physiological features of human body. Therefore, no information is embedded in ROI to preserve it. Cryptography is integrated only for generation and exchange of the secret key of ROI using Elliptic curve cryptography. Patient information and secret key is embedded into NROI using wavelet-based hybrid watermarking technique. The proposed work is tested on varieties of medical image dataset of MRI, CT scan and X-ray against various intentional and unintentional attacks and evaluated with performance metrics PSNR (Peak signal to Noise Ratio), SSIM (Structural Similarity Index), NC (Normalized Correlation) and BER (Bit Error Ratio). Secret key is matched at receiving end to authenticate the
V. Conclusion	
Authors	
Figures	
References	
Citations	
Keywords	
Metrics	

More Like This

An Image Watermarking Algorithm for Medical Computerized Tomography Images
2019 5th Iranian Conference on Signal Processing and Intelligent Systems (ICSPIS)
Published: 2019

X-ray medical image processing using directional wavelet transform
1996 IEEE International Conference on Acoustics, Speech, and Signal Processing Conference Proceedings
Published: 1996

Show More



ICDSMLA 2020 pp 717–726

Design of Secure Biometric System Using Cancelable Techniques

[Aarti Laxman Gilbile](#)  & [Pramod D. Ganjewar](#)

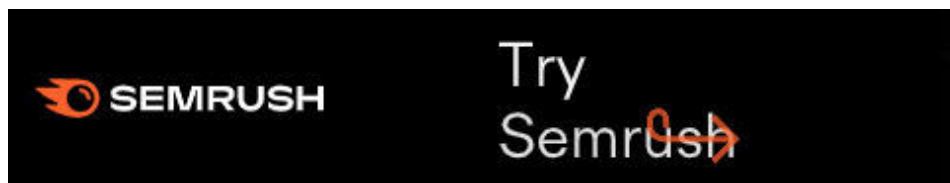
Conference paper | [First Online: 09 November 2021](#)

591 Accesses

Part of the [Lecture Notes in Electrical Engineering](#) book series (LNEE, volume 783)

Abstract

Individual identification can be accurately done by measuring biological parameters termed as biometrics. These have been proved as an unusual tool for identity verification. Recognition of biometrics and applications based on it is increased tremendously, so the privacy protection monitors are raising the privacy concerns. For reducing the privacy threats, the research work has increased to find methods to protect the biometric data. Security of biometric template is that the most challenging aspect of biometric identification system. The biometric data are stored as it is within the database which increases the rate of compromising it. This can also cause serious threat or misuse of



AIP

Conference Proceedings

HOME

BROWSE

MORE ▼

[Home](#) > [AIP Conference Proceedings](#) > [Volume 2417, Issue 1](#) > [10.1063/5.0072779](#)

< PREV

NEXT >



No Access

Published Online: 19 October 2021

CFD analysis of exhaust pipe of a diesel engine

AIP Conference Proceedings **2417**, 060002 (2021); <https://doi.org/10.1063/5.0072779>Pawankumar Yadav^{a)} and Pramod Kothmire^{b)}[View Affiliations](#)[View Contributors](#)

Topics ▼

ABSTRACT



PDF



E-READER

Conferences > 2021 2nd Global Conference fo... ?

Design & Development of Insurance Money Predictor to Claim with Insurance Company

Publisher: IEEE Cite This PDF

Ankita Jadhav ; Mayuri Kulkarni ; Pranav Abute ; Prachi Rajarapolu All Authors

1
Paper
Citation

34
Full
Text Views

Alerts

Manage Content Alerts

Add to Citation Alerts

Abstract

Document Sections

I. Introduction

II. Literature Review

III. Methodology Implemented

IV. System Development

V. Results

Show Full Outline

Authors

Figures

References

Citations

Keywords

Metrics

Download PDF

Abstract:In this pandemic situation of Covid-19, the whole world had suffered a lot. Whatever issues occurred is very uncertain and unexpected. In the life cycle of a human being,... **View more**

► Metadata

Abstract:

In this pandemic situation of Covid-19, the whole world had suffered a lot. Whatever issues occurred is very uncertain and unexpected. In the life cycle of a human being, it is always desirable to be safe and have a secure lifestyle in every aspect. To face sudden, unexpected situation insurance is one of the solutions. Nowadays due to increasing awareness among the society people are more inclined towards taking medical insurance from various companies. As we know there are several companies in ensuring the various diseases, climatic hazards, man-made and natural emergencies. Insurance money is going to support the human in morally and financially. The insurance companies are having their own rules and regulations for giving money/claims to a client. Some hidden calculations are always out of reach to the common man. Day by day accurate insurance calculation and claim for money become a challenging task for society. In this paper, a system has been developed using a machine learning algorithm for accurate claim calculation. Implemented system will help the client to claim monthly or quarterly premiums based on various parameters like the number of family members you want to insure, the total income of the family, the expected amount of insurance, age group of family members, etc. To make the process more user-friendly and fast, we have developed a website.

More Like This

News-EDS: News based Epidemic Disease Surveillance using Machine Learning

2020 14th International Conference on Open Source Systems and Technologies (ICOSST)

Published: 2020

Analysis and design of epidemic disease monitoring cloud platform

2022 IEEE 6th Information Technology and Mechatronics Engineering Conference (ITOEC)

Published: 2022

Show More

Conferences > 2021 2nd Global Conference fo... ?

Crack Detection on Metal Surfaces Using Image Processing Techniques

Publisher: IEEE

Cite This

PDF

Megharaj Sonawane ; Aditya Borse ; Hrishikesh Sonawane ; Aashish Mali ; Prachi Raj...

All Authors

School of Electrical Engineering MIT Academy of Engineering, Pune, India

64 Full Text Views

Alerts

Manage Content Alerts

Add to Citation Alerts

Abstract

Document Sections

I. Introduction

II. Literature Review

III. Methodology Implemented

IV. Algorithm Implemented

V. Result

Show Full Outline

Authors

Figures

References

Keywords

Metrics

More Like This

Download PDF

Abstract:It is impossible to imagine an industry without a machine. Huge number of machines are working together in industry. Many times if the failure occurs in machine it become... [View more](#)

Metadata

Abstract:

It is impossible to imagine an industry without a machine. Huge number of machines are working together in industry. Many times if the failure occurs in machine it becomes a challenging task to identify it. Fault may occur due to various reasons. Here the main focus is on identifying the fault occurred due to the fine crack on metal body. Faulty spare parts can be easily identified and can be replaced. But finding a fault due to the crack on metal body is becomes difficult to work out. To find out such type of faults machine disassembling is the only option. Disassembling any machine is not that much easy task and hence a system is developed here which will help in identifying the crack on metal body without disassembling any machine. It is possible to detect the exact size, location of the crack. Digital image processing concepts are used to identify the crack on a metal body. Scanning of metal body will be done to identify the crack on metal body, with the help of scanning mechanism (using ultrasonic, xray, gamma rays Radiography). The image of metal body will get captured which will get inputted to the systems for the processing purpose and by using the different algorithms of image processing, image will get processed. Firstly image will get converted into black and white form and then the digitization of image will be done. Based on the digitized data, using the segmentation

More Like This

A Hybrid Fault Diagnosis Approach for Blade Crack Detection using Blade Tip Timing

2020 IEEE International Instrumentation and Measurement Technology Conference (I2MTC)

Published: 2020

An automated thermographic image segmentation method for induction motor fault diagnosis

IECON 2014 - 40th Annual Conference of the IEEE Industrial Electronics Society

Published: 2014

Show More

https://ieeexplore.ieee.org/document/9587516

1/3

Conferences > 2021 International Conference... ?

Lecture Summarization using Video Processing and Automatic Text Summarization

Publisher: IEEE

Cite This

PDF

Janhavi Chadawar ; Vivek Deshmukh ; Sahil Kharade ; Tushar Shelar ; Nilesh Bhandare All Authors

75 Full Text Views

Alerts

Manage Content Alerts

Add to Citation Alerts

Abstract

Document Sections

I. Introduction

II. Literature Survey

III. Methodology

IV. Work/Module Description

V. Proposed Project Design

Show Full Outline

Authors

Figures

References

Keywords

Metrics

More Like This

Download PDF

Abstract:Nowadays machine learning has achieved a lot of success in technical fields. One of these is video processing but text is recognized which is in a computer readable forma... **View more**

► Metadata
Abstract:
Nowadays machine learning has achieved a lot of success in technical fields. One of these is video processing but text is recognized which is in a computer readable format, our paper is focusing on detection of handwritten text and summarizing the document for which we found a better result with some methods which are clearly explained in this paper. This paper is following three modules to achieve the better result as from video selecting keyframes without losing whiteboard data, after selecting keyframes to identify the text which is a difficult task can be achieved. Preparing short notes with more accuracy is required for that this paper shows some ML libraries.These paper will give us a brief idea about which methods are used for modules to achieve a good accuracy.

Published in: 2021 International Conference on Intelligent Technologies (CONIT)

Date of Conference: 25-27 June 2021 **INSPEC Accession Number:** 21467270

More Like This

A BiCMOS continuous-time filter for video signal processing applications
IEEE Journal of Solid-State Circuits
Published: 1998

A single chip video signal processing architecture for image processing, coding, and computer vision
IEEE Transactions on Circuits and Systems for Video Technology
Published: 1995

Show More

Conferences > 2021 International Conference... ?

Surveillance Through Semi-Autonomous Bot

Publisher: IEEE

Cite This

PDF

<< Results

Rohit Kadhane ; Akshit Kumar ; Kushal Bhattad ; Ashish Srivastava All Authors

Back to Results

22 Full Text Views

Alerts

Manage Content Alerts

Add to Citation Alerts

Abstract

Document Sections

I. Introduction

II. System Design and Implementation

III. Result

IV. Conclusion

Authors

Figures

References

Keywords

Metrics

More Like This

Download PDF

Abstract:This paper consists of the design and implementation of the semi-autonomous surveillance bot. The idea presented in the paper is to monitor a surrounding or unknown area.... **View more**

Metadata

Abstract:
This paper consists of the design and implementation of the semi-autonomous surveillance bot. The idea presented in the paper is to monitor a surrounding or unknown area. This paper carries the different phases of realization such as the motion of the robot, obstacle avoidance, and video capturing and streaming. After the video has been captured the recorded clip is streamed to a remote server which assesses the surrounding. For the implementation of the idea, different tools were required for the execution of the precursor. For building the model, the hardware required was Raspberry Pi, infrared sensors, L293D motor driver. Raspberry Pi consisting of a Raspbian operating system running on python language for video capturing and obstacle sensing was used.

Published in: 2021 International Conference on Design Innovations for 3Cs Compute Communicate Control (ICDI3C)

Date of Conference: 10-11 June 2021 **INSPEC Accession Number:** 21142299

Date Added to IEEE Xplore: 27 September 2021

More Like This

A design of mobile robot based on Network Camera and sound source localization for intelligent surveillance system
2008 International Conference on Control, Automation and Systems
Published: 2008

ERS-210 Mobile Video Surveillance System
2005 portuguese conference on artificial intelligence
Published: 2005

Show More

Conferences > 2021 Innovations in Power and...

?

Comparative Analysis of Nine level T-Type MLI

Publisher: IEEE

Cite This

PDF

<< Results

Vijay Pise ; Gajanan Dhakne ; Vishal Waghmare ; Akash Waghmare ; Mandar Bhalekar

All Authors

11 Full Text Views

Alerts

Manage Content Alerts

Add to Citation Alerts

Abstract

Document Sections

I. Introduction

II. Multilevel Inverter Topology

III. Simulation Result

IV. Comparative Table

V. Conclusion

Authors

Figures

References

Keywords

Metrics

More Like This

Download PDF

Abstract:This paper is a comparison between Traditional Cascaded H-Bridge Multilevel Inverter (MLI) and Modern T-Type MLI. The most suitable topology to be used in Electrical/E-ve... [View more](#)

► Metadata

Abstract:

This paper is a comparison between Traditional Cascaded H-Bridge Multilevel Inverter (MLI) and Modern T-Type MLI. The most suitable topology to be used in Electrical/E-vehicle to get smooth AC for increasing the performance is found based on comparison of the use of the number of power devices, THD values, and FFT analysis. The MATLAB simulation results of both topologies for Nine level AC output are compared and presented systematically.

Published in: 2021 Innovations in Power and Advanced Computing Technologies (i-PACT)

Date of Conference: 27-29 November 2021**INSPEC Accession Number:** 21705344

Date Added to IEEE Xplore: 08 February 2022**DOI:** 10.1109/i-PACT52855.2021.9696693

► ISBN Information:**Publisher:** IEEE

More Like This

Classification Based Method Using Fast Fourier Transform (FFT) and Total Harmonic Distortion (THD) Dedicated to Proton Exchange Membrane Fuel Cell (PEMFC) Diagnosis

2017 IEEE Vehicle Power and Propulsion Conference (VPPC)

Published: 2017

Identification of harmonic loads using fast fourier transform and radial basis Function Neural Network

2017 International Electronics Symposium on Engineering Technology and Applications (IES-ETA)

Published: 2017

Show More

Conferences > 2021 Innovations in Power and... ?

Smart Metering of Electricity

Publisher: IEEE

Cite This

PDF

<< Results

Khushal Babu ; Sainath Meharkar ; Chaitanya Pujari ; Shwetambari Thakare ; Mandar ... All Authors

Back to Results

35 Full Text Views

Alerts

Manage Content Alerts

Add to Citation Alerts

Abstract

Document Sections

I. Introduction

II. System Configuration

III. Block Diagram

IV. Hardware Implementation

V. Methodology

Show Full Outline

Authors

Figures

References

Keywords

Metrics

More Like This

Download PDF

Abstract:As population rises the demand of electricity also increases and energy theft becomes a major issue in countries like India. A large loss is faced by the utility of elect... **View more**

► Metadata

Abstract:
As population rises the demand of electricity also increases and energy theft becomes a major issue in countries like India. A large loss is faced by the utility of electricity every year due to power theft. The automatic meter reading (AMR) system already exists but with potentially reduced reliability and risk of loss of privacy. To collect consumption, diagnostic and status data by visiting consumers' places every time is tedious work. In this paper, an attempt is made based on a microcontroller ESP32 for monitoring, detecting and controlling energy theft remotely. The Internet is used for communication to the central utility system. The consumer will be motivated to use electrical appliances effectively by sharing the real time usage with it.

Published in: 2021 Innovations in Power and Advanced Computing Technologies (i-PACT)

Date of Conference: 27-29 November 2021 **INSPEC Accession Number:** 21562942

More Like This

Hardware Design of Automatic Meter Reading System Based on Internet 2008 IEEE International Symposium on Knowledge Acquisition and Modeling Workshop
Published: 2008

Internet of Things Enabled Power Theft Detection and Smart Meter Monitoring System 2020 International Conference on Communication and Signal Processing (ICCSP)
Published: 2020

Show More

Conferences > 2021 International Conference... ?

Personalization of Information using Graph Convolutional Network

Publisher: IEEECite ThisPDF

<< Results

Aditi Pandey ; Kaustubh Patil ; Sanskar Sharma ; Mayura Kulkarni All Authors

11Full Text Views

Alerts

Manage Content Alerts

Add to Citation Alerts

More Like This

Application of an Improved Nearest Neighbor Method

2021 International Applied Computational Electromagnetics Society (ACES-China) Symposium

Published: 2021

Rumour Detection Based on Graph Convolutional Neural Net

IEEE Access

Published: 2021

Show More

Abstract

Document Sections

I. Introduction

II. Related Work

III. Proposed Approach

IV. Implementation

V. Performance Evaluation

Show Full Outline ▾

Authors

Figures

References

Keywords

Metrics

Download PDF

Abstract: There exists several researches that have been done on link-based search engines for instance, Clever and Google. They involve the use of link structure to get precise results. View more

Metadata

Abstract: There exists several researches that have been done on link-based search engines for instance, Clever and Google. They involve the use of link structure to get precise results. Generally, search engines based on link structure give users high-quality results than search engines which are text based. However, those search engines encounter difficulty producing the result fitting to a specific user's profile. Personalization means knowing the user intimately enough to not only meet their needs but also predict them. This paper presents an analogy to a personalized search engine using an already existing GCN (Graph Convolutional Network) architecture on (Cora) the paper citation dataset (similar to web pages) and additionally followed by KNN algorithm to rank the personalized citations in best consonance with a user's profile.

Published in: 2021 International Conference on Advancements in Electrical, Electronics, Communication, Computing and Automation (ICAECA)

Date of Conference: 08-09 OctoberINSPEC Accession Number:

Conferences > 2021 9th International Confer... ?

Design and Development of Gamification Tool for Teenagers for Selection of Higher Education Path Based on Personality Traits

Publisher: IEEE Cite This PDF

<< Results

Deepali Bhalerao ; Dhiraj Bagul ; Nikhil Kesapure ; Deven Bharati ; Rupa Hiremath ; N... All Authors

60 Full Text Views

Alerts

Manage Content Alerts

Add to Citation Alerts

More Like This

Intelligent Computer-Aided Instruction Modeling and a Method to Optimize Study Strategies for Parallel Robot Instruction IEEE Transactions on Education Published: 2013

How to Improve the Quality and Effect of Computer Aided Instruction's Application in Classroom Teaching in Institutes of Higher Learning 2010 Second International Workshop on Education Technology and Computer Science Published: 2010

Show More

Abstract

Document Sections

I. Introduction

II. Methodology

III. Story Development

IV. System Analysis

V. System Architecture

Show Full Outline

Authors

Figures

References

Keywords

Abstract: Gamification is used as a powerful way to connect and engage player in an effective and enjoyable funny mood. The current research work demonstrates how gamification is d... View more

Metadata

Abstract: Gamification is used as a powerful way to connect and engage player in an effective and enjoyable funny mood. The current research work demonstrates how gamification is designed and developed in an innovative way to find out different personality traits of the teenagers and recommends the possible career choices available for them based on their personality traits connecting it to the requirements of different professional careers. OCEAN model is used to find out different personalities and gamification concepts like design, elements and storytelling are used to develop gamified system.

Published in: 2021 9th International Conference on Reliability, Infocom Technologies and Optimization (Trends and Future Directions) (ICRITO)

Date of Conference: 03-04 September INSPEC Accession Number: 2021 21437139



ICCCE 2021 pp 675–680

Efficient Use of Convolutional Neural Networks for Classification of Sugarcane Leaf Diseases

[Swapnil Dadabhau Daphal](#)  & [S. M. Koli](#)

Conference paper | [First Online: 16 May 2022](#)

133 Accesses

Part of the [Lecture Notes in Electrical Engineering](#) book series (LNEE, volume 828)

Abstract

Early identification and diagnosis of plant diseases are more crucial for holistic development of the agriculture sector in India. Farmer's general estimates and observations are time costly, sometimes vague and misjudged. For this purpose, a appropriate deep neural network is proposed for the automatic identification of sugarcane disease. The classification involves 5 types of diseases and 1 healthy class. Experimentation is performed over the manually collected dataset of size 1470 images. Performance estimation of the network is dependent on the choice of optimization. In this paper comparative analysis for different optimizers



ICCCE 2021 pp 859–869

Recent Trends and Techniques of CBIR to Enhance Retrieval Performance

[Prajakta Ugale](#)  & [Suresh Mali](#)

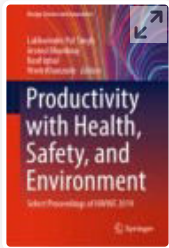
Conference paper | [First Online: 16 May 2022](#)

130 Accesses

Part of the [Lecture Notes in Electrical Engineering](#) book series (LNEE, volume 828)

Abstract

The vast growth in social media platforms such as Twitter, Instagram, Whatsapp, Facebook, etc. leads to the uploading of billions of images on the web. Content-Based Image Retrieval (CBIR) is essential to improve the performance of the data search. Computer vision research community facing research challenges related to the retrieval of relevant images from large databases. Most of the current search engines use text-based search whose performance highly depends on text Annotation and metadata of the images. In this paper, we aim to present an extensive survey of recent work carried out on CBIR based on various

**Productivity with Health, Safety, and Environment** pp 47–54

To Study the Stress Management of Women Police in Pune Urban Area

[Nandini Patole](#), [Shilpi Bora](#), [Mahesh D. Goudar](#) & [Abhijit Malge](#)

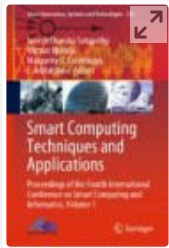
Conference paper | [First Online: 14 May 2022](#)

28 Accesses

Part of the [Design Science and Innovation](#) book series (DSI)

Abstract

Work-related stress and allied physical and psychological well-being issues are not addressed for women police personnel in Indian context with sufficient importance. In this study, the specialist has embraced distinct research structure to explore and examine the given issue. Depictions being made on the bases of logical perceptions are disclosed to be more exact by applying different techniques. The universe of this study is constrained to Pune District. 50 women police were selected randomly. A suitability sampling method (percentage) is used for selecting sample in the study. Majority part of the respondents faces issues



Smart Computing Techniques and Applications pp 525–536

Yield Estimation and Drought Monitoring Through Image Processing Using MATLAB

[Shaikh Akbar Shaikh Rasul](#) , [Jadhav Swamini Narendra](#) & [Dipti Y. Sakhare](#)

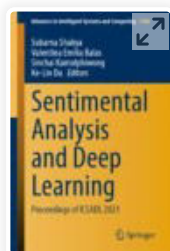
Conference paper | [First Online: 08 July 2021](#)

279 Accesses

Part of the [Smart Innovation, Systems and Technologies](#) book series (SIST,volume 225)


Abstract

This paper elucidates the pre-harvest yield estimation method and technique for cotton crop by image processing. This pixel-based image analysis of image processing is done using the image processing toolbox of the MATLAB 2019b. The images for abovementioned purpose are taken through camera armed drone (quadrotor). Further, there is a need for a better and transparent surveying method to assess the eligibility of a particular farm, for claiming the agricultural insurance. From the findings of proposed research, a suggestion for Agriculture Insurance Companies



Sentimental Analysis and Deep Learning, pp 451–464

Covid-19 Data Analysis to Predict the Level of Hospitalization

[Advet Jadhav](#) , [Maheshwari Satpute](#), [Utkarsh Rai](#),
[Apeksha Wadibhasme](#) & [Usha Verma](#)

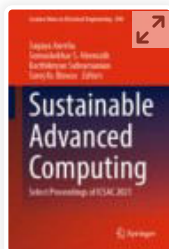
Conference paper | [First Online: 26 October 2021](#)

510 Accesses

Part of the [Advances in Intelligent Systems and Computing](#) book series (AISC, volume 1408)

Abstract

The spread of Coronavirus has resulted in a global pandemic. It has caused a heavy burden on medical facilities world over. The analysis of Covid-19 data presented in the paper may help the medical experts to categorize the patient into four levels of hospitalization based on their age, symptoms, and any previous medical history. Different prediction analysis algorithms are implemented, and results are presented to verify the accuracy of the implemented methods. Naive Bayes algorithm is found useful to categorize the patients with highest accuracy and R square score. Its results are compared with some of the traditional machine



Sustainable Advanced Computing pp 381–394

Region-Based Stabilized Video Magnification Approach

[Sanket Yadav](#) , [Prajakta Bhalkare](#) & [Usha Verma](#)

Conference paper | [First Online: 31 March 2022](#)

96 Accesses

Part of the [Lecture Notes in Electrical Engineering](#) book series (LNEE, volume 840)

Abstract

Eulerian video magnification (EVM) is used to magnify the imperceptible signals inside the video in the form of color. For this, it requires the jitter-free stable video of the target occupying the major part of the frame. And most of the time, the real-world/real-time videos cannot satisfy the above requirements completely. This is where EVM lacks optimal results. And this thought motivated authors to develop a new region-based stabilized video magnification (RSVM) approach. This preprocesses the input by stabilization of video, then detection–tracking–cropping of ROI, to get the motion-free-modulated input which satisfies requirements of EVM. Further, performance of both methods is

PAPER • OPEN ACCESS

Aqueous Two-Phase Separation (ATPS) Methods for Oleic acid extraction from Neem leaves

To cite this article: Shubham Gawade *et al* 2022 *IOP Conf. Ser.: Mater. Sci. Eng.* **1224** 012016

View the [article online](#) for updates and enhancements.

You may also like

- [Neoteric Media as Tools for Process Intensification](#)
C C Beh, R Mammucari and N R Foster
- [Liquid-liquid extraction of Pt\(IV\) from hydrochloric acid solutions using PPG 425 – NaCl – H₂O system](#)
I V Zinov'eva
- [Metallic and semiconducting carbon nanotubes separation using an aqueous two-phase separation technique: a review](#)
Malcolm S Y Tang, Eng-Poh Ng, Joon Ching Juan et al.

Aqueous Two-Phase Separation (ATPS) Methods for Oleic acid extraction from Neem leaves

Shubham Gawade, Sandeep P. Shewale and Amravati Gode

School of Chemical Engineering, MIT Academy of Engineering, Alandi (D), Pune, India-412105

Corresponding author's e-mail address: agode@mitaoe.ac.in

Abstract. The aqueous two-phase separation system (ATPS) signifies an environmentally responsible approach for the extraction of bioactive compounds from a plants basis, as it is a liquid-liquid fractionation technique centred on the inconsistency of two aqueous solutions. In this investigation, various experimental parameters are optimized as the speed of agitation (200, 300 400 and 500 rpm) and solvent ratio (1:1, 2:3 and 3:2) with 20 % (w/w) of Ammonium Sulphate (AMS) salt composition and 30 % (w/w) of Polyethelyene Glycol (PEG). The obtained extract contains alkaloids, flavonoids, tannins, glycosides, acids and total phenolic compounds (TPC). The extracted Oleic acid by the ATPS method was measured with gallic acid equivalent (GAE) of TPC extracted from neem leaves powder. The determined concentration of oleic acid in the practice of TPC is 8.033 mg of GAE/g from the optimized experimental parameter. The optimized results can be cast off for a commercial process on an industrialized scale. Also, the mathematical modelling investigation was done to intent the critical impeller speed (Njs) with the Zwittering model. The identified model calculates the essential speed of agitation (rpm) for maximum extraction yield.

Keywords: Oleic acid, Total phenolic compounds (TPC), Aqueous Two-Phase Separation System (ATPS), Gallic Acid Equivalent (GAE), Critical Impeller Speed (Njs).

1. Introduction

Herbs are used for flavouring, food, medicine, or perfume from ancient times. Culinary use naturally differentiates herbs are implying the leafy green portions of spice also a product from a different part of the plant containing seeds, roots, bark, and fruits. Furthermore, medicinal contents available in the plant's parts are used for the production of some pharmaceutical products such as aspirin, colchicine, ephedrine, morphine, physostigmine, pilocarpine, quinidine, reserpine and vincristine, etc [1-2]. The approach of isolating the bioactive components from the medicinal plants and used for the manufacturing of some pharmaceutical products are becoming prominent. Generally, organic solvents such as methanol, ethanol and diethyl ether are usually helped for extracting the bioactive compounds as of plant basis by the outmoded extraction arrangements. These solvents are relatively expensive,



needs distinctive processing conditions and most importantly disposal of the solvents is a major concern as they are not environmental responsive [3].

Conventional extraction processes are time-consuming and need more solvent for carrying out an operation, also after extraction, the added cost of purification and solvents recovery makes the process uneconomical.

Whereas, ATPS two-stage extraction is developing as a successful and flexible green system for the downstream handling of biomolecules. Fluid two-stage frameworks are low unpredictability frameworks with high adaptability [4]. That is, an expansive assortment might be acquired utilizing substances that pursue the Green Chemistry guideline on ecotoxicity, biodegradability, bioaccumulation and constancy, limiting waste and amplifying yields. Furthermore, they conform to the guideline of changeover of naturally safe structures to permit work under air weight. Since the 1970s numerous classified and out examinations have announced the filtration of proteins and other biologic materials utilizing ATPS, and numerous specialists have considered different operations of ATPS for the extraction and cleaning of organic products [5]. However, the utilization of such frameworks for the recuperation of phenolic mixes from plant materials is extremely constrained. In addition, there is broad writing about the thermodynamic properties of ATPS be that as it may, to the best of our insight, their application to crude unpurified examples has been very constrained [6].

Subsequently, the late nineteenth-century fluid two-phase extraction has been identified to the entire world. Aqueous two-phase can be framed through an extensive diversity of characteristics or else engineered water-solvent polymers& salt blends [7]. Watery two-phase extraction is developed for protected, sparing partition and cleaning of biomolecules, for example, proteins and catalyst extraction. Fluid extraction has numerous favourable circumstances; it is biocompatible, has low interfacial surface pressure among stages and it has high water content, the procedure can incorporate and the ability for strengthening [8-9].

Likewise, the level of corruption for biomolecules is low. In any case, two-polymer and polymer-based salt frameworks have developed quickly and a considerable measure of effort has been placed keen on concentrate this strategy utilizing these sorts of aqueous two-phase separation systems (ATPS). Aqueous two-phase extraction is known as an operative, adaptable and significant developing green method for the subsequential treating of biomolecules. This strategy has points of interest completed traditional extraction systems similar to, simplicity of scaling-up, condition benevolent, minimal effort, fit for nonstop activity and is effective for some sorts of trials exceptionally for the fixation and refinement of biomolecules. The utilization of partiality in ATPS can affect the developed recuperation earnings and developed refinement bends of bio consistent items such as it is an essential phase recuperation strategy [10]. Water as the foremost constituent of together stages in ATPS practices a moderate setting for bioactive molecules to distinct and polymers steady to the assembly and biotic doings through further liquid-liquid extraction approaches could impairment natural goods since of the development circumstances and biological solvents such method reduces the purity of active ingredient present in the extract.

There are two fundamental sorts of ATPS: polymer-polymer and polymer-salt frameworks. The mind-boggling expense of some shaping stage polymers (e.g dextran) limits the use of these frameworks, just legitimized when the expense of the result of intrigue is extensive. Consequently, the choice of the more temperate polymer-salt frameworks is profoundly suggested [10-11].

The novelty of the proposed work is that during the extraction itself two different layers of aqueous solution and salt is obtained, which can help further to reduce the cost of separating components. Also, the systems can be designed by partying a diversity of components in water and two-polymer and polymer-salt systems have developed quickly. The said work majorly focuses on the extraction of oleic acid from neem leaves to powder using ATPS (water + polymer + salt) based on PEG and ammonium sulphate. The aim is to optimize various experimental parameters (time, ATPS composition, particle size) for the removal of Oleic acid from neem leaves powder and its additional practices as natural antioxidants.

2. Material and Methods

The Neem powder was obtained from Hari Parshuram Aushdhalya, Pune., Polyethelyene Glycol (PEG) was procured from SRL Chemicals Pvt Ltd, Mumbai. Folin Ciocalteu's reagent was procured from Qualigens Fine Chemicals, Mumbai. Ammonium Sulphate (AMS) was procured from S.D. Fine Chemicals Pvt Ltd, Mumbai.

2.1. Batch extraction

Batch extractions are a modest method for the extraction of bioactive compounds. The stages in this method are equipped with a 50 ml glass reactor with a four-bladed glass turbine impeller and the combination to be divided is supplementary. Subsequently collaborating, phase parting is proficient each by resolving below gravity. The stages are disconnected and investigated to improve the alienated constituents of the preliminary mixture. The object product would be focused at any of the stages and the pollutants in the additional form. In various cases, reclamation and attentiveness of the product that produces beyond 90% can be attained with a particular extraction stage.

One particular phase removal does not give adequate retrieval, recurrent extractions can be supported obtainable in a sequence of communicating and parting components [12]. The fluid dividers into two stages, each covering added 80% liquid. When basic biomolecules are supplementary to these combinations, biomolecules and cell wreckages are dividers among the stages; by choosing suitable circumstances, cell remains can be limited to one stage as the object bioactive molecule barriers. The segregating of biomolecules among segments mostly be contingent on the equilibrium connection of the arrangement. The partition coefficient is demarcated as [12-13].

$$K = \frac{C_{AT}}{C_{AB}}$$

Where C_{AT} is the equilibrium attentiveness of constituent A in the upper phase and C_{AB} is the equilibrium adsorption of A in the lesser phase. If constituent A helps the greater stage the worth of K will be better. In numerous aqueous arrangements, K is continual finished with an extensive collection of deliberations, as long as the molecular possessions of the stages are not transformed. The theoretic yield in the topmost stage, Y_T , can be premeditated relative to the capacity ratio of the stages, R (up to volume / below volume), and the partition coefficient K of the object molecule as follows [12-13]:

$$Y_T = \frac{V_T C_{AT}}{V_O C_O} = \frac{V_t C_{AT}}{V_t C_{AT} + V_B C_{AB}} = \frac{1}{1 + [\frac{1}{KR}]}$$

Similarly, the theoretic yield in the bottommost stage, Y_B is known by,

$$Y_B = \frac{1}{1 + [\frac{1}{KR}]}$$

Consequently, by changing anyone like K or R we can effortlessly upsurge or reduction the profit of the object particle [14]. Additional constraint recycled to describe two-phase partitioning is the concentration factor, δ_c , distinct as the ratio of produce attentiveness in the favoured stage to the original product attentiveness.

$$\delta_{C,T} = \frac{C_{AT}}{C_{Ao}} \quad (\text{Product partitions to the higher phase})$$

$$\delta_{C,B} = \frac{C_{AB}}{C_{Ao}} \quad (\text{Product partitions to the lower phase})$$

2.2. Determination of the binodal

By settlement, the constituent mainly in the lower layer is represented as abscissa and the predominant element in the upper stage is represented as ordered. The three systems are explained realistically.

2.2.1 Turbidometric titration

In the tubing, with suitable backup solutions, formulate systems through different configurations of recognized weight. Note the added size due to titration, for example, if 5 g methods are organized, use 10 ml tubes. As an example, shows the systems for different systems that can use PEG-phosphate and PEG-dextran, and the essential designs. This can be replicated in a worksheet to permit easy intention. Note down the mass of the tube and titration drop by drop, with suitable dilution till the scheme is zeroed, i.e., a stage is formed.

This can be done through the scheme is continuously mixing or accumulation a droplet, collaborating, adding a second drop and continues the same process. To confirm that it has formed a single-stage system, the schemes must be centrifuged (for example 1000-2000 g, 5 min). Record the concluding mass of the tube and estimate the mass of the additional dilution just before the formation of a phase. Since the number of graduate systems is relative to the total of points in the binodal, superior precision is obtained with a superior number of schemes [15].

2.2.2 Cloud point method

Balance 5 g of a standard solution of constituent X into a 25 ml narrowed flask. Then add drop by drop, a reserve solution of the Y component up to the principal indication of turbidity, which is the cloud point. Note the weight of the Y component necessary for the mixture to become cloudy. This provides the first point in the binodal. Also, add a known weight of diluent lower the cloud point and duplication as indicated [15-16].

2.2.3 Determination of the Tie line

Measuring the connection line for polymeric schemes comprising an optically active composite, for example, PEG-dextran, PEG-Ficoll and ethylene oxide-propylene as well as oxide-Reppal PES 100.

2.2.3.1 Polymeric Methods Comprehending One Optically Active Polymer

Formulate a standard curve for the lively constituent, in the variety of 0 to 10% (p / v), i.e. inside the linear series, through the identical sections arrange a second standard curve for the refractive measure of the index. If the scheme is arranged in a shield, the average curves for the clean constituents must be completed with a similar safeguard, since the salts similarly subsidize the refractive index. Get ready the phased scheme for investigation, assembly sure that the phase components mix well; let the phases separate.

To ensure complete separation, centrifuge at low speed (for example 1000-2000 g, 5 min). The system proportions should be appropriate to permit deduction of at least 5 g upper and lower stage for phase concentration investigation and an additional quantity for density extents. Distinct the higher and subordinate stages building certain not to origin stage relations. Make the suitable dilutions, for example, watery 5 g of phase with the suitable solvent to 25 ml in a volumetric container. Extend the visual revolution for every stage and estimate the individual concentrations. The concentration of another constituent is resolute by determining the refractive index of the developed and subordinate stage and deducting the influence of the refractive index acquired from the optically lively constituent [17].

2.2.3.2 Polymer-Salt Systems

Formulate a standard curve aimed at salt conductivity within the linear series (in% w / v). Arrange the stage schemes as indicated above and eliminate 5 g of samples of the higher too subordinate phases and

diluted with liquid and lyophilized, then note the dehydrated weight. Eliminate an additional section from the higher and subordinate stage, diluted with water and extent the conductivity of every stage. Estimate the salt absorption and deduct the mass involvement of the dehydrated mass of the section [16-18].

3. Results and Discussion

In this investigation, various experimental parameters were optimized such as speed of agitation (200 rpm, 300 rpm, 400 rpm & 500 rpm) and solvent ratio (1:1, 2:3 and 3:2). Extract samples were pipette out at specific time intervals like every 15 min and further standard Folin–Ciocalteu's method was used for analysis purposes. The obtained outcomes indicated that the TPC concentration of TPC in the extraction stage at a specific time. By changing the parameters speed of agitation and solvent ratio in the batch reactor at different times the results were optimized and used for further study.

3.1 Speed of agitation

About 5 g of powder of neem leaves was weighted and fed to 50 ml of batch reactor along with AMS salt (20 %w/w) and 50 ml of PEG (30 %w/w) at a temperature of 30°C till the extraction rate was a steady-state. The maximum speed of agitation produces high turbulence in the batch reactor and increases the rate of mass transfer [11]. The results of various experiments were performed for multiple agitation speeds is shown in figure 3.1 The experimental results shows that the concentration of TPC at 200 rpm significantly low as compared to 500 rpm, but there could be a marginal difference of TPC concentration of 400 and 500 rpm, speed of agitation., therefore for the further study, speed of agitation (400 rpm) was used. The circulation of TPC compounds from the neem leaves powder in the solvents could expand with the accumulative agitation speed. An added rise in the agitation speed has no substantial effect on final extraction yield; it clues that external mass transfer fighting is inconsequential at 400 rpm

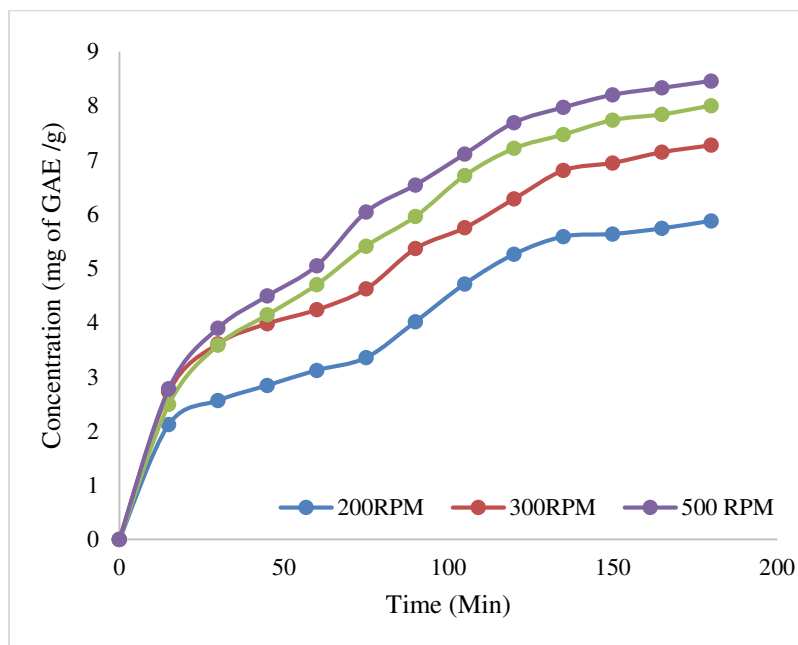


Fig. 3.1 Concentration of TPC obtained from Batch at temp 30°C speed of agitation 200, 300, 400 & 500 rpm)

3.2 Effect of Solvent Ratio (AMS: PEG)

The TPC concentration values in the extract were considered for changed extraction times at different solvent ratios (1:1, 2:3 & 3:2) and the same is shown in Figure 3.2. About 5 g of powder of neem leaves

was weighted and fed to 50 ml of batch reactor along with AMS salt (20 %w/w) and 50 ml of PEG (30 %w/w) at a temperature of 30°C till the extraction rate was a steady-state. There was an increase in TPC concentration and experiential for solvent ratio 01:01. A substantial quantity of solvent favours an additional concentration gradient and cuts diffusional resistance that rises the rate of extraction rate. There was a rise in TPC concentration, for the solvent ratio of 1:1 to 3:2. A substantial quantity of solvent tends to the added concentration gradient and drops diffusional resistance that rises the rate of extraction [11].

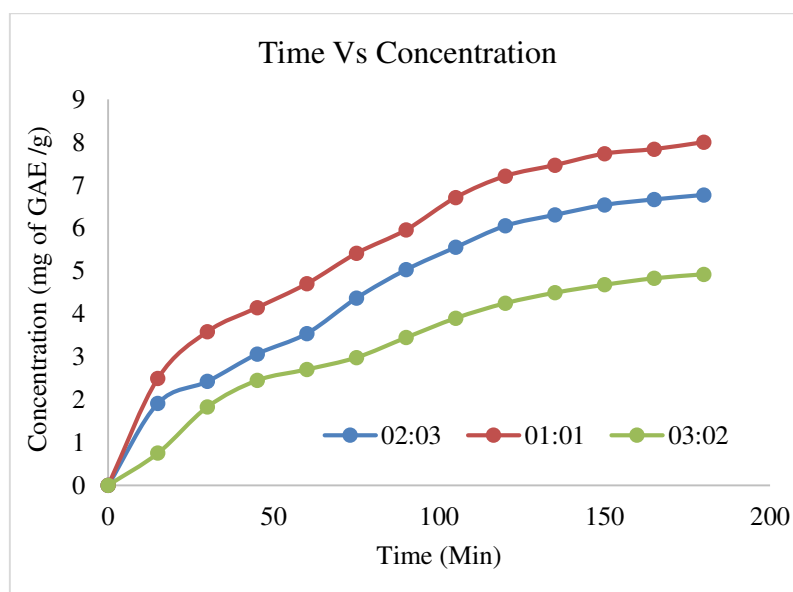


Fig.3.2 Effect of Solvent Ratio (AMS: PEG)

4. Conclusion

The investigation of the ATPS method was beneficial for the sub sequential treating of biomolecules. Also, the experimental parameters were optimized such as speed of agitation and solvent ration and the optimized parameters as 400 rpm and 01:02 solvent ration respectively with AMS salt (20 % w/w) & PEG (30 % w/w). The obtained extract also contains alkaloids, flavonoids, tannins, glycosides, acids and total phenolic compounds (TPC). The extracted Oleic acid by ATPS technique was measured with gallic acid equivalent (GAE) of TPC extracted from neem leaves powder. The determined concentration of oleic acid in the practice of TPC is 8.033 mg of GAE/g from the optimized experimental parameter. The optimized results can be used for a commercial process on an industrial scale.

References

- [1] Alasalvar C, Karamac M, Amarowicz R, Shahidi F, 2006. Antioxidant and antiradical activities in extracts of hazelnut kernel (*Corylus avellana* L.) and hazelnut green leafy cover. *J Agric Food Chem* 54: 4826-4832.
- [2] Babitskaia V, Shcherba V, Lkonnikova N, 2000. Melanin complex of the fungus *Inonotus obliquus*. *Prikl Biokhim Mikrobiol* 36(4): 439-444.
- [3] Dallora N, Klemz J, Filho P, 2007. Partitioning of model proteins in aqueous two-phase systems containing polyethylene glycol and ammonium carbamate. *Biochem Eng J* 34(1): 92-97.
- [4] Karakatsanis A, Liakopoulou M, 2007. Comparison of PEG/ fractionated dextran and PEG/industrial grade dextran aqueous two-phase systems for the enzymic hydrolysis of starch. *Eng* 80(4): 1213-1217.
- [5] Alencar L.V.T.D., Passos L.M.S., Martins M.A.R., Barreto I.M.A., Soares C.M.F., Lima A.S., Souza R.L., 2020. The complete process for the selective recovery of textile dyes using an

aqueous two-phase system. *Sep. Purif. Technol.* 253: <https://doi.org/10.1016/j.seppur.2020.117502>.

- [6] Ying H, Diyun C, Shuqi C, Minhua S, Yongheng C, Yixiong P, Gutha Y, 2021. A green method for recovery of thallium and uranium from wastewater using polyethylene glycol and ammonium sulfate based on the aqueous two-phase system. *J. Clean. Prod.* 297: <https://doi.org/10.1016/j.jclepro.2021.126452>.
- [7] Leitner M, Vandelle E, Gaupels F, Bellin D, Delledonne M, 2009. NO signals in the haze: Nitric oxide signalling in plant defence. *Curr Opin Plant Biol* 12(4): 451-458.
- [8] Liu SP, Zong ZM, Wei Q, Wei XY, 2010. Study on organic compounds in aqueous two phase system phase forming and distribution. *Chem Ind Times* 24(12): 21-24.
- [9] Ahareh AS, Gholamreza P, Javad RS, Shahla S, Naghmeh H, 2020. Separation of erythromycin using aqueous two-phase system based on acetonitrile and carbohydrates. *Fluid Phase Equilib.* 505: <https://doi.org/10.1016/j.fluid.2019.112360>
- [10] Perla JV, Salvador VG, Iran AT, Yolanda SM, Leticia GC, Artemio PL, Diana GR, 2020. Separation of bioactive compounds from epicarp of 'Hass' avocado fruit through aqueous two-phase systems. *Food Bioprod. Process.* 123:238-250.
- [11] Sandeep Shewale & Virendra K. Rathod (2018) Extraction of total phenolic content from *Azadirachta indica* or (neem) leaves: Kinetics study, Preparative Biochemistry & Biotechnology, 48:4, 312-320, DOI: 10.1080/10826068.2018.1431784
- [12] Singh SB, Jayasuriya H, Dewey R, Polishook JD, Dombrowski AW, Zink DL, Guan Z, Collado J, Platas G, Pelaez F, Felock PJ, Hazuda DJ, 2003. Isolation, structure, and HIV-1 integrase inhibitory activity of structurally diverse fungal metabolites. *J Ind Microbiol Biotechnol* 30(12): 721-731.
- [13] Srinivas ND, Barhate RS, Raghavarao KSMS, 2002. Aqueous two-phase extraction in combination with ultrafiltration for down-stream processing of *Ipomoea peroxidase*. *J Food Eng* 54(1): 1-6.
- [14] Uma DB, Ho CW, Wan Aida WM, 2010. Optimization of extraction parameters of total phenolic compounds from Henna (*Lawsonia inermis*) leaves. *Sains Malaysiana* 39(1): 119-128.
- [15] Wang SY, Wu JH, Cheng SS, Lo CP, Chang HN, Shyur LF, Chang ST, 2004. Antioxidant activity of extracts from *Calocedrus formosana* leaf, bark, and heartwood. *J Wood Sci* 50: 422-426.
- [16] Zhao YX, Miao KJ, Zhang MM, Wei ZW, Zheng WF, 2009. Effects of nitric oxide on production of antioxidant phenolic compounds in *Phaeoporus obliquus*. *Mycosystema* 28(5): 750-754.
- [17] Zheng WF, Zhao YX, Zhang MM, Wei ZW, Miao KJ, Sun WG, 2009. Oxidative stress response of *Inonotus obliquus* induced by hydrogen peroxide. *Med Mycol* 47: 814-823.
- [18] Zheng WF, Miao KJ, Liu YB, Zhao YX, Zhang MM, Pan SY, Dai YC, 2010. Chemical diversity of biologically active metabolites in the sclerotia of *Inonotus obliquus* and submerged culture strategies for up-regulating their production. *Appl Microbiol Biotechnol* 87(4): 1237-1254.

Simulation of M-ary QAM and M-ary PSK Modulation Techniques Using MATLAB GUI

Pranjal Dwivedi^a, Alok Ranjan^a, Ashish Srivastava^{a*}

^a*Department of Electronics & Telecommunication, MIT Academy of Engineering, Pune, India*

Abstract

The world has seen a transformation due to the recent pandemic. The field of education is drastically affected by it. There is a need to move from classroom teaching to online teaching, and the biggest hurdle is to impart practical knowledge. This paper attempts to study the concepts like M-ary Phase shift keying (PSK) and M-ary Quadrature amplitude modulation (QAM), used in modern-day communication systems, using a simulation platform. For this purpose, simulation using a graphical user interface (GUI) is proposed to study various M-ary PSK and M-ary QAM types. MATLAB is used to implement the GUI. The modulation, transmission, demodulation, and recovery of a signal implemented through the GUI will help learners understand the concepts better. Moreover, the constellation diagrams for M-ary PSKs and M-ary QAMs can be examined using the developed GUI.

Keywords- *Phase Shift Keying (PSK), Quadrature Amplitude Modulation (QAM), Constellation diagram, Graphical User Interface (GUI)*

© 2021 – Authors.

1. Introduction

The field of digital communication is growing and evolving rapidly, modulation techniques and their enhancements have become important. The digital modulation techniques must be tested and analyzed using the latest mathematical simulation platforms for improvements and effectiveness. With the development of communication techniques, the demand for reliable and fast data transmission has increased, which is also a reason for the simulation and analysis of these modulation techniques. Now that we know about increasing the data rate by changing the envelope, phase, and frequency of the carrier signal, different digital modulation schemes based on keying techniques are used to implement digital communication systems. These modulation schemes map the baseband data into more than four possible carrier signals because the degrees of freedom are two, i.e., phase and amplitude. In M-ary signaling, two or more bits are grouped, and symbols have some energy associated with them, known as symbol energy. The number of signals that can be generated is given by $M=2^m$, where m is an integer indicating the number of bits. Different modulation types like amplitude shift keying,

* Corresponding author.

E-mail address: aksrivastava@entc.mitaoe.ac.in

frequency-shift keying, and phase-shift keying exist depending on whether the amplitude, phase, or frequency is changed. The modulation technique is called Quadrature Amplitude Modulation (QAM) when the amplitude and phase are varied.

These days communication systems are studied through the simulation environment Sadinov et al., 2017. Implementation and calculation of the BER of M-PSK and M-QAM can be done using the signal space approach Lu et al., 1999. Laboratory sessions can be conducted in three ways, first, the live hands-on sessions, second, through simulation, and third remote laboratories Nickerson et al., 2006. Conducting laboratory sessions for engineering education needs a careful lookout, with detailed dos and don'ts Krivickas et al., 2007. A different approach needs to have opted for teaching-learning in distance learning mode Tomei, 2010. Digital communication experiments can have a wide range of concepts from basics to complex like jamming Wickert, 2011. MATLAB is used as the simulation platform and is a suitable platform for explaining wireless communication concepts to undergraduate students Zheng et al., 2007. Simulink being graphical, this programming environment gives good visualization of the results Hirst et al., 2013. The advanced applications of digital communication can be designed using MATLAB Yuting et al., 2010. The GUI can be converted to a mobile application for ease of access. Also, GUI will help in increasing learning efficiency. Interactive learning software can improve the learning experience of the students Naim et al., 2016. The programming approach can help the learners to understand software engineering Douglas 2005. The further sections elaborate on the concerning theory and methodology that were undertaken to implement the idea presented in the paper. The second section describes the considered modulation technique along with the role of noise in the communication system. The third section deals with the discussion and interpretations of the developed GUI. The conclusion drawn through the implementation and execution of is the presented idea is elaborated in the fourth section.

2. The Modulation Techniques

The section describes the theory behind the considered modulation technique and methodology opted to implement the GUIs. It is essential to emphasize the importance of M-ary encoding and the modulation techniques. The section concludes with a brief description of noise in the communication system in general and developed GUI in particular.

2.1. M-ary Encoding

To represent a signal using more than two bits, we use the word *M-ary*. The term *M* defines the number of bits being used to transmit one symbol, and it also gives an insight into the combinations and energy levels. M-ary encoding plays a critical role in digital modulation and communication. It improves the SNR, increases power and bandwidth efficiency in a modulation scheme. Different M-ary encoding is used in the digital world. Due to the features mentioned above, the encoding techniques are known with specific names. For instance, a 2-ary Phase Shift Keying modulation (2-PSK) is known as Binary Phase Shift Keying. Similarly, 4-PSK is known as Quadrature Phase Shift Keying.

In these modulation techniques, two or more bits are considered together to form a symbol, and the symbols $S_1(t)$, $S_2(t)$, ..., $S_m(t)$ are transmitted during the symbol period T . The possible number of signals depends on the value of M .

These modulation techniques find attractive application in the band-limited channels because of their higher bandwidth efficiency at the expense of power efficiency. There are certain drawbacks of these modulation techniques, like, poor error performance because of the minimal separation between the signals. Another

important point that needs to be taken into consideration is the bit rate and baud rate. Different modulation techniques result in different baud rates, which vary the bandwidth requirement of the signals.

As the value of M goes on increasing for a particular modulation scheme, the number of bits transmitted per symbol also increases, the resulting combination of bits forming a signal increases and, in turn, increasing the constellation points in a constellation diagram. With the rise in the constellation points, there tends to be some inter symbol interference (ISI) between the points. This results in distortion and corruption of the transmitted signal as the decision boundary of one symbol start interfering with the other symbols' boundary.

2.2. BPSK

It is a two-phase modulation. A binary message with 0 and 1 is represented by two different phase states, i.e., 0° and 180° for 0 and 1, respectively. For generating a BPSK signal, a basis function is chosen. Once we get the basis function, any vector present in the signal space can be represented as a linear combination of this function. In BPSK the modulation is done by varying the phase of the basis function depending on the message bits. The phase states of the carrier signal can be represented as follows:

$$S_1(t) = A_c \cos 2\pi f_c t, \quad 0 \leq t \leq T_b \text{ for binary 1} \quad (1)$$

$$S_0(t) = A_c \cos(2\pi f_c t \pm \pi), \quad 0 \leq t \leq T_b \text{ for binary 0} \quad (2)$$

Here A_c represents the amplitude of the sinusoidal signal, f_c is the carrier frequency calculated in Hz, t is the instantaneous time in seconds, and T_b is the bit period in seconds. The signals S_0 and S_1 denote the modulated signal when information 0 and 1 are transmitted, respectively.

The BPSK transmitter can be implemented using the nonreturn to zero (NRZ) polar coding method and multiplying the output by a reference oscillator running at carrier frequency f_c . In this case, it is convenient to choose the oversampling factor as the ratio of sampling frequency (f_s) and the carrier frequency (f_c).

2.3. QPSK

In this modulation technique, two information bits that are combined as one symbol are modulated. The modulator is required to select one of the four possible carrier phase shift states. A QPSK signal with a symbol duration T is defined as:

$$S(t) = A_c \cos(2\pi f_c t + \theta_n), \quad 0 \leq t \leq T \text{ for } n = 1, 2, 3, 4 \quad (3)$$

and the signal phase is defined as:

$$\theta_n = (2n - 1)\pi/4, \quad (4)$$

Therefore, the possible phase outcomes are $\pi/4$, $3\pi/4$, $5\pi/4$ and $7\pi/4$. Equation [4] above requires two orthogonal basis functions, which are in-phase and quadrature signaling points.

For the generation of a QPSK signal, a splitter is used to separate the odd and even bits from the generated information bits. The odd bits and even bits are converted to NRZ polar at the same time. It is to be noted here that the BPSK modulation requires a symbol duration same as that of bit duration, but when QPSK is used, the

symbol duration becomes twice as that of bit duration. Hence, QPSK sends a message at a rate that is twice as compared to the BPSK.

2.4. *M*-ary QAM

Quadrature amplitude modulation is a modulation technique that encodes the information or message signal with the carrier signal by varying the carrier signal's amplitude and phase. The carrier signal is subdivided into two signals which are 90° out of phase from each other. These signals are termed In-phase and Quadrature phase signals. Since both the amplitude and phase are constantly varied, the signal envelope is not constant and has a higher bandwidth efficiency than other *M*-ary signaling schemes with the same power consumption. Suppose M_1 and M_2 represent the number of possible values of amplitudes and phases, respectively. The total number of bits per symbol transmitted is the combination of amplitude and phase modulation and is given by $\log_2(M_1M_2)$.

Constellation diagram is used for graphical representation of the envelope of the state of the symbol and is considered an essential tool in analyzing the performance of QAM. The x-axis and the y-axis of the diagram represent the in-phase and the quadrature-phase components of the modulated signal, respectively. The separation between the signals in the constellation diagram tells us about the difference between the modulation schemes and how the receiver distinguishes them.

To measure the modulation schemes' performance, one needs to calculate the bit error rate (BER) while assuming that the systems contain additive white Gaussian noise (AWGN).

2.5. Noise

Noise is the unwanted electrical signal that is present in almost every electrical system. It interferes with the signal and leads to improper or distorted production and reception of the transmitted signal. Due to this, interference generates specific errors in the signal analysis and affects the sensitivity of receivers.

The noise is present in almost all communication systems and is the primary disturbance in those systems. AWGN has typically zero mean. The deviation of the received signals with noise increases with an increase in the variance. This noise is used to model any communication systems where the noise interferences are kept in check.

3. Results and Discussions

A Graphical User Interface Development Environment (GUIDE) can be used to create custom applications and user interfaces. A GUI can be made by dragging and dropping components. GUIDE generates two files, one contains layout information, and the other has implementation code. The simulation of discussed modulation techniques through GUIs was developed comprising a random signal, converting it into integer representation, modulation using inbuilt MATLAB functions, adding noise, simulation of the channel, demodulation using the inbuilt MATLAB function.

The GUI can also take desired inputs from the user and simulate the modulation and demodulation to show the results. Different parameters can be studied and analyzed through the developed GUI. Used parameters paved the way to compare the modulation techniques. The GUI of the modulation techniques along with constellation diagram was developed with the help of 'push button', 'box' and 'axes' widgets in MATLAB.

Various modulation techniques, including BPSK, QPSK, and QAM, can be learned using the options available on the GUI, as seen in Figure 1.

Figure 1 shows in-phase, and quad-phase components of the signal are depicted separately along with the combined modulated signal. From this figure, different phases can be observed at the message transitions from 0 to 1 or 1 to 0. Similarly, we can obtain BPSK, 8-PSK, and 16-PSK modulated signals by clicking on the corresponding push button on the GUI. On clicking the “Navigate to QAM” push button, the other GUI for QAM will open. In the second GUI, options for 4, 8, 16, and 64 QAM are provided. The learner can click on the desired technique to be studied. For example, on clicking the push button for 8-QAM, the results of this will pop up, as shown in Figure 2. A message signal is shown in the digital format (in terms of bits). The number of symbols is represented in terms of discrete signals in which there are M number of distinct amplitude levels. The symbols are separated by fixed symbol duration. Modulated signals in analog form can also be seen in the figure. In the same GUI for 8-QAM, the constellation diagram is also depicted. The reference constellation is adjusted to the desired constellation. Eight yellow points represent the transmitted symbol. The distance between each point and origin is different, which specifies the change in amplitude. Similarly, each point is located at a different location and specifies the phase change. With the help of the constellation diagram, the learner can easily find out the Euclidian distance for a particular modulation scheme.

Through Figure 3, the 16-QAM can be studied, and it gives the learner a better insight for understanding the modulated signal and the constellation diagram. The different information signal in digital format is considered as an input for the 16-QAM. Here also one can observe sixteen different amplitude levels in symbol representation in discrete form. Continuous, modulated signal can also be seen in Figure 3.

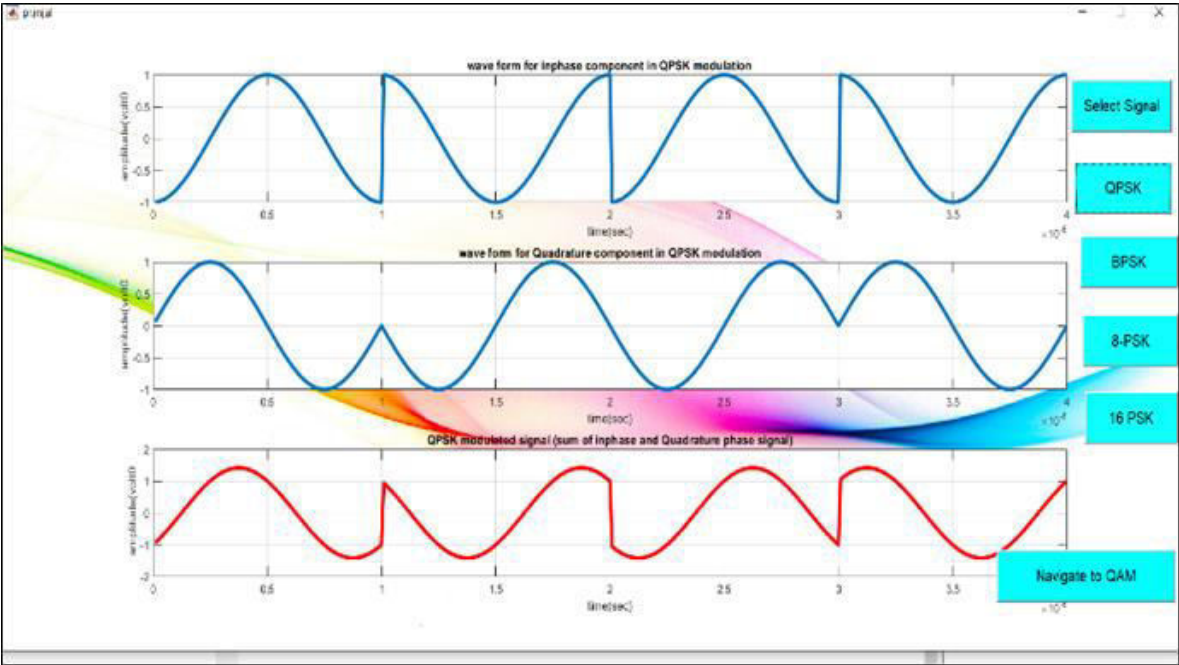


Fig. 1. In-phase, Quad-phase, and Modulated QPSK Signal

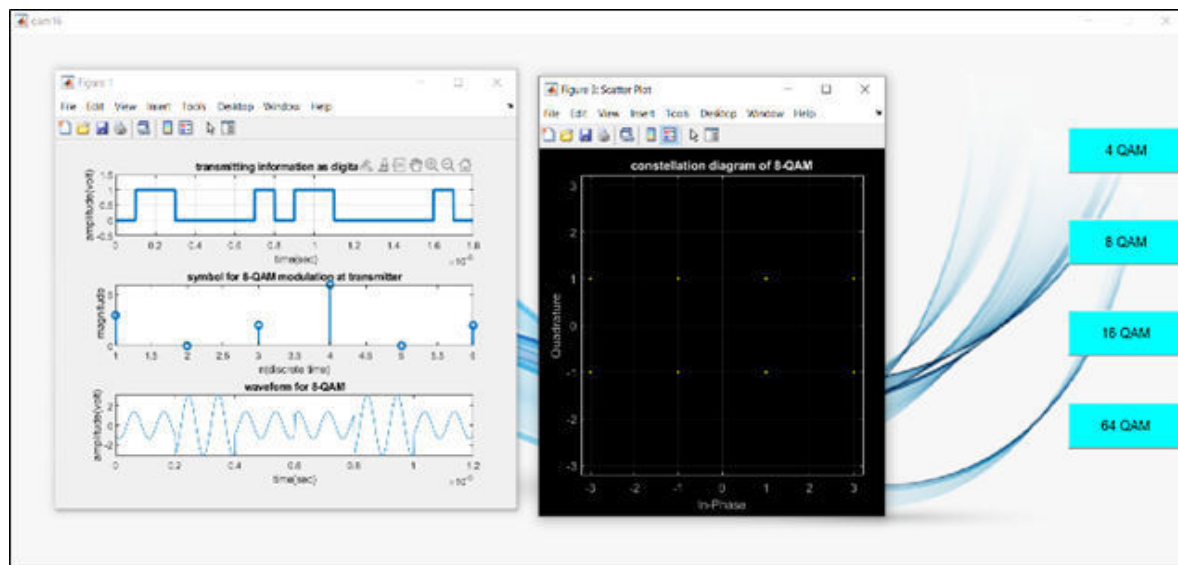


Fig. 2. 8-QAM Modulated Signal with Constellation Diagram

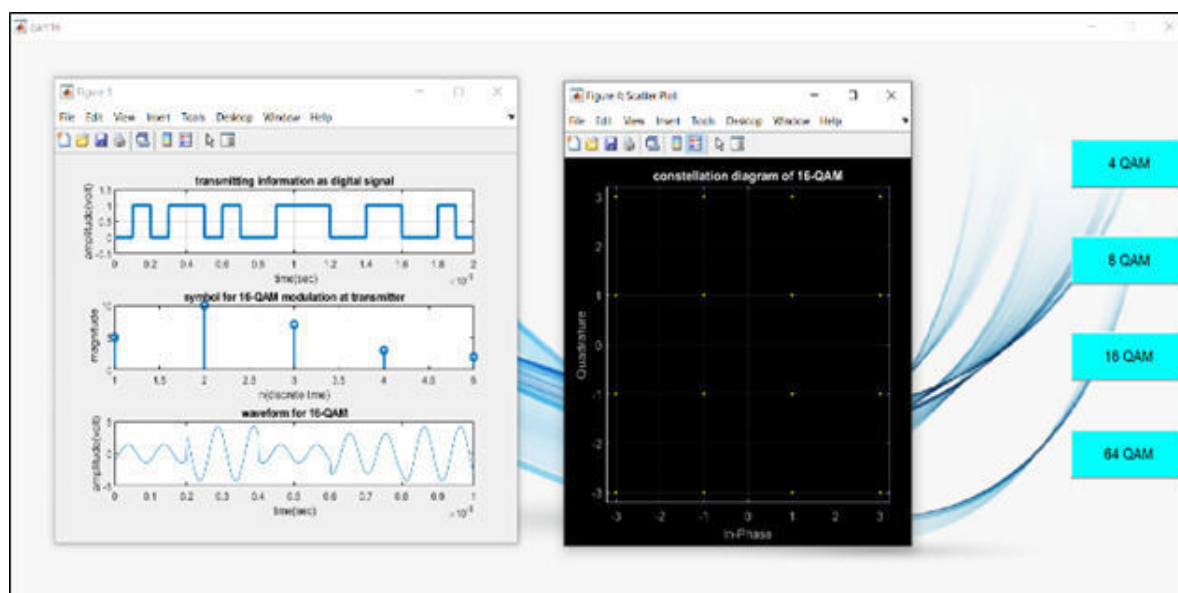


Fig. 3. 8-QAM Modulated Signal with Constellation Diagram

4. Conclusions

The paper elaborates the M-ary modulation techniques using MATLAB environment. The motivation for the paper's central theme was employed from the fact that practical teaching has been very difficult in pandemic situations and will raise an alarming situation if something is not done. Teaching-learning through the use of the developed GUI will efficiently help the students to visualize and understand different modulation schemes. The modulations considered are phase shift keying variants (BPSK, QPSK, 8-PSK, 16-PSK) and Quadrature Amplitude Modulation (4-QAM, 8-QAM, 16-QAM, 64-QAM). The developed GUIs will provide a better learning experience to the learner. The results show different stages of modulation of the message signal. The constellation diagram of the received signal after passing through the channel in the presence of noise can also be observed. With the increase in modulation order, Euclidian distance decreases; thus bit error rate increases. The lower value of modulation has disadvantages such as transmission problems, lesser bandwidth efficiency, and lesser power efficiency. The theoretical concepts of digital modulation techniques can be taught to a learner using the developed GUI for an improved learning experience without compromising on practical aspects in online or distance learning mode.

References

- S. M. Sadinov, May 22- 26, 2017, "Simulation Study of M-ARY QAM Modulation Techniques using Matlab/Simulink." MIPRO 2017, Opatija, Croatia
- Jianhua Lu, K. B. Letaief, Justin C-I Chuang, and Ming L. Liou, 2nd February 1999, "M-PSK and M-QAM BER Computation Using Signal-Space Concepts", IEEE Transactions On Communications, Vol. 47, No.
- J. Ma and J. Nickerson, pp. 1-24, 2006, "Hands-On, Simulated, and Remote Laboratories: A Comparative Literature Review," Journal of ACM Computing Surveys, vol. 38, no. 3.
- R. Krivickas and J. Krivickas, 2007, "Laboratory Instruction in Engineering Education," Global Journal of Engineering Education, vol. 11, no. 2, pp. 191-196.
- Lawrence A. Tomei, 2010, Designing Instruction for the Traditional, Adult, and Distance Learner: A New Engine for Technology-Based Teaching, Information Science Reference, New York, USA.
- M. Wickert, 2011 IEEE, 2011, "Digital Communication with Jamming Experiments for a Signal Processing First Course," Digital Signal Processing Workshop and IEEE Signal Processing Education Workshop (DSP/SPE), pp.101-106.
- J. Z. Zhang, R.D. Adams & K. Burbank, 2007 UICEE, "Using MATLAB to Improve Learning Effectiveness and Quality in an Undergraduate Course on Wireless Communications and Systems," Global J. of Engng. Educ., Vol.11, No.1, Australia, pp. 45-54.
- Brice A. Hirst and Yahong R. Zheng, 2013, "Utilization of MATLAB Simulink Exercises for an Undergraduate Communications Course," Proceedings of the 2013 American Society for Engineering Education Annual Conference & Exposition, American Society for Engineering Education.
- D. Yuting and F Lijun, 2010, "The Simulation Design of MATLAB applied to the Mode Technology of Digital Communication System," Third International Symposium on Information Science and Engineering, IEEE Computer Society, pp.438-441.
- Naim, Nani Fadzlina, et al. "Interactive Learning Software for Engineering Subjects Based on MATLAB-GUI." Journal of Telecommunication, Electronic and Computer Engineering (JTEC) 8.6 (2016): 77-81.
- Douglas Bell, 2005., Software Engineering for Students: A Programming Approach. 4th Edition, Pearson Education Limited, Harlow, England.



Pranjal Dwivedi is a student in the Department of Electronics and Telecommunication Engineering, School of Electrical Engineering, MIT Academy of Engineering Pune. He had been working in the field of wired and wireless communications as a research enthusiast.



Alok Ranjan is a student in the Department of Electronics and Telecommunication Engineering, School of Electrical Engineering, MIT Academy of Engineering Pune. For the last two years, he has been working in the communication domain and has a firm grip over the simulation platforms and latest technical tools.



Ashish Srivastava is working as an Assistant Professor in the Department of Electronics and Telecommunication Engineering, School of Electrical Engineering, MIT Academy of Engineering Pune. He is a Doctoral candidate in the National Institute of Technology Patna. Ashish's research interest lies in the field of communication engineering.

Robust Control Algorithm for Piezo-electric Energy Scavenging

Shailesh Shinde^{a*}, Ashitosh Chavan^{a†}, Aniket Gundecha^a, Kaliprasad Mahapatro^b

^aMIT Academy of Engineering, Alandi(D), Pune, Maharashtra, INDIA

^bAvantika University, Ujjain, MP, INDIA

Abstract

The paper proposes a robust control algorithm for the piezoelectric energy scavenging in the presence of uncertainties. The nonlinear dynamics makes the piezoelectric actuators unstable and shows substantial uncertainty and disturbances in the output. In this study a closed loop step down DC–DC converter along with the Extended State Observer (ESO) is implemented. This paper proposes step by step design of buck converter and its linear mathematical model. The output of a buck converter is taken as a feedback along with the heuristic implementation of ESO. Extended state observer is designed such that it estimates the state and lumped uncertainties. The proposed algorithm is addressed to maintain the output voltage constant in the piezoelectric energy harvester under the uncertainties. The efficacy of the proposed algorithm is verified using MATLAB Simulink and the result shown in this paper showcase a better voltage regulation in the presence of uncertainties and wide range of dynamic input voltage.

Keywords- *Buck Converter, Extended State Observer (ESO), Piezoelectric Energy Scavenging*

© 2021 – Authors.

1. Introduction

The demand for renewable energy sources is increasing day by day. The process of the conversion of renewable energy into electrical energy is referred to as energy scavenging and it can be utilized in many applications including portable electronics, wireless gadgets and power systems Lu et al., 2010. Energy harvester is used to recharge the battery and the input for the harvester is dynamic, as it is obtained from environmental energy sources such as sunlight, wind, etc. Lu et al., 2010. Different energy harvesting methodologies are available such as piezoelectric Ayrikyan et al., 2017, wind Wu et al., 2013, thermoelectric Hu et al., 2020 and solar Carvalho and Paulino, 2010. Because of better liberal vibration accessibility and good harvesting material property, piezoelectric energy harvesting based method is selected Ayrikyan et al., 2017.

In piezoelectric approach, due to unstable vibration status the output voltage is also changing Grace et al., 2011. In order to scavenge as much energy as possible, a run-time adaptive mechanism is required to track the output voltage with the vibration of piezoelectric element Chao et al., 2007. Energy scavenging systems provide constant output voltage with the growing application of DC–DC converter Gundecha et al., 2016,

* Corresponding author.

E-mail address: srshinde@entc.maepune.ac.in

† Corresponding author.

E-mail address: adchavan@mitaoe.ac.in.

Nguyen et al., 2021. The piezoelectric sensors are used to stimulate the development of specific converters to operate such actuators Bellmund et al., 2007. Different switching converter topologies have been employed to drive such actuators, buck Lakshmi and Raj, 2014, boost Gundecha et al., 2016, and buck-boost Lefeuvre et al., 2007.

The voltage in the output cannot be considered as constant and it should be controlled by different strategies. A variety of controlling strategies like PID controller Djmel et al., 2019, fuzzy logic Ardhenta et al., 2020, and sliding mode control Utomo et al., 2020 are available to control the power converter. The effects of uncertainties and disturbance in control are estimated by introducing some observing methods like disturbance observer (DO), State and disturbance observer (SDO) Chavan et al., 2019, Discrete Kalman Filter and High Gain Observers Ali et al., 2019, H_∞ Wang et al., 2020, Luenberger Observer Wang and Li, 2020. Extended state observer (ESO) Han, 2009 is a better observing technique that can estimate both state as well as disturbance with less plant information Li et al., 2011. The ESO is used to estimate the present uncertainty and disturbance in order to minimize the effect in the output Bin et al., 2014. ESO has been widely applied in various areas like motion control systems Mahapatro et al., 2019, robot control systems Ma et al., 2020 and vibrations Shi et al., 2021.

Based on the literature, most commonly used control algorithms and the observers are listed in Table 1.

Table 1. Literature on control algorithms & observers

Control Algorithms	Observers	
PID Control	Disturbance Observer (DO)	State & Disturbance Observer (SDO)
Sliding Mode Control (SMC)	High Gain Observers	Discrete Kalman Filter Observers
Fuzzy Logic Control	H_∞ Observer	

The rest of the paper is organized as follows: Section 2 introduces piezoelectric energy scavenging system. Section 3 describes the operation of a DC–DC buck converter. Section 4 gives the mathematical modelling of DC–DC buck converter. Section 5 explains the concept of control design. The results are shown with related discussion in section 6. The paper is concluded in section 7.

2. Piezoelectric Energy Scavenging

Piezoelectric materials are used for energy scavenging to convert mechanical strain into an electrical form due to their small size and the piezoelectric effect. The equivalent circuit of a vibrating piezoelectric element can be modeled as a source of sinusoid current $i_P(t)$ parallel to its C_p electrode capacitor.

AC–DC rectifier is required as the output of piezoelectric material is an AC signal. The magnitude of the polarization current I_p depends on the level of mechanical excitation of the piezoelectric element, frequency of mechanical vibration and hence the rectifier voltage may not be constant Ottman et al., 2003. The ability to achieve and maintain constant output voltage is accomplished by placing a DC–DC step-down converter between the rectifier and the electronic load as shown in Fig.1. A DC–DC step-down converter is known as buck converter. A buck converter is placed between the rectifier and the electronic load. The control approach used an extended state observer (ESO) for estimating state as well as lumped disturbance. This strategy gives constant and regulated output voltage by using ESO in the presence of certain uncertainties.

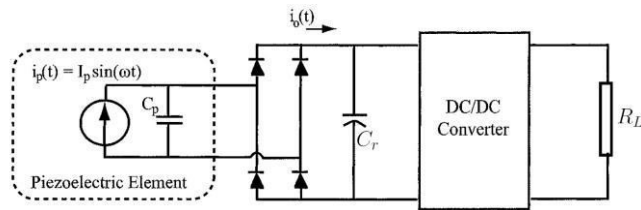


Fig. 1. Energy harvesting circuitry

The DC component of the output current and the rectifier capacitor voltage give the power of the piezoelectric element Ottman et al., 2003 are shown as;

$$\dot{i}_o(t) = \frac{2I_p}{\pi} - \frac{2V_r \omega C_p}{\pi} \quad P(t) = \frac{2V_r}{\pi} (I_p - V_r \omega C_p)$$

Where V_r is the rectifier capacitor voltage and ω is the resonating frequency.

The controller of the converter is designed to achieve and maintain the constant output voltage in presence of the uncertainties. The output obtained from the piezoelectric sensor is characterized and studied for selection of proper voltage levels for further interface. The frequency of vibration plays an important role in the generation of the corresponding electrical voltage Ottman et al., 2003, Vulture. The characteristics of a piezoelectric sensor when operated in different conditions are shown in Table 2. The tip mass range is considered from 0 gram to 7.8 gram and their corresponding variation in frequency, AC voltage and rectified DC voltage is stated in Table I. The system efficiency depends on the rectification output in conjunction with the DC-DC converter. A step down converter is used to maintain the constant output voltage.

Table 2. Characteristics of piezoelectric sensor

Tip Mass (gram)	Frequency (Hz)	Open Ckt. Vtg (rms)	Rectified O/P (V _{dc})	Tip Mass (gram)	Frequency (Hz)	Open Ckt. Vtg (rms)	Rectified O/P (V _{dc})
0	120	3.2	3.11	2.4	75	6.5	7.7
0	120	4.4	4.8	2.4	75	7.5	9.17
0	120	5.5	6.3	2.4	75	11.5	14.81
0	120	10.1	12.84	7.8	50	10.3	13.12
2.4	75	4.7	5.22	7.8	50	15.4	20.31

3. Buck Converter

Buck converter is referred to as step down converter. In a buck converter, an unregulated DC input voltage is converted to a regulated low DC output voltage. A typical buck converter is shown in Fig 2. The buck converter comprises a power MOSFET Ramirez et al., 2006 used as a controllable switch Q with two states $\mu = 0$ and $\mu = 1$, a diode D , an inductor L , and a filter capacitor. The buck converter is connected to a DC source which is rectified from piezoelectric output of voltage E that provides a regulated DC voltage V_o to the load resistor R .

When the MOSFET Q is ON, the diode D is reversed biased and the input current, I_L flows through the inductor L and resistor R . When the MOSFET Q is OFF, the diode D gets conducted and the inductor current flows through the inductor, capacitor and resistor.

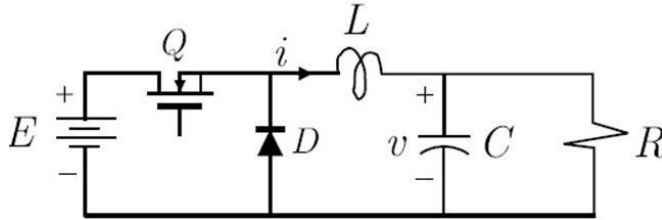


Fig. 2. Circuit diagram of buck converter

Therefore the output voltage depends on the input voltage, duty cycle and it is always less than the input voltage. The inductor value depends upon the frequency, load and ripple current, input and output voltages Lakshmi and Raja, 2014. Designing a good performance buck converter, the inductor ripple current should lie between 10% to 20% of the output current. The output voltage ripple is the most important criterion for selecting the capacitors.

The output voltage, value of inductance and capacitor are given as;

$$V_0 = E \times d \quad L = \frac{(E - V_{out}) \times d}{f_s \times \Delta I_L} \quad C = \frac{I_L}{8 \times f_s \times \Delta V_{out}}$$

Where d is the duty cycle.

4. Modeling of Buck Converter

Consider the ideal configuration as shown in Fig. 2, to describe the dynamics of DC-DC buck converter. The mathematical modeling of a DC-DC buck converter is based on the controlling action of switch Wang et al., 2015.

When the switch is ON (i.e. at $\mu = 1$), the equation is obtained by applying Kirchhoff's laws to the circuit shown in Fig. 2.

$$\frac{di_L}{dt} = \frac{E - V_0}{L} \quad (1)$$

$$\frac{dV_0}{dt} = \frac{i_L}{C} - \frac{V_0}{RC} \quad (2)$$

Where i_L is the inductor current and V_0 is the output voltage.

When the switch is OFF (i.e. at $\mu = 0$), the equation is obtained by applying Kirchhoff's laws to the circuit shown in Fig. 2.

$$\frac{di_L}{dt} = \frac{-V_0}{L} \quad (3)$$

$$\frac{dV_0}{dt} = \frac{i_L}{C} - \frac{V_0}{RC}$$

Then combining equation (1), (2), (3), (4) and when $\mu \in [0, 1]$, the average model can be written as;

$$\frac{di_L}{dt} = \frac{\mu E - V_0}{L} \quad (5)$$

$$\frac{dV_0}{dt} = \frac{i_L}{C} - \frac{V_0}{RC} \quad (6)$$

In practice, the load resistance may vary and the assumed nominal value of R is R_0 .

Let $z_1 = (V_0 - V_{ref})$ and $z_2 = \left(\frac{i_L}{C}\right) - \left(\frac{V_0}{R_0 C}\right)$ be the state variables, hence the model is rewritten as;

$$\dot{z}_1 = \frac{i_L}{C} - \frac{V_0}{RC} + \varphi_1(t) \quad (7)$$

Where $\varphi_1(t) = -\frac{V_0}{RC} + \frac{V_0}{R_0 C}$ is the mismatched disturbance.

Therefore;

$$\dot{z}_2 = \frac{\mu E - V_0}{LC} - \frac{1}{R_0 C} \left(\frac{i_L}{C} - \frac{V_0}{RC} \right) \quad (8)$$

It can be simplified as;

$$\dot{z}_2 = \frac{\mu E - V_{ref}}{LC} - \frac{z_1}{LC} - \frac{1}{R_0 C} \left(\frac{V_0}{R_0 C} - \frac{V_0}{RC} \right) \quad (9)$$

Denoting; $u = \frac{\mu E - V_{ref}}{LC}$ and $\varphi_2(t) = -\frac{1}{R_0 C} \left(\frac{V_0}{R_0 C} - \frac{V_0}{RC} \right)$

The model can be simplified using equation (7) and (9) as;

$$\dot{z}_1 = z_2 + \varphi_1(t) \quad (10)$$

$$\dot{z}_2 = u - \frac{z_1}{LC} - \frac{z_2}{R_0 C} + \varphi_2(t) \quad (11)$$

5. Control Design

A robust control for variable load in a DC-DC buck converter is designed in this section with a piezoelectric energy scavenging system. The ESO is used to estimate two states as well as disturbance Han, 2009. A proposed control configuration is shown in Fig. 3.

Consider the mismatched disturbance estimation of $\varphi_1(t)$, based on the ESO technique is designed as;

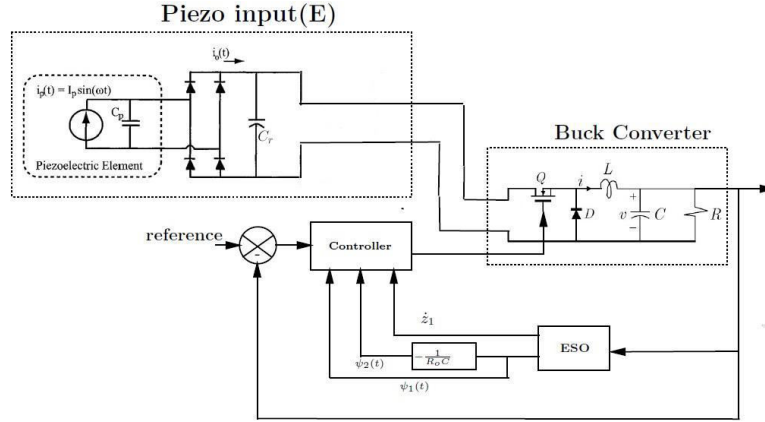


Fig. 3. Proposed control configuration

$$\hat{z}_1 = \hat{z}_2 + z_2 - \beta_1(\hat{z}_1 - z_1) \quad (12)$$

$$\hat{z}_2 = -\beta_3(\hat{z}_1 - z_1) \quad (13)$$

Where, $z_1 = \hat{z}_1$, $z_2 = \hat{\varphi}_1(t)$ and $\beta_1 > 0$, $\beta_2 > 0$.

From the equation (7), (8), (9) and (10) the relationship between φ_1 and φ_2 is given by;

$$\hat{\varphi}_2(t) = -\frac{1}{R_0 C} \hat{\varphi}_1(t) \quad (14)$$

In a buck converter, ESO is employed to observe and estimate the disturbance φ_i of a plant and which is based on control input and plant output. The proposed ESO-based system under mismatched disturbance is designed in Gundecha et al., 2016, Mahpatro et al., 2015 as;

$$u = \left[\frac{z_1}{LC} + \frac{z_2}{R_0 C} - \hat{\varphi}_2 - k_1 \hat{z}_1 - k_2 (z_2 + \hat{\varphi}_1) \right] \quad (15)$$

6. Results and Discussion

The proposed algorithm has been tested for voltage tracking in a buck converter with piezoelectric energy scavenging system. The responses of variable output load resistance and dynamic changes in input voltage are tested on the propose algorithm.

The proposed work is used to control and analyse the effect of dynamic variation in piezoelectric input. From Ottman et al., 2003 the trajectory as shown in Fig. 4(a) is designed. For variable input voltage E , the

load resistance is changed from 200Ω to 150Ω . From Fig. 4(b), it is observed that the controller design in equation (11) estimates the changes in the state and adjusts the duty cycle for getting output voltage at $4.5V$.

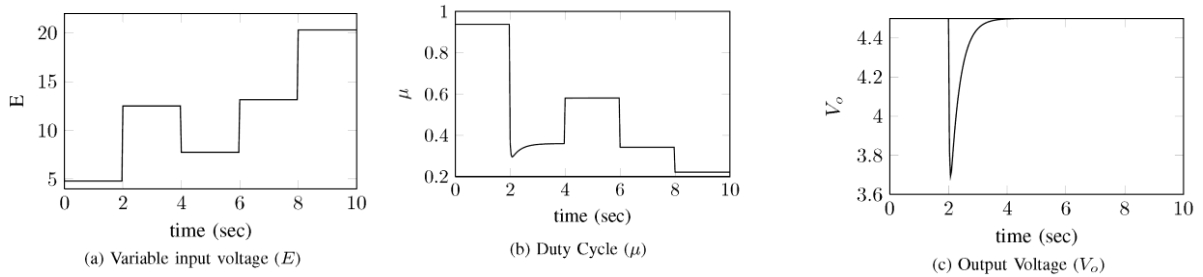


Fig. 4. Dynamic variation in piezoelectric input

Case 1: Variable Load Resistance (R_L)

The buck converter is evaluated under variable load resistance conditions for tracking the reference voltage. The input voltage is considered as, $E = 8V$, reference voltage as, $V_{ref} = 4.5V$. The tracking and estimation performance for 180Ω resistance is shown in Fig. 5. The duty cycle (μ) and the controlled output are shown in Fig. 5(c), 5(d). The results are tested for different R_L range from 140Ω to 240Ω . The cumulative results for *Case 1* are illustrated in Table 3.

Table 3. Performance result for variable load resistance

R_L (Ω)	μ (V_{ms})	Tracking Error ($z_1 = V_{ref} - V_0$)	Estimation Error ($e = z_1 - \hat{z}_1$)	R_L (Ω)	μ (V_{ms})	Tracking Error ($z_1 = V_{ref} - V_0$)	Estimation Error ($e = z_1 - \hat{z}_1$)
180	0.5466	0	0.0026	230	0.5861	0	0.0051
200	0.5777	0	0.0031	240	0.5962	0	0.0076

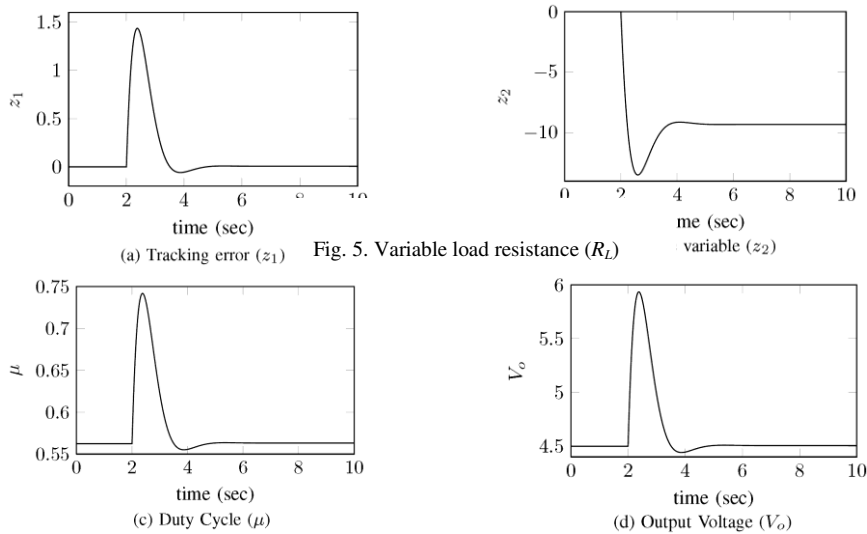


Fig. 5. Variable load resistance (R_L)

Case 2: Variable Input Voltage (E)

The estimation and tracking performance for an input voltage is tested for different E range from 8V to 16V. The results are illustrated in Table 4.

Table 4. Performance result for variable input voltage

E (V)	μ (V_{rms})	Tracking Error ($z_1 = V_{ref} - V_0$)	Estimation Error ($e = z_1 - \hat{z}_1$)	E (V)	μ (V_{rms})	Tracking Error ($z_1 = V_{ref} - V_0$)	Estimation Error ($e = z_1 - \hat{z}_1$)
8	0.5548	0	0.0013	12	0.3698	0	0.0013
10	0.4438	0	0.0013	14	0.3170	0	0.0013

Case 3: Variable Reference Voltage (V_{ref})

The reference voltage is varied from 3.8V to 5.8V and the load resistance $R_L = 200$ with the input voltage $E = 8V$. The proposed controller is suitable to regulate the required output voltage. The results for variable reference varied from 3.8V to 5.8V are shown in Table 5.

Table 5. Performance result for variable reference voltage

V_{ref} (V)	μ (V_{rms})	Tracking Error ($z_1 = V_{ref} - V_0$)	Estimation Error ($e = z_1 - \hat{z}_1$)	V_{ref} (V)	μ (V_{rms})	Tracking Error ($z_1 = V_{ref} - V_0$)	Estimation Error ($e = z_1 - \hat{z}_1$)
3.8	0.4685	0	0.0011	4.5	0.5548	0	0.0013
4.0	0.4931	0	0.0012	5.8	0.7150	0	0.0017

The proposed work shows the robust voltage tracking of buck converters for piezoelectric energy harvesting and the results are verified in simulation. The different cases of the piezoelectric energy scavenging are considered and obtain better voltage tracking results with various dynamic constants. The effects of disturbances are compensated by ESO, caused by load and input uncertainties.

7. Conclusions

The paper proposed a robust control approach for DC–DC buck converter for scavenging electrical energy from a mechanically excited piezoelectric element. The disturbances caused by variation in load and input are compensated by using ESO. A good disturbance rejection against input and load resistance variation is obtained with better voltage tracking performance and state estimation. A robust control strategy with application to piezoelectric energy scavenging for uncertain dynamics is confirmed.

References

- [1] J. Lu, S. Liu, Q. Wu, and Q. Qiu, 2010. "Accurate modeling and prediction of energy availability in energy harvesting real-time embedded systems," in International Green Computing Conference. Chicago: IEEE, pp. 469–476.
- [2] Ayrikyan, A. Kastner, N. H. Khansur, S. Yasui, M. Itoh and K. G. Webber, 2017. "Lead-Free Multilayer Piezoceramic Composites: Effect of Cosintering on Electromechanical Properties," in IEEE Transactions on Ultrasonics, Ferroelectrics, and Frequency Control, vol. 64, no. 7, pp. 1127–1134, doi: 10.1109/TUFFC.2017.2701882.
- [3] Y. Wu, W. Liu, and Y. Zhu, 2013. "Design of a wind energy harvesting wireless sensor node," in International Conference on Information Science and Technology (ICIST). Yangzhou: IEEE, pp. 1494–1497.
- [4] Z. Hu, E. Mu and Z. Wu, 2020. "MEMS thermoelectric power chip for large scale thermal energy harvesting," 2020 IEEE 8th Electronics System-Integration Technology Conference (ESTC), pp. 1-6, doi: 10.1109/ESTC48849.2020.9229864.
- [5] C. Carvalho and N. Paulino, 2010. "A mosfet only, step-up dc-dc micro power converter, for solar energy harvesting applications," in 17th International Conference on Mixed Design of Integrated Circuits and Systems (MIXDES). Warsaw: IEEE, pp. 499–504.
- [6] E. Grace, D. Rajan, and A. clarence asis, 2011. "Performance evaluation of different rectifiers for piezo-electric energy harvesting applications," in International Conference on Recent Advancements in Electrical, Electronics and Control Engineering. IEEE, pp. 248–252.
- [7] L. Chao, C.-Y. Tsui, and W.-H. Ki, 2007. "Vibration energy scavenging and management for ultra-low power applications," in Low Power Electronics and Design (ISLPED). Portland: IEEE, pp. 316–321.
- [8] D. Gundecha, V. Gohokar, K. A. Mahapatro, and P. V. Suryawanshi, 2016. "Control of DC–DC converter in presence of uncertain dynamics," in Intelligent Systems Technologies and Applications, vol. 384. Springer, pp. 315–326.
- [9] S. H. Nguyen, H. Richardson and R. Amirtharajah, 2021. "A Bias-Flip Interface and Dual-Input DC-DC Converter for Piezoelectric and RF Energy Harvesting," International Symposium on Circuits and Systems (ISCAS), pp. 1-5, doi 10.1109/ISCAS51556.2021.9401590.
- [10] O. Gomis-Bellmunt, D. Montesinos-Miracle, S. Galceran-Arellano, and A. Sudri-Andreu, 2007. "A buck-boost bidirectional converter to drive piezoelectric actuators," in Power Electronics and Applications. Aalborg: IEEE, pp. 1–7.
- [11] S. Lakshmi and T. S. R. Raja, 2014. "Design and implementation of an observer controller for a buck converter," Turkish Journal of Electrical Engineering & Computer Sciences, pp. 562–572.
- [12] E. Lefeuvre, D. Audigie, C. Richard, and D. Guyomar, 2007. "Buck-boost converter for sensorless power optimization of piezoelectric energy harvester," in Power Electronics, vol. 22. IEEE, pp. 2018–2025.
- [13] O. Djamel, G. Dhaouadi, S. Youcef and M. Mahmoud, 2019. "Hardware Implementation of Digital PID Controller for DCDC Boost Converter," International Conference on Power Electronics and their Applications (ICPEA), pp. 1-4, doi: 10.1109/ICPEA1.2019.8911129.
- [14] L. Ardhenta, M. R. Ansyari, R. K. Subroto and R. N. Hasanah, 2020. "DC Voltage Regulator using Buck-Boost Converter Based PID-Fuzzy Control," Electrical Power, Electronics, Communications, Controls and Informatics Seminar (EECCIS), pp. 117-121, doi: 10.1109/EECCIS49483.2020.9263425.
- [15] T. Utomo, G. T. A. Wedangga and L. Ardhenta, 2020. "Sliding Mode Control based on Power Information of Boost Converter for Voltage Regulator," 2020 10th Electrical Power, Electronics, Communications, Controls and Informatics Seminar (EECCIS), pp. 37-42, doi: 10.1109/EECCIS49483.2020.9263442.
- [16] D. Chavan, A. D. Gundecha, K. A. Mahapatro, and P. V. Suryawanshi, 2019. "State and disturbance observer for robust motion control," in International Conference on Recent Trends on Electronics, Information, Communication & Technology. IEEE, pp. 1252–1256.
- [17] D. Ali, M. Asim, F. Wallam, Z. Qazi, A. Abbas and Y. Naudhani, 2019. "Experimental Testing of Observers Comprising Discrete Kalman Filter and High-Gain Observers," International Conference on Computing, Mathematics and Engineering Technologies (iCoMET), pp. 1-5, doi: 10.1109/ICOMET.2019.8673453.
- [18] G. Wang, M. Chadli and S. Mammar, 2020. "H_∞ memory observer design for vehicle suspension state estimation and unknown road reconstruction," Mediterranean Conference on Control and Automation (MED), pp.479-483, doi: 10.1109/MED48518.2020.9183121.
- [19] P. Wang, N. Li, X. Sun and C. Wang, 2020. "Deadbeat Predictive Current Control for PMSM Based on Improved Luenberger Observer," Chinese Control Conference (CCC), pp. 2373-2377, doi: 10.23919/CCC50068.2020.9189403.
- [20] J. Han, "From pid to active disturbance rejection control," in Industrial Electronics, vol. 56. Beijing: IEEE, 2009, pp. 900–906.
- [21] W. Bin, Y. Jun, W. Junxiao, and L. Shihua, 2014. "Extended state observer based control for DC–DC buck converters subject to mismatched disturbances," in Chinese Control Conference. Nanjing: IEEE, pp. 8080–8085.
- [22] S. Li and Z. Liu, 2009. "Adaptive speed control for permanent-magnet synchronous motor system with variations of load inertia," in Industrial Electronics, vol. 56. Nanjing: IEEE, pp. 3050–3059.

- [23] K. A. Mahapatro, A. D. Gundecha, A. D. Chavan, and P. V. Suryawanshi, 2019. "Disturbance rejection in motion control based on equivalent input disturbance approach with experimental validation," in International Conference on Recent Trends on Electronics, Information, Communication & Technology. IEEE, pp. 1247–1251.
- [24] Z. Ma, Y. Xiao, P. Wang and Y. Zhao, 2020. "Linear-Extended-State- Observer Based Pinning Control of Nonlinear Multi-Robots System," in IEEE Access, vol. 8, pp. 144522-144528, doi: 10.1109/ACCESS. 2020.3014399.
- [25] W. Shi, K. Liu and W. Zhao, 2021. "Active Vibration Isolation of a Maglev Inertially Stabilized Platform Based on an Improved Linear Extended State Observer," in IEEE Access, vol. 9, pp. 743-751, doi: 10.1109/ACCESS.2020.3046886.
- [26] G. K. Ottman, H. F. Hofmann, and G. A. Lesieutre, 2003. "Optimized piezoelectric energy harvesting circuit using Step-Down converter in discontinuous conduction mode," in IEEE Transactions on Power Electronics, vol. 18. IEEE, pp. 696–703.
- [27] Vulture, Piezoelectric Energy Harvestors, MIDE.
- [28] H. Sira-Ramirez and R. Silva-Ortigoza, 2006. Control Design Techniques in Power Electronics Devices. Springer-Verlag London limited.
- [29] J. Wang, S. Li, JunYang, BinWu, and Q. Li, 2015. "Extended state observer based sliding mode control for PWM-based DC–DC buck power converter systems with mismatched disturbances," in IET Control Theory and Applications, vol. 9. China: IET, pp. 579–586.



Shailesh S Shinde is Master's student in the Department of Electronics at MIT Academy of Engineering, Alandi (D), Pune, India. His research interests cover Uncertainty and Disturbance Estimation, Hybrid Renewable Energy Sources, Energy Scavenging.



Ashitosh Dilip Chavan is an Assistant Professor in the Department of Electronics and Telecommunication at MIT Academy of Engineering, Alandi (D), Pune, India. His thrust research interests cover robust control, sliding mode control (SMC) for dynamical systems, active disturbance rejection control (ADRC) for linear and nonlinear systems, uncertainty and disturbance estimation, observer designs, control law design of motion control and application in automotive domain. He is author and co-author of different research studies of journals, conference proceedings.



Dr. Aniket D. Gundecha is an Assistant Professor in the Department of Electronics and Telecommunication at MIT Academy of Engineering, Alandi (D), Pune, India. His research interests cover Uncertainty and Disturbance Estimation, Observer Designs, Active Disturbance Rejection Control for Linear and Nonlinear Systems, Hybrid Renewable Energy Sources, Energy Scavenging, Embedded Control Design for Control Systems. He has various publications in journals, conferences and book chapters of national and international repute.



Kaliprasad A Mahapatro is an Assistant Professor at Avantika University, Ujjain, MP. He is a researcher and academician with interest in Control System Design. Being a passionate researcher, Kaliprasad has published several papers in high indexed journal and conferences like IEEE, Springer etc. His primary research areas include, sliding mode control, active disturbance rejection control for linear and nonlinear systems, PID Control design and applications, control law design of energy scavenging from renewable energy sources.

Access provided by:
MIT Academy Of Engineering

Sign Out

Browse▼My Settings▼Help▼

Access provided by:
MIT Academy Of Engineering

Sign Out

All

Q

ADVANCED SEARCH

Conferences > 2021 International Conference... ?

Signature Recognition Models: Performance Comparison

Publisher: IEEE

Cite This

PDF

Atharva Gadre ; Pradyumna Pund ; Gouri Ajmire ; Shubhangi Kale All Authors

16 Full Text Views

Alerts

Manage Content Alerts

Add to Citation Alerts

Abstract

Document Sections

I. Introduction

II. Proposed Systems and Methodology

III. Dataset

IV. Pre-Processing

V. Result (Performance Analysis)

Show Full Outline

Download PDF

Abstract:In recent times Signature Verification has become an act of absolute necessity in the area of biometric verification. Unlike other verification problems, every small deta... **View more**

► Metadata

Abstract:
In recent times Signature Verification has become an act of absolute necessity in the area of biometric verification. Unlike other verification problems, every small detail between genuine and forged signatures needs to be observed because a skilled forgery can only differ by only some specific kind of features of the real signature. The task of verifying signatures has become even harder in writing independent scenarios. In this paper, with the help of Siamese Network, VGG16 model and DEEP CNN models we have modeled a system that will verify signatures offline. Siamese networks use two images as input with shared weights, which can be trained to learn the features of both the images to find out the similarity between them. This is done by passing sets of similar and dissimilar images to the network so that it can learn to reduce the loss and Euclidean distance between similar images and increase it in dissimilar images. As for VGG 16, it is a pre-trained 16-layer model that is based on CNN, these 16 layers consist of max layer, pooling layers, and many more. CNN is simply a convolutional neural network on which both Siamese and VGG models are based. The performance analysis shows the VGG16 to have best accuracy about 85-90%, Siamese shows 65-70% and CNN shows 65-70% and the Siamese network to have the highest speed in identification.

Authors

Figures

References

Keywords

Metrics

More Like This

A Novel Approach for Handwriting Recognition in Malayalam Manuscripts using Contour Detection and Convolutional Neural Nets

2018 International Conference on Advances in Computing, Communications and Informatics (ICACCI)

Published: 2018

Rumour Detection Based on Graph Convolutional Neural Net

IEEE Access


Published: 2021

Show More



Smart Trends in Computing and Communications pp 619–627

Apriori Algorithm with Dynamic Parameter Selection and Pruning of Misleading Rules

[Aditya Veer](#) , [Mohit Gurav](#), [Shreyansh Dange](#), [Shubham Chandgude](#) & [Vaishali Wangikar](#)

Conference paper | [First Online: 26 October 2021](#)

287 Accesses

Part of the [Lecture Notes in Networks and Systems](#) book series (LNNS, volume 286)

Abstract

In the field of knowledge discovery in databases (KDD), the effectiveness of association rules is important. Association rules are a technique of data mining, wherein we identify the relationship between one item to another. For mining, the association rules Apriori algorithm is widely used. The idea of the Apriori algorithm is to find the frequent sets from a transactional database. Through the frequent sets, association rules are obtained, and these rules must satisfy the minimum confidence threshold. This paper presents an improved method for deciding an optimum



Advanced Data Mining Tools and Methods for Social Computing

Hybrid Computational Intelligence for Pattern Analysis

2022, Pages 107-125

Chapter 6 - A machine learning approach to aid paralysis patients using EMG signals

Manisha Choudhary ^a, Monika Lokhande ^a, Rushikesh Borse ^a, Avinash Bhute ^b

Show more ▾

Outline | Share | Cite

<https://doi.org/10.1016/B978-0-32-385708-6.00013-8>

[Get rights and content](#)

Abstract

This work focuses on hand movement classification from electromyography (EMG) signals using machine learning algorithms. The use of EMG signals for the human–human interface to move a paralyzed person is discussed. EMG signals are generated when the electric potential of the muscles changes after receiving signals from the brain due to the contraction or expansion of muscles. EMG signals were collected by connecting electrodes to a person's arm and they were recorded using the BYB Spike Recorder App. Features were extracted from these signals and a dataset was obtained using these features. Hand movement of the person using this dataset was classified using various algorithms like k-nearest neighbor (KNN), support vector machine, naive Bayes, and decision tree. All algorithms offered a promising accuracy of around 90%, except KNN, whose accuracy was 60%. Thus, they can be used to control movements of people with disabilities by a human–human interface.

[<](#) Previous

Next [>](#)

Keywords

EMG signals; Feature extraction; Machine learning; Human–human interface

[Recommended articles](#)

Cited by (0)

Copyright © 2022 Elsevier Inc. All rights reserved.



Copyright © 2022 Elsevier B.V. or its licensors or contributors.
ScienceDirect® is a registered trademark of Elsevier B.V.

RELX™

PAPER • OPEN ACCESS

Aqueous Two-Phase Separation (ATPS) Methods for Oleic acid extraction from Neem leaves

To cite this article: Shubham Gawade *et al* 2022 *IOP Conf. Ser.: Mater. Sci. Eng.* **1224** 012016

View the [article online](#) for updates and enhancements.

You may also like

- [Neoteric Media as Tools for Process Intensification](#)
C C Beh, R Mammucari and N R Foster
- [Liquid-liquid extraction of Pt\(IV\) from hydrochloric acid solutions using PPG 425 – NaCl – H₂O system](#)
I V Zinov'eva
- [Metallic and semiconducting carbon nanotubes separation using an aqueous two-phase separation technique: a review](#)
Malcolm S Y Tang, Eng-Poh Ng, Joon Ching Juan et al.

Aqueous Two-Phase Separation (ATPS) Methods for Oleic acid extraction from Neem leaves

Shubham Gawade, Sandeep P. Shewale and Amravati Gode

School of Chemical Engineering, MIT Academy of Engineering, Alandi (D), Pune, India-412105

Corresponding author's e-mail address: agode@mitaoe.ac.in

Abstract. The aqueous two-phase separation system (ATPS) signifies an environmentally responsible approach for the extraction of bioactive compounds from a plants basis, as it is a liquid-liquid fractionation technique centred on the inconsistency of two aqueous solutions. In this investigation, various experimental parameters are optimized as the speed of agitation (200, 300 400 and 500 rpm) and solvent ratio (1:1, 2:3 and 3:2) with 20 % (w/w) of Ammonium Sulphate (AMS) salt composition and 30 % (w/w) of Polyethelyene Glycol (PEG). The obtained extract contains alkaloids, flavonoids, tannins, glycosides, acids and total phenolic compounds (TPC). The extracted Oleic acid by the ATPS method was measured with gallic acid equivalent (GAE) of TPC extracted from neem leaves powder. The determined concentration of oleic acid in the practice of TPC is 8.033 mg of GAE/g from the optimized experimental parameter. The optimized results can be cast off for a commercial process on an industrialized scale. Also, the mathematical modelling investigation was done to intent the critical impeller speed (Njs) with the Zwittering model. The identified model calculates the essential speed of agitation (rpm) for maximum extraction yield.

Keywords: Oleic acid, Total phenolic compounds (TPC), Aqueous Two-Phase Separation System (ATPS), Gallic Acid Equivalent (GAE), Critical Impeller Speed (Njs).

1. Introduction

Herbs are used for flavouring, food, medicine, or perfume from ancient times. Culinary use naturally differentiates herbs are implying the leafy green portions of spice also a product from a different part of the plant containing seeds, roots, bark, and fruits. Furthermore, medicinal contents available in the plant's parts are used for the production of some pharmaceutical products such as aspirin, colchicine, ephedrine, morphine, physostigmine, pilocarpine, quinidine, reserpine and vincristine, etc [1-2]. The approach of isolating the bioactive components from the medicinal plants and used for the manufacturing of some pharmaceutical products are becoming prominent. Generally, organic solvents such as methanol, ethanol and diethyl ether are usually helped for extracting the bioactive compounds as of plant basis by the outmoded extraction arrangements. These solvents are relatively expensive,



needs distinctive processing conditions and most importantly disposal of the solvents is a major concern as they are not environmental responsive [3].

Conventional extraction processes are time-consuming and need more solvent for carrying out an operation, also after extraction, the added cost of purification and solvents recovery makes the process uneconomical.

Whereas, ATPS two-stage extraction is developing as a successful and flexible green system for the downstream handling of biomolecules. Fluid two-stage frameworks are low unpredictability frameworks with high adaptability [4]. That is, an expansive assortment might be acquired utilizing substances that pursue the Green Chemistry guideline on ecotoxicity, biodegradability, bioaccumulation and constancy, limiting waste and amplifying yields. Furthermore, they conform to the guideline of changeover of naturally safe structures to permit work under air weight. Since the 1970s numerous classified and out examinations have announced the filtration of proteins and other biologic materials utilizing ATPS, and numerous specialists have considered different operations of ATPS for the extraction and cleaning of organic products [5]. However, the utilization of such frameworks for the recuperation of phenolic mixes from plant materials is extremely constrained. In addition, there is broad writing about the thermodynamic properties of ATPS be that as it may, to the best of our insight, their application to crude unpurified examples has been very constrained [6].

Subsequently, the late nineteenth-century fluid two-phase extraction has been identified to the entire world. Aqueous two-phase can be framed through an extensive diversity of characteristics or else engineered water-solvent polymers& salt blends [7]. Watery two-phase extraction is developed for protected, sparing partition and cleaning of biomolecules, for example, proteins and catalyst extraction. Fluid extraction has numerous favourable circumstances; it is biocompatible, has low interfacial surface pressure among stages and it has high water content, the procedure can incorporate and the ability for strengthening [8-9].

Likewise, the level of corruption for biomolecules is low. In any case, two-polymer and polymer-based salt frameworks have developed quickly and a considerable measure of effort has been placed keen on concentrate this strategy utilizing these sorts of aqueous two-phase separation systems (ATPS). Aqueous two-phase extraction is known as an operative, adaptable and significant developing green method for the subsequential treating of biomolecules. This strategy has points of interest completed traditional extraction systems similar to, simplicity of scaling-up, condition benevolent, minimal effort, fit for nonstop activity and is effective for some sorts of trials exceptionally for the fixation and refinement of biomolecules. The utilization of partiality in ATPS can affect the developed recuperation earnings and developed refinement bends of bio consistent items such as it is an essential phase recuperation strategy [10]. Water as the foremost constituent of together stages in ATPS practices a moderate setting for bioactive molecules to distinct and polymers steady to the assembly and biotic doings through further liquid-liquid extraction approaches could impairment natural goods since of the development circumstances and biological solvents such method reduces the purity of active ingredient present in the extract.

There are two fundamental sorts of ATPS: polymer-polymer and polymer-salt frameworks. The mind-boggling expense of some shaping stage polymers (e.g dextran) limits the use of these frameworks, just legitimized when the expense of the result of intrigue is extensive. Consequently, the choice of the more temperate polymer-salt frameworks is profoundly suggested [10-11].

The novelty of the proposed work is that during the extraction itself two different layers of aqueous solution and salt is obtained, which can help further to reduce the cost of separating components. Also, the systems can be designed by partying a diversity of components in water and two-polymer and polymer-salt systems have developed quickly. The said work majorly focuses on the extraction of oleic acid from neem leaves to powder using ATPS (water + polymer + salt) based on PEG and ammonium sulphate. The aim is to optimize various experimental parameters (time, ATPS composition, particle size) for the removal of Oleic acid from neem leaves powder and its additional practices as natural antioxidants.

2. Material and Methods

The Neem powder was obtained from Hari Parshuram Aushdhalya, Pune., Polyethelyene Glycol (PEG) was procured from SRL Chemicals Pvt Ltd, Mumbai. Folin Ciocalteu's reagent was procured from Qualigens Fine Chemicals, Mumbai. Ammonium Sulphate (AMS) was procured from S.D. Fine Chemicals Pvt Ltd, Mumbai.

2.1. Batch extraction

Batch extractions are a modest method for the extraction of bioactive compounds. The stages in this method are equipped with a 50 ml glass reactor with a four-bladed glass turbine impeller and the combination to be divided is supplementary. Subsequently collaborating, phase parting is proficient each by resolving below gravity. The stages are disconnected and investigated to improve the alienated constituents of the preliminary mixture. The object product would be focused at any of the stages and the pollutants in the additional form. In various cases, reclamation and attentiveness of the product that produces beyond 90% can be attained with a particular extraction stage.

One particular phase removal does not give adequate retrieval, recurrent extractions can be supported obtainable in a sequence of communicating and parting components [12]. The fluid dividers into two stages, each covering added 80% liquid. When basic biomolecules are supplementary to these combinations, biomolecules and cell wreckages are dividers among the stages; by choosing suitable circumstances, cell remains can be limited to one stage as the object bioactive molecule barriers. The segregating of biomolecules among segments mostly be contingent on the equilibrium connection of the arrangement. The partition coefficient is demarcated as [12-13].

$$K = \frac{C_{AT}}{C_{AB}}$$

Where C_{AT} is the equilibrium attentiveness of constituent A in the upper phase and C_{AB} is the equilibrium adsorption of A in the lesser phase. If constituent A helps the greater stage the worth of K will be better. In numerous aqueous arrangements, K is continual finished with an extensive collection of deliberations, as long as the molecular possessions of the stages are not transformed. The theoretic yield in the topmost stage, Y_T , can be premeditated relative to the capacity ratio of the stages, R (up to volume / below volume), and the partition coefficient K of the object molecule as follows [12-13]:

$$Y_T = \frac{V_T C_{AT}}{V_O C_O} = \frac{V_t C_{AT}}{V_t C_{AT} + V_B C_{AB}} = \frac{1}{1 + [\frac{1}{KR}]}$$

Similarly, the theoretic yield in the bottommost stage, Y_B is known by,

$$Y_B = \frac{1}{1 + [\frac{1}{KR}]}$$

Consequently, by changing anyone like K or R we can effortlessly upsurge or reduction the profit of the object particle [14]. Additional constraint recycled to describe two-phase partitioning is the concentration factor, δ_c , distinct as the ratio of produce attentiveness in the favoured stage to the original product attentiveness.

$$\delta_{C,T} = \frac{C_{AT}}{C_{Ao}} \quad (\text{Product partitions to the higher phase})$$

$$\delta_{C,B} = \frac{C_{AB}}{C_{Ao}} \quad (\text{Product partitions to the lower phase})$$

2.2. Determination of the binodal

By settlement, the constituent mainly in the lower layer is represented as abscissa and the predominant element in the upper stage is represented as ordered. The three systems are explained realistically.

2.2.1 Turbidometric titration

In the tubing, with suitable backup solutions, formulate systems through different configurations of recognized weight. Note the added size due to titration, for example, if 5 g methods are organized, use 10 ml tubes. As an example, shows the systems for different systems that can use PEG-phosphate and PEG-dextran, and the essential designs. This can be replicated in a worksheet to permit easy intention. Note down the mass of the tube and titration drop by drop, with suitable dilution till the scheme is zeroed, i.e., a stage is formed.

This can be done through the scheme is continuously mixing or accumulation a droplet, collaborating, adding a second drop and continues the same process. To confirm that it has formed a single-stage system, the schemes must be centrifuged (for example 1000-2000 g, 5 min). Record the concluding mass of the tube and estimate the mass of the additional dilution just before the formation of a phase. Since the number of graduate systems is relative to the total of points in the binodal, superior precision is obtained with a superior number of schemes [15].

2.2.2 Cloud point method

Balance 5 g of a standard solution of constituent X into a 25 ml narrowed flask. Then add drop by drop, a reserve solution of the Y component up to the principal indication of turbidity, which is the cloud point. Note the weight of the Y component necessary for the mixture to become cloudy. This provides the first point in the binodal. Also, add a known weight of diluent lower the cloud point and duplication as indicated [15-16].

2.2.3 Determination of the Tie line

Measuring the connection line for polymeric schemes comprising an optically active composite, for example, PEG-dextran, PEG-Ficoll and ethylene oxide-propylene as well as oxide-Reppal PES 100.

2.2.3.1 Polymeric Methods Comprehending One Optically Active Polymer

Formulate a standard curve for the lively constituent, in the variety of 0 to 10% (p / v), i.e. inside the linear series, through the identical sections arrange a second standard curve for the refractive measure of the index. If the scheme is arranged in a shield, the average curves for the clean constituents must be completed with a similar safeguard, since the salts similarly subsidize the refractive index. Get ready the phased scheme for investigation, assembly sure that the phase components mix well; let the phases separate.

To ensure complete separation, centrifuge at low speed (for example 1000-2000 g, 5 min). The system proportions should be appropriate to permit deduction of at least 5 g upper and lower stage for phase concentration investigation and an additional quantity for density extents. Distinct the higher and subordinate stages building certain not to origin stage relations. Make the suitable dilutions, for example, watery 5 g of phase with the suitable solvent to 25 ml in a volumetric container. Extend the visual revolution for every stage and estimate the individual concentrations. The concentration of another constituent is resolute by determining the refractive index of the developed and subordinate stage and deducting the influence of the refractive index acquired from the optically lively constituent [17].

2.2.3.2 Polymer-Salt Systems

Formulate a standard curve aimed at salt conductivity within the linear series (in% w / v). Arrange the stage schemes as indicated above and eliminate 5 g of samples of the higher too subordinate phases and

diluted with liquid and lyophilized, then note the dehydrated weight. Eliminate an additional section from the higher and subordinate stage, diluted with water and extent the conductivity of every stage. Estimate the salt absorption and deduct the mass involvement of the dehydrated mass of the section [16-18].

3. Results and Discussion

In this investigation, various experimental parameters were optimized such as speed of agitation (200 rpm, 300 rpm, 400 rpm & 500 rpm) and solvent ratio (1:1, 2:3 and 3:2). Extract samples were pipette out at specific time intervals like every 15 min and further standard Folin–Ciocalteu's method was used for analysis purposes. The obtained outcomes indicated that the TPC concentration of TPC in the extraction stage at a specific time. By changing the parameters speed of agitation and solvent ratio in the batch reactor at different times the results were optimized and used for further study.

3.1 Speed of agitation

About 5 g of powder of neem leaves was weighted and fed to 50 ml of batch reactor along with AMS salt (20 %w/w) and 50 ml of PEG (30 %w/w) at a temperature of 30°C till the extraction rate was a steady-state. The maximum speed of agitation produces high turbulence in the batch reactor and increases the rate of mass transfer [11]. The results of various experiments were performed for multiple agitation speeds is shown in figure 3.1 The experimental results shows that the concentration of TPC at 200 rpm significantly low as compared to 500 rpm, but there could be a marginal difference of TPC concentration of 400 and 500 rpm, speed of agitation., therefore for the further study, speed of agitation (400 rpm) was used. The circulation of TPC compounds from the neem leaves powder in the solvents could expand with the accumulative agitation speed. An added rise in the agitation speed has no substantial effect on final extraction yield; it clues that external mass transfer fighting is inconsequential at 400 rpm

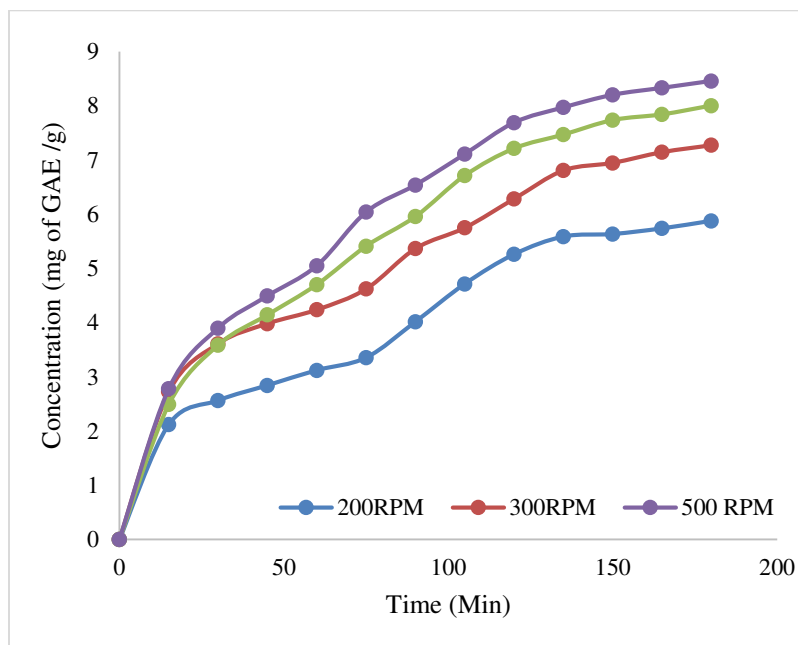


Fig. 3.1 Concentration of TPC obtained from Batch at temp 30°C speed of agitation 200, 300, 400 & 500 rpm)

3.2 Effect of Solvent Ratio (AMS: PEG)

The TPC concentration values in the extract were considered for changed extraction times at different solvent ratios (1:1, 2:3 & 3:2) and the same is shown in Figure 3.2. About 5 g of powder of neem leaves

was weighted and fed to 50 ml of batch reactor along with AMS salt (20 %w/w) and 50 ml of PEG (30 %w/w) at a temperature of 30°C till the extraction rate was a steady-state. There was an increase in TPC concentration and experiential for solvent ratio 01:01. A substantial quantity of solvent favours an additional concentration gradient and cuts diffusional resistance that rises the rate of extraction rate. There was a rise in TPC concentration, for the solvent ratio of 1:1 to 3:2. A substantial quantity of solvent tends to the added concentration gradient and drops diffusional resistance that rises the rate of extraction [11].

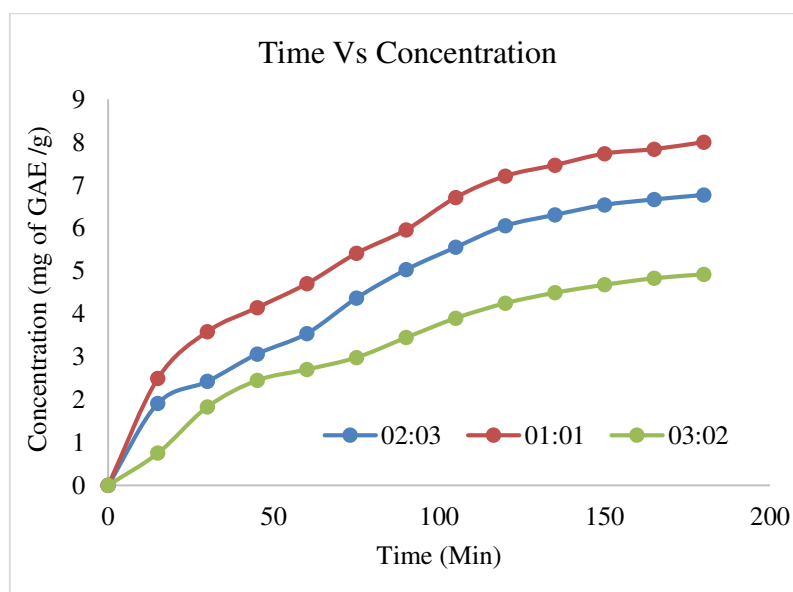


Fig.3.2 Effect of Solvent Ratio (AMS: PEG)

4. Conclusion

The investigation of the ATPS method was beneficial for the sub sequential treating of biomolecules. Also, the experimental parameters were optimized such as speed of agitation and solvent ration and the optimized parameters as 400 rpm and 01:02 solvent ration respectively with AMS salt (20 % w/w) & PEG (30 % w/w). The obtained extract also contains alkaloids, flavonoids, tannins, glycosides, acids and total phenolic compounds (TPC). The extracted Oleic acid by ATPS technique was measured with gallic acid equivalent (GAE) of TPC extracted from neem leaves powder. The determined concentration of oleic acid in the practice of TPC is 8.033 mg of GAE/g from the optimized experimental parameter. The optimized results can be used for a commercial process on an industrial scale.

References

- [1] Alasalvar C, Karamac M, Amarowicz R, Shahidi F, 2006. Antioxidant and antiradical activities in extracts of hazelnut kernel (*Corylus avellana* L.) and hazelnut green leafy cover. *J Agric Food Chem* 54: 4826-4832.
- [2] Babitskaia V, Shcherba V, Lkonnikova N, 2000. Melanin complex of the fungus *Inonotus obliquus*. *Prikl Biokhim Mikrobiol* 36(4): 439-444.
- [3] Dallora N, Klemz J, Filho P, 2007. Partitioning of model proteins in aqueous two-phase systems containing polyethylene glycol and ammonium carbamate. *Biochem Eng J* 34(1): 92-97.
- [4] Karakatsanis A, Liakopoulou M, 2007. Comparison of PEG/ fractionated dextran and PEG/industrial grade dextran aqueous two-phase systems for the enzymic hydrolysis of starch. *Eng* 80(4): 1213-1217.
- [5] Alencar L.V.T.D., Passos L.M.S., Martins M.A.R., Barreto I.M.A., Soares C.M.F., Lima A.S., Souza R.L., 2020. The complete process for the selective recovery of textile dyes using an

aqueous two-phase system. *Sep. Purif. Technol.* 253: <https://doi.org/10.1016/j.seppur.2020.117502>.

- [6] Ying H, Diyun C, Shuqi C, Minhua S, Yongheng C, Yixiong P, Gutha Y, 2021. A green method for recovery of thallium and uranium from wastewater using polyethylene glycol and ammonium sulfate based on the aqueous two-phase system. *J. Clean. Prod.* 297: <https://doi.org/10.1016/j.jclepro.2021.126452>.
- [7] Leitner M, Vandelle E, Gaupels F, Bellin D, Delledonne M, 2009. NO signals in the haze: Nitric oxide signalling in plant defence. *Curr Opin Plant Biol* 12(4): 451-458.
- [8] Liu SP, Zong ZM, Wei Q, Wei XY, 2010. Study on organic compounds in aqueous two phase system phase forming and distribution. *Chem Ind Times* 24(12): 21-24.
- [9] Ahareh AS, Gholamreza P, Javad RS, Shahla S, Naghmeh H, 2020. Separation of erythromycin using aqueous two-phase system based on acetonitrile and carbohydrates. *Fluid Phase Equilib.* 505: <https://doi.org/10.1016/j.fluid.2019.112360>
- [10] Perla JV, Salvador VG, Iran AT, Yolanda SM, Leticia GC, Artemio PL, Diana GR, 2020. Separation of bioactive compounds from epicarp of 'Hass' avocado fruit through aqueous two-phase systems. *Food Bioprod. Process.* 123:238-250.
- [11] Sandeep Shewale & Virendra K. Rathod (2018) Extraction of total phenolic content from *Azadirachta indica* or (neem) leaves: Kinetics study, Preparative Biochemistry & Biotechnology, 48:4, 312-320, DOI: 10.1080/10826068.2018.1431784
- [12] Singh SB, Jayasuriya H, Dewey R, Polishook JD, Dombrowski AW, Zink DL, Guan Z, Collado J, Platas G, Pelaez F, Felock PJ, Hazuda DJ, 2003. Isolation, structure, and HIV-1 integrase inhibitory activity of structurally diverse fungal metabolites. *J Ind Microbiol Biotechnol* 30(12): 721-731.
- [13] Srinivas ND, Barhate RS, Raghavarao KSMS, 2002. Aqueous two-phase extraction in combination with ultrafiltration for down-stream processing of *Ipomoea peroxidase*. *J Food Eng* 54(1): 1-6.
- [14] Uma DB, Ho CW, Wan Aida WM, 2010. Optimization of extraction parameters of total phenolic compounds from Henna (*Lawsonia inermis*) leaves. *Sains Malaysiana* 39(1): 119-128.
- [15] Wang SY, Wu JH, Cheng SS, Lo CP, Chang HN, Shyur LF, Chang ST, 2004. Antioxidant activity of extracts from *Calocedrus formosana* leaf, bark, and heartwood. *J Wood Sci* 50: 422-426.
- [16] Zhao YX, Miao KJ, Zhang MM, Wei ZW, Zheng WF, 2009. Effects of nitric oxide on production of antioxidant phenolic compounds in *Phaeoporus obliquus*. *Mycosystema* 28(5): 750-754.
- [17] Zheng WF, Zhao YX, Zhang MM, Wei ZW, Miao KJ, Sun WG, 2009. Oxidative stress response of *Inonotus obliquus* induced by hydrogen peroxide. *Med Mycol* 47: 814-823.
- [18] Zheng WF, Miao KJ, Liu YB, Zhao YX, Zhang MM, Pan SY, Dai YC, 2010. Chemical diversity of biologically active metabolites in the sclerotia of *Inonotus obliquus* and submerged culture strategies for up-regulating their production. *Appl Microbiol Biotechnol* 87(4): 1237-1254.



Gavin Publishers is an international open access journal publisher peer reviewed articles.

AIP

Conference Proceedings

HOME

BROWSE

MORE ▼

[Home](#) > [AIP Conference Proceedings](#) > [Volume 2417, Issue 1](#) > [10.1063/5.0072779](#)

< PREV

NEXT >



No Access

Published Online: 19 October 2021

CFD analysis of exhaust pipe of a diesel engine

AIP Conference Proceedings **2417**, 060002 (2021); <https://doi.org/10.1063/5.0072779>Pawankumar Yadav^{a)} and Pramod Kothmire^{b)}[View Affiliations](#)[View Contributors](#)

Topics ▼

ABSTRACT



PDF



E-READER

PAPER • OPEN ACCESS

Rectangular and Square Cross-Sections Microchannel Heat Sink CFD Simulation and Analytical Validation Using Liquid Water & Water- Aluminium Oxide Nanofluid as a Cooling Medium

To cite this article: Saurabh Narayan Pawar *et al* 2021 *IOP Conf. Ser.: Mater. Sci. Eng.* **1145** 012093

View the [article online](#) for updates and enhancements.

You may also like

- [Mono and hybrid nanofluid based heat sink technologies - A review](#)
A Chandravadhana, V NandaKumar and K Venkatramanan
- [Role of 1,2-benzisothiazolin-3-one \(BIT\) in the Improvement of Barrier CMP Performance with Alkaline Slurry](#)
Tengda Ma, Baimei Tan, Yuling Liu et al.
- [CFD Simulation and Analytical Validation of Rectangular and Square microchannel heat sink with liquid water as cooling medium](#)
Saurabh Narayan Pawar and Nilesh Balkishanji Totla

Retraction

Retraction: Rectangular and Square Cross-Sections Microchannel Heat Sink CFD Simulation and Analytical Validation Using Liquid Water & Water-Aluminium Oxide Nanofluid as a Cooling Medium (*IOP Conf. Ser.: Mater. Sci. Eng.* **1145 012093)**

Published 23 February 2022

This article (and all articles in the proceedings volume relating to the same conference) has been retracted by IOP Publishing following an extensive investigation in line with the COPE guidelines. This investigation has uncovered evidence of systematic manipulation of the publication process and considerable citation manipulation.

IOP Publishing respectfully requests that readers consider all work within this volume potentially unreliable, as the volume has not been through a credible peer review process.

IOP Publishing regrets that our usual quality checks did not identify these issues before publication, and have since put additional measures in place to try to prevent these issues from reoccurring. IOP Publishing wishes to credit anonymous whistleblowers and the [Problematic Paper Screener](#) [1] for bringing some of the above issues to our attention, prompting us to investigate further.

[1] Cabanac G, Labbé C and Magazinov A 2021 arXiv:[2107.06751v1](#)

Retraction published: 23 February 2022



Content from this work may be used under the terms of the [Creative Commons Attribution 3.0 licence](#). Any further distribution of this work must maintain attribution to the author(s) and the title of the work, journal citation and DOI.

Published under licence by IOP Publishing Ltd

Rectangular and Square Cross-Sections Microchannel Heat Sink CFD Simulation and Analytical Validation Using Liquid Water & Water-Aluminium Oxide Nanofluid as a Cooling Medium

Saurabh Narayan Pawar¹ Jugal Shrinivas Makam¹ Nilesh Balkishanji Totla²

¹Student, MIT Academy of Engineering, Pune, India.

²Sr Assistant Professor, MIT Academy of Engineering, Pune, India.

¹snpawar@mitaoe.ac.in ²jsmakam@mitaoe.ac.in, ³nbtotla@mech.maepune.ac.in

Abstract. In this study, cooling performance of copper material based microchannel heat sink was investigated using two different approaches which are CFD and Analytical. Microchannel heat sink with two different cross-sectional geometries of rectangular and square was considered for the present study. In the present work CFD simulation is carried out using two different cooling fluids which are liquid water and water- Al_2O_3 nanofluid. Nanofluid volume fraction of 0.3% was used for present study. Re number in between 200-1000 was used for the present study. For CFD simulation purpose heat sink of dimension of $25.4\text{mm} \times 25.4\text{mm} \times 2.384\text{mm}$ is considered in the study. Boundary condition of constant heat flux is assumed by providing heat flux at constant rate at bottom of the assembly. To compare between square and rectangular cross section microchannel heat sink, the hydraulic diameter is kept same in both the cases and CFD simulation was conducted. With using water- Al_2O_3 nanofluid as the working fluid the rectangular cross section is showing better performance in terms of cooling as compare to the square cross section. Drop in pressure results in rectangular section calculated using water Al_2O_3 nanofluid using both CFD and Analytical approach are in good agreement with difference of 13.4%

Keywords: Computational fluid dynamics, Heat transfer, Microchannel heat sink, ICEM-Fluent CFD.

1. Introduction

In this modern era, use of smaller and compact devices has been increased tremendously. Modern computers that uses smaller electronic devices is the best example of it. Along with using this device, the problem of dissipation of heat has been increased also as if it is not removed then it might damage the component. Many researchers have presented their work regarding effective heat transfer and faster cooling of these devices so as to protect these devices using microchannels and minichannels. Microchannel and minichannel heat sink study has been carried out in various literature using different working fluids and different geometries for investigating the cooling performance and enhancing the heat transfer rate. [1] presented thermodynamic investigation results in circular tube for fully developed turbulent forced convection with water- Al_2O_3 nanofluid using entropy generation minimization method. Volume fraction of nanofluid in range of 0% to 6% was used and Reynolds number ranging from 5000 to 180000 were used. Using velocity and temperature fields obtained during CFD analysis the entropy



generation rates were numerically determined. It has been proved that at each Reynolds number there is a cross sectional area which is optimum for which there is minimum entropy generation in tube and as with increase in Reynolds number the optimal area of cross section increases. [2] investigated nanofluid application on the system of parabolic trough collector. Using Al_2O_3 /synthetic oil nanofluid and using Finite Element Method the multifield coupling simulation of PTC system was implemented for performance investigation. The Al_2O_3 particle concentration effects on PTC system were also studied. Good agreement was observed between experimental data and numerical results. Using Al_2O_3 /synthetic nanofluid there is a great reduction in absorber maximum temperature and temperature gradient. [3] explored effects of various aspects which include heat source/sink location, number of tubes, average Nusselt number, Rayleigh number, volume concentration. By employing Finite Volume based control volume technique, governing equations are numerically solved. In the studied cavity, considerable enhancement in heat transfer was observed using nanofluids. [4] presented numerical study results of parabolic trough solar collector of high concentration ratio on the thermodynamic and thermal performance. In this study, 80° rim angle and 113 concentration ratio parabolic trough system was used. The thermal physical properties temperature dependency have been considered for both copper nanoparticles and base fluid. The combination of CFD and Monte-Carlo ray tracing procedures was used in numerical analysis. [5] numerically investigated different microstructures microchannels with forced convection heat transfer. In microstructural grooves vortices will appear. Using Nusselt number the microchannel geometries influence on performance of heat transfer was evaluated. The highest heat transfer performance was possessed by microstructure with V shaped groove.

[6] investigated numerically forced convection heat transfer of laminar flow in corrugated channel of trapezoidal section using copper water nanofluid. The Reynolds number ranging between 100 to 700 and volume fraction of nanoparticles in range of 0% to 5% was considered. The geometrical parameter effects like corrugated channel wavelength and amplitude have been presented. It was observed that with increasing volume fraction of nanoparticles the average Nusselt number increases with increase in pressure drop. [7] studied microchannel and minichannel using single phase liquid flow. Microscale liquid flow fundamental issue was addressed by author and relation for single phase liquid flow pressure drop calculations were given. Researchers in [8] conducted investigation experimentally and explored conventional sized channel based classical correlation validity for predicting single phase flow thermal behaviour in rectangular microchannel. Width of microchannels considered ranged between $194\mu m$ to $534\mu m$. Deionized water was used for analysis with Reynolds number ranging from 300 to 3500. Classical and continuum approach based numerical predictions and experimental data were found to be in good agreement with showing 5% of average deviation. [9] used three nanofluid types namely carbon nanotubes-Ga, copper-Ga, diamond-Ga and carried out natural convection investigation of enhancement of heat transfer and generation of the entropy in cavity which is differentially heated. In this volume fraction of nanofluids is in between 0.01 to 0.15. Model of two-phase mixture is used for simulation of the nanofluid flow. Results showed that with Grashof number increment local entropy generation, heat transfer and convective intensity increases. [10] studied numerically heat transfer and analysis of fluid flow in channel having blocks at bottom wall. Nanofluid is used in this study. Channel inlet temperature of fluids are taken less than walls. Using control volume approach the governing equations are solved numerically. Results concluded that by using blocks on hot walls and using nanoparticles there is enhancement in channel heat transfer. By simulation, upto 60% enhancement in channel heat transfer is shown due to nanoparticles and blocks.

[11] investigated experimentally Foam/NEPCM composite heat transfer with phase change with foam porosity effect consideration. 47° Wall temperature reduction is provided which is maximum by Foam/NEPCM composite as compared to pure NEPCM. [12] employed CFD approach and studied serpentine tube heat exchanger for thermo hydraulic performance extensive exploration. The volume flow rates in the range of 1L/min to 5L/min was used. The Al_2O_3 /water based nanofluid influence was broadly studied on thermo hydraulic performance using 1%, 3% and 5% nanoparticles concentrations. Higher performance of heat transfer was provided as compared to other cases using low to high serpentine tube. At the expense of pressure drop which is negligible the higher coefficient of heat transfer

was provided using nanoparticles which are highly concentrated. [13] showed that by swirl flows, vortices and thermal boundary layer subsequent breaking the heat exchanger thermal efficiency is augmented by vortex generator. For this numerical study which is 3D validated vortex generator of triangular winglet type is selected. Working fluids which are air, water and nanofluids of two different types are analyzed with vortex generator which is non-central. [14] showed that less important role is played by O_2 and SO_2 in water and MEA losses than evaporation. For capturing CO_2 ionic liquids at room temperature are proposed potential candidates recently. IL to MEA aqueous solution addition reduced MEA and water losses. [15] stated that in many industrial applications the essential tool is surface cooling. In enhancement of heat transfer the important factor is area of the wetted surface utilization effectively. The vortex generator surface texture effects on vortex dynamics and heat transfer are studied, with pressure drop which is minimal the surface temperature found to reduce by vortex stretching. [16] have presented their work in microchannel heat sink using microchannel with rectangular and square cross section keeping the hydraulic diameter same in both of the cross sections. Liquid water was used as a cooling medium. As comparing with microchannel with square cross section, the better cooling performance was shown by rectangular cross section. In the present study, microchannel heat sink with rectangular and square cross section are considered and studied using two different types of fluid which are liquid water and water- Al_2O_3 nanofluid of 0.3% volume fraction. Using CFD approach both the cross sections are compared using both of the cooling fluids.

2. Physical Model & CFD Simulation

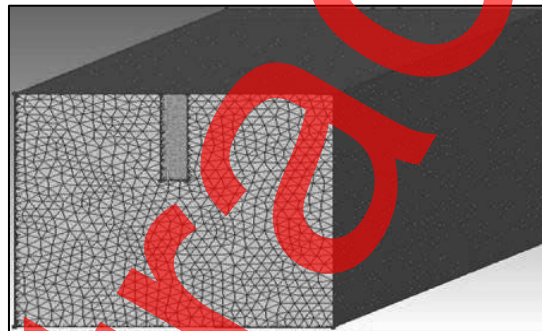


Figure 1. Rectangular microchannel heat sink model with meshing

CFD is a tool which is used to solve many engineering problems which involves fluid flow and heat transfer. CFD stands for Computational Fluid Dynamics. To get the heat sink machining was done on square block of copper with dimensions of 25.4 length, 25.4mm width and 70mm height. Now the dimension of rectangular section are considered to be 25.4mm length (L), 25.4mm width (W) and 2.384mm height (H) for CFD analysis in the present study. The rectangular section dimensions are same as that in [8]. There are N=10 straight parallel rectangular cross section microchannels in microchannel heat sink block same as that used in [8], but in the present study for CFD work, one rectangular cross section was considered and analysis was conducted as shown in Figure 1. The results obtained by CFD analysis of the rectangular and square heat sink was studied by using same hydraulic diameter in both the cases. The cooling fluids used in both the cases were liquid water and water- Al_2O_3 nanofluid of 0.3% volume fraction. The results of both the cross sections were compared using two cooling fluids mentioned. Re number was considered from 200 to 1000 for both of the cross sections.

Table 1. Dimensions of Rectangular and Square cross sections

Microchannel Dimensions	D_h	Height	Width
Rectangular	0.318 mm	$H_r=0.884$ mm	$W_r=0.194$ mm
Square	0.318 mm	$H_s=0.318$ mm	$W_s=0.318$ mm

The dimensions and notations used in table 1. Are same as those which were used in [16]. As shown in Figure 1. The fluid flows from inlet to outlet through the rectangular cross section microchannel. Constant heat flux was provided at bottom of the heat sink so that heated assembly temperature was brought down by cooling fluid by increment in temperature of cooling fluid from inlet to outlet. Using ICEM-CFD module the meshing of the assembly was done. Using GSF of 6 and tetra/mixed mesh type meshing was done. GSF stands for global scale factor. Fluent_V6 output solver and ANSYS solver was used. Keeping mesh density same the solid and fluid zones were meshed. The ICEM output was used and then using fluent software further analysis was done. It used navier stokes equation to solve the problem related to heat transfer and fluid flow. While analysis viscous laminar flow was selected and energy equation was kept on. Copper was selected as solid material.

3. Boundary conditions and assumptions:

1. Single phase laminar flow was used.
2. Working fluid and solid properties were treated as constant.
3. Three dimensional steady state fluid flow was considered.
4. Velocity values of 0.8149m/s, 1.6298m/s, 2.444m/s, 3.2596m/s, 4.0745m/s were obtained for Reynolds number of 200, 400, 600, 800, 1000 respectively using water- Al_2O_3 nanofluid of 0.3% volume fraction.
5. Outlet pressure was considered to be 0 Pa gauge with pressure outlet condition.
6. 450000 W/m^2 heat flux was provided at bottom.
7. Insulation was considered at assembly top surface.

The further analysis was done using CFD post processing section.

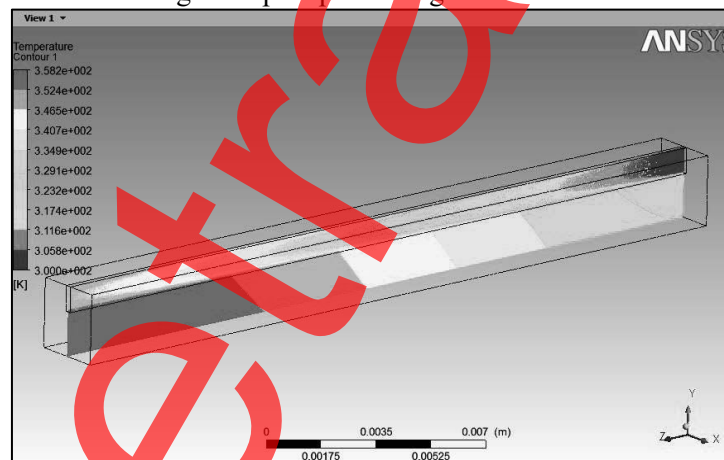


Figure 2. Temperature variation in rectangular cross section microchannel at 200 Reynolds number using water Al_2O_3 nanofluid of 0.3% volume fraction

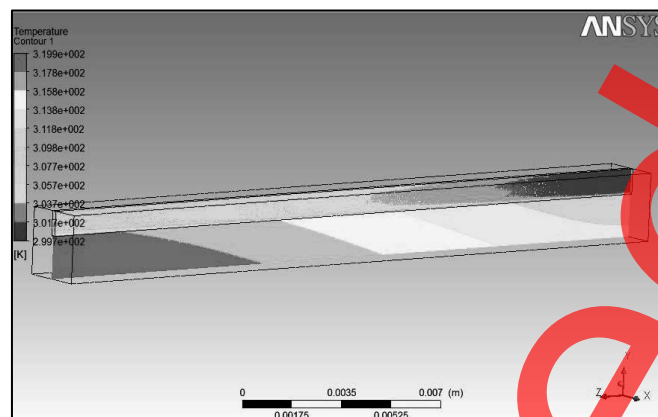


Figure 3. Temperature variation in rectangular cross section microchannel at 1000 Reynolds number using water- Al_2O_3 nanofluid of 0.3% volume fraction

Figure 2 and Figure 3. Represent temperature variation in rectangular cross section microchannel. As heat flux at constant rate was supplied at bottom of the assembly the assembly gets heated which is cooled by the working fluid flowing from inlet to outlet through the rectangular microchannel.

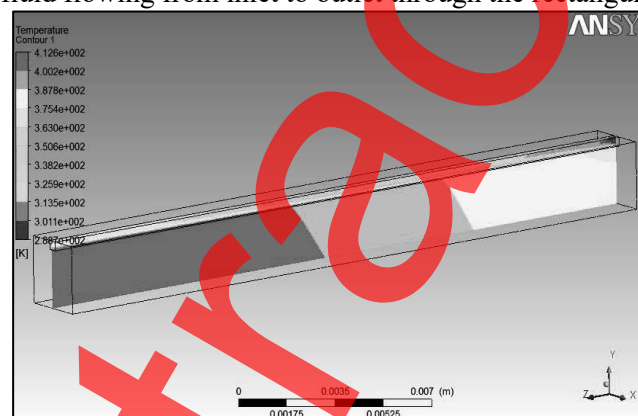


Figure 4. Temperature variation in square cross section microchannel at 200 Reynolds number using water Al_2O_3 nanofluid of 0.3% volume fraction

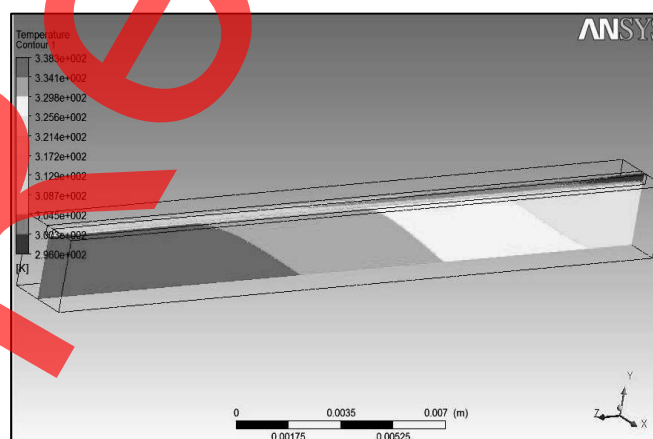


Figure 5. Temperature variation in square cross section microchannel at 200 Reynolds number using water- Al_2O_3 nanofluid of 0.3% volume fraction

Figure 4 and Figure 5. Represent the temperature variation in the square cross section microchannel. Fluid temperature increases as flows from inlet to outlet by absorbing heat from the heated assembly and it cools down the heated assembly.

4. Data Reduction from CFD Results

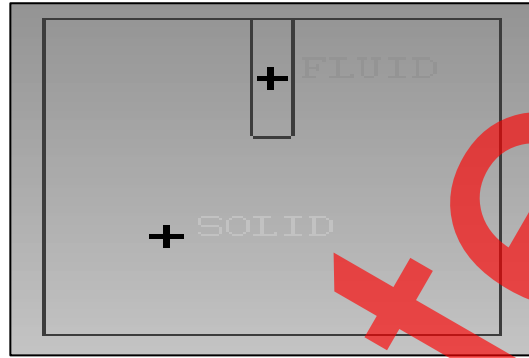


Figure 6. Rectangular microchannel heat sink front view

The Figure 6 was taken from [16]. Heat transfer takes place from the heated assembly to the cooling fluid by forced convection as fluid is flowing with certain velocity. For conduction CFD analysis, 2 zones were created namely solid and fluid zone. Lines were created in the assembly, 3 in fluid and 1 in solid part. From inlet to outlet the 3 lines were created at fluid section, one at top, one at middle and one at bottom.

Temperature difference between fluid inlet and outlet temperatures,

$$(\Delta T)_f = T_{f,o} - T_{f,i} \quad (1)$$

The average temperature of fluid was given as,

$$T_{f,avg} = (T_{f,i} + T_{f,o})/2 \quad (2)$$

Average fluid temperature and average wall temperature difference was given as,

$$(\Delta T) = T_{w,avg} - T_{f,avg} \quad (3)$$

Mass flow of the fluid passing through the microchannel was calculated as,

$$\dot{m} = \rho A_{cs} V \quad (4)$$

The hydraulic diameter is given as,

$$D_h = (4A_{cs})/P \quad (5)$$

The formula for Reynolds number is,

$$Re = (\rho V D_h) / \mu \quad (6)$$

Heat absorbed by the cooling fluid as it flows through the microchannel is given as,

$$Q = \dot{m} C_p (\Delta T)_f \quad (7)$$

And the heat transfer coefficient associated with the above forced convection heat transfer process is given as,

$$Q = h A_s (\Delta T) \quad (8)$$

All Equations from (1)-(8) used are same as those which were used in [16].

5. Results & Discussions

Microchannel with different cross sections was used and between them comparison was conducted using liquid water and water- Al_2O_3 nanofluid of 0.3% volume fraction as a cooling medium. With both of the fluids the rectangular cross section was better with respect to the heat transfer as that of square cross section.

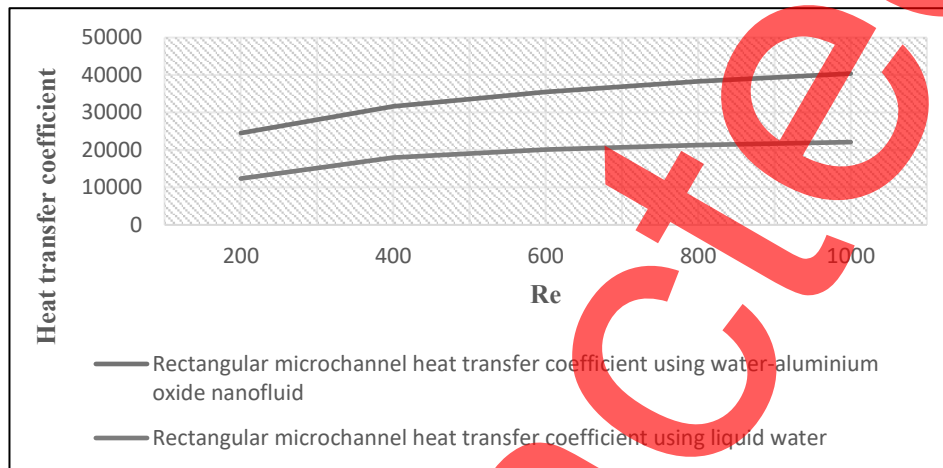


Figure 7. Comparison of heat transfer coefficient in rectangular microchannel using liquid water and water-aluminium oxide nanofluid

As shown in Figure 7. The values of heat transfer coefficient expressed in W/m^2K obtained for rectangular microchannel using nanofluid are higher compared to the values obtained with liquid water. The heat transfer coefficient values for rectangular microchannel using liquid water at Reynolds number of 600, 800 and 1000 are taken from [16]. The percentage increase in heat transfer coefficient using nanofluid in rectangular microchannel was observed to be 49.5%, 43.09%, 43.3%, 44% and 45% for Reynolds number of 200, 400, 600, 800 and 1000 respectively and average percentage increment of 45%.

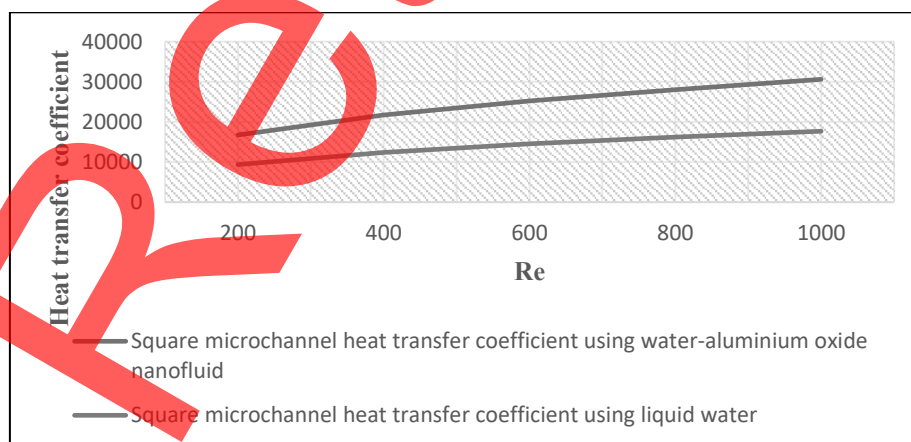


Figure 8. Comparison of heat transfer coefficient in square microchannel using liquid water and water-aluminium oxide nanofluid

As shown in Figure 8. In each case the nanofluid is giving better heat transfer coefficient values expressed in W/m^2K as compared to the liquid water in square cross section microchannel. The heat transfer coefficient values at Reynolds number of 600, 800 and 1000 for square cross section using liquid water are taken from [16]. The percentage increase in heat transfer coefficient values using nanofluids as compare to using water for Reynolds number of 200, 400, 600, 800 and 1000 in square microchannel was observed to be 44%, 42.9%, 42%, 42% and 42% respectively with average percentage increment of 42.5%.

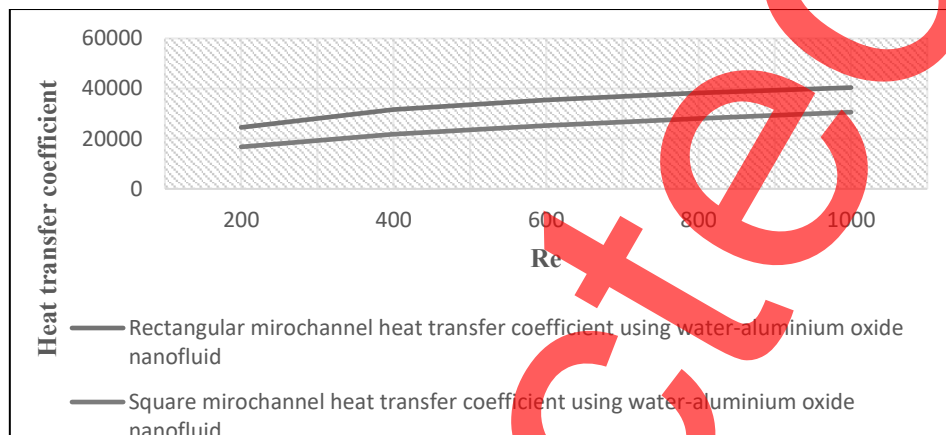


Figure 9. Comparison of heat transfer coefficient in rectangular and square microchannel using water-aluminium oxide nanofluid

From Figure 9. We can conclude that rectangular microchannel is giving better performance as that of square section while using nanofluid as cooling medium. The percentage increase in heat transfer coefficient values expressed in W/m^2K using rectangular microchannel as compared to square using nanofluid as a cooling medium was observed to be 31.6%, 31%, 29%, 26.7% and 24% for the Reynolds number of 200, 400, 600, 800 and 1000 with average percentage increment of 28.4%.

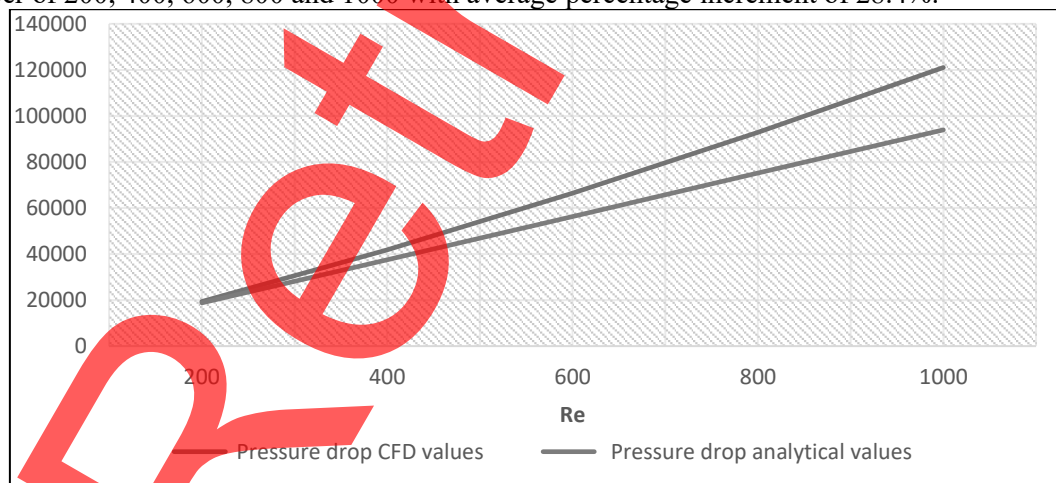


Figure 10. Pressure drop values in rectangular cross section using water-aluminium oxide nanofluid

The values of pressure drop in Pa are expressed in Figure 10. Using CFD and Analytical approach. With the flow pressure drop increases because of the frictional head loss. The analytical values of pressure drop are calculated using formula given in [7]. The percentage variation between the pressure drop values obtained using CFD Analytical approach for Reynolds number of 200, 400, 600, 800 and 1000 was observed to be 3.05%, 10%, 15.2%, 19.12% and 19.9% with average variation of 13.4%.

6. Conclusion

Present study was conducted using liquid water and water- Al_2O_3 nanofluid with 0.3% volume fraction. As compared to liquid water the nanofluid is showing better heat transfer performance. The rectangular is better to use as compared to square cross section microchannel as heat will be effectively removed by rectangular cross section because heat transfer coefficient values obtained are higher for rectangular than square cross section.

1. Average percentage increment in heat transfer coefficient values in rectangular microchannel with water- Al_2O_3 nanofluid as cooling medium as compared to the liquid water was obtained to be 45%.
2. Average percentage increment in heat transfer coefficient values in square microchannel with water- Al_2O_3 nanofluid as cooling medium as compared to the liquid water was obtained to be 42.5%.
3. Average percentage increment in heat transfer coefficient values in rectangular microchannel as compared to the square microchannel with water- Al_2O_3 nanofluid as cooling medium was obtained to be 28.4%.
4. Average pressure drop variation in rectangular microchannel with water- Al_2O_3 nanofluid as cooling medium using analytical and CFD approach was observed to be 13.4%.
So it is better to use rectangular as that of square microchannel and nanofluid as compared to liquid water.

References

- [1] Aggrey Mwesigye, Zhongjie Huan, *Thermodynamic analysis and optimization of fully developed turbulent forced convection in a circular tube with water- Al_2O_3 nanofluid*, International Journal of Heat and Mass Transfer **89** (2015), pp 694-706.
- [2] Yanjuan Wang, Jinliang Xu, Qibin Liu, Yuanyuan Chen, Huan Liu, *Performance analysis of a parabolic trough solar collector using Al_2O_3 /synthetic oil nanofluid*, Applied Thermal Engineering **107** (2016), pp 469-478.
- [3] Yulin Ma, Mojtaba Jamiatia, Alireza Aghaei, Mohammad Sepehrirad, Amin Dezfulizadeh, Masoud Afrand, *Effect of differentially heated tubes on natural convection heat transfer in a space between two adiabatic horizontal concentric cylinders using nano-fluid*, International Journal of Mechanical Sciences **163** (2019), p 105148.
- [4] Aggrey Mwesigye, Zhongjie Huan, Josua P. Meyer, *Thermal performance and entropy generation analysis of a high concentration ratio parabolic trough solar collector with Cu – Therminol® VP-1 nanofluid*, Energy Conversion and Management **120** (2016) , pp 449-465.
- [5] Yang Liu, Jing Cui, WeiZhong Li, Ning Zhang, *Effect of Surface Microstructure on Microchannel Heat Transfer Performance*, Journal of Heat Transfer, DECEMBER 2011, **133** / , pp 124501-1.
- [6] M.A. Ahmed, M.Z. Yusoff, N.H. Shuaib, *Effects of geometrical parameters on the flow and heat transfer characteristics in trapezoidal-corrugated channel using nanofluid*, International Communications in Heat and Mass Transfer **42** (2013) , pp 69-74.
- [7] Satish G. Kandlikar, *Single-Phase Liquid Flow in Minichannels and Microchannels*, Heat Transfer and Fluid Flow in Minichannels and Microchannels, 2014 Elsevier Ltd.
- [8] Poh-Seng Lee, Suresh V. Garimella, Dong Liu, *Investigation of heat transfer in rectangular microchannels*, International Journal of Heat and Mass Transfer **48** (2005) , pp 1688–1704.
- [9] Xiaoming Zhou, Yanni Jiang, Xunfeng Li, Keyong Cheng, Xiulan Huai, Xidong Zhang, Hulin Huang, *Numerical investigation of heat transfer enhancement and entropy generation of natural convection in a cavity containing nano liquid-metal fluid*, International Communications in Heat and Mass Transfer **106** (2019) , pp 46-54.

- [10] H. Heidary, M.J. Kermani, *Heat transfer enhancement in a channel with block(s) effect and utilizing Nano-fluid*, International Journal of Thermal Sciences **57** (2012) , pp 163-171.
- [11] W.Q. Li, S.J. Guo, L. Tan, L.L. Liu, W. Ao, *Heat transfer enhancement of nano-encapsulated phase change material (NEPCM) using metal foam for thermal energy storage*, International Journal of Heat and Mass Transfer **166** (2021) , p 120737.
- [12] M. Awais, M. Saad, Hamza Ayaz, M.M. Ehsan, Arafat A. Bhuiyan, *Computational assessment of Nano-particulate (Al_2O_3 /Water) utilization for enhancement of heat transfer with varying straight section lengths in a serpentine tube heat exchanger*, Thermal Science and Engineering Progress **20** (2020) , p 100521.
- [13] Man-Wen Tian, Saleh Khorasani, Hazim Moria, Samira Pourhedayat, Hamed Sadighi Dizaji, *Profit and efficiency boost of triangular vortex-generators by novel techniques*, International Journal of Heat and Mass Transfer **156** (2020) , p 119842.
- [14] H. Anandakumar and K. Umamaheswari, A bio-inspired swarm intelligence technique for social aware cognitive radio handovers, Computers & Electrical Engineering, vol. **71**, pp. 925–937, Oct. 2018. doi:10.1016/j.compeleceng.2017.09.016
- [15] R. Arulmurugan and H. Anandakumar, Early Detection of Lung Cancer Using Wavelet Feature Descriptor and Feed Forward Back Propagation Neural Networks Classifier, Lecture Notes in Computational Vision and Biomechanics, pp. 103–110, 2018. doi:10.1007/978-3-319-71767-8_9.
- [16] Saurabh Narayan Pawar, Nilesh Balkishanji Totla, *CFD Simulation and Analytical Validation of Rectangular and Square microchannel heat sink with liquid water as cooling medium*, 3rd International Congress on Advances in Mechanical Sciences, IOP Conf. Series: Materials Science and Engineering 998 (2020) 012030, IOP Publishing, doi:10.1088/1757-899X/998/1/012030.

2022 | OriginalPaper | Chapter

Reverse Supply Chain Network for Plastic Waste Management

Authors: Rakshit Shetty, Neha Sharma, Vishal A. Bhosale

Published in: Emerging Research in Computing, Information, Communication and Applications

Publisher: Springer Singapore

Login to get access

Show more

Please log in to get access to this content

Log in

Register for free

previous chapter

next chapter

Literature

Metadata





Smart Technologies for Energy, Environment and Sustainable Development, Vol 1 pp 707–723

A Study on Women Police Bullet-Proof Jacket Considering Anthropometry Data, Comfort and Safety in Pune, India

[Chinmayanand Prakash Jagtap](#), [Shilpi Bora](#), [Pranjal Arun Patil](#), [Abhijeet Malge](#) & [Mahesh Goudar](#)

Conference paper | [First Online: 25 February 2022](#)

200 Accesses

Part of the [Springer Proceedings in Energy](#) book series (SPE)

Abstract

An effective study was held with a survey carried out by interacting with a number of lady police about the current Bullet-Proof vest available, which are bullet resistant to a particular threat level. These are not manufactured according to the concern of women. This study helps in figuring out the need for a new bullet-proof vest for women. The survey gave many aspects which need to be changed. The paper flows by briefing today's availability and condition for women's working in various defence sectors. With current scenarios and the changes

2022 | OriginalPaper | Chapter

Improvement in Liquid and Plastic Limit for Black Cotton Soil by Addition of RBI Grade 81

Authors: Prashant Khedkar, Shraddha Shinde, Sakshi Wayal, Bhaskar Wabhitkar

Published in: Smart Technologies for Energy, Environment and Sustainable Development, Vol 1

Publisher: Springer Nature Singapore

Login to get access

Show more

Please log in to get access to this content

Log in

Register for free

previous chapter

next chapter

Literature

Metadata



Smart Technologies for Energy, Environment and Sustainable Development, Vol 1 pp 261–272

Shear Strength Improvement of Black Cotton Soil Reinforced with Waste Plastic Bottle Strips

[Nilesh Shirpurkar](#) , [Dhanraj Saste](#), [Vaibhav Varpe](#) & [Bhaskar Wabhitkar](#)

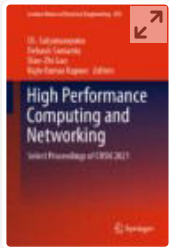
Conference paper | [First Online: 25 February 2022](#)

200 Accesses

Part of the [Springer Proceedings in Energy](#) book series (SPE)

Abstract

India generates an average of 26,000 tons of plastic a day. The plastic processing industry is producing 13.4 MT in 2015 and growing to 22 million tons (MT) a year by 2020 (TOI article 2019) [1]. Black cotton soil has a very low-bearing capacity. Due to its characteristics, it forms a very poor foundation material. Black cotton soil falls under a major constituent of soil in India. The soil undergoes volumetric changes when soil is present on the water table. Increase in water content causes the swelling of the soils and loss of strength. Decrease in moisture content resulting in soil shrinkage. BC



High Performance Computing and Networking pp 425–436

SquashCord: Video Conferencing Application Using WebRTC

[Adhiksha Thorat](#) & [Avinash Bhute](#) 

Conference paper | [First Online: 23 March 2022](#)

165 Accesses

Part of the [Lecture Notes in Electrical Engineering](#) book series (LNEE, volume 853)

Abstract

WebRTC is a framework that helps to facilitate real-time communication between browsers. It provides services through application programming interface (API) and allows web applications and sites to exchange video and audio streams in real time. It is an open-source software developed by Google. The research presented in this paper delves into the development of a multi-peer video conferencing application that is developed using technologies like WebRTC, Node.js and Socket.io. WebRTC establishes a peer-to-peer network, and Socket.io (a library in Node.js) acts as a signalling mechanism for exchanging data necessary for establishing this network. The developed application works well on

Conferences > 2021 International Conference... ?

Signature Recognition Models: Performance Comparison

Publisher: IEEE [Cite This](#) PDF

Atharva Gadre ; Pradyumna Pund ; Gouri Ajmire ; Shubhangi Kale All Authors

16
Full
Text Views



Alerts

Manage Content Alerts

Add to Citation Alerts

More Like This

A Novel Approach for Handwriting Recognition in Malayalam Manuscripts using Contour Detection and Convolutional Neural Nets
2018 International Conference on Advances in Computing, Communications and Informatics (ICACCI)
Published: 2018

Rumour Detection Based on Graph Convolutional Neural Net
IEEE Access
Published: 2021

Show More

Abstract

Document Sections

I. Introduction

II. Proposed Systems and Methodology

III. Dataset

IV. Pre-Processing

V. Result (Performance Analysis)

Show Full Outline ▾

Authors

Figures

References

Keywords

Metrics

Download PDF


Abstract:In recent times Signature Verification has become an act of absolute necessity in the area of biometric verification. Unlike other verification problems, every small deta... [View more](#)

► Metadata
Abstract:
In recent times Signature Verification has become an act of absolute necessity in the area of biometric verification. Unlike other verification problems, every small detail between genuine and forged signatures needs to be observed because a skilled forgery can only differ by only some specific kind of features of the real signature. The task of verifying signatures has become even harder in writing independent scenarios. In this paper, with the help of Siamese Network, VGG16 model and DEEP CNN models we have modeled a system that will verify signatures offline. Siamese networks use two images as input with shared weights, which can be trained to learn the features of both the images to find out the similarity between them. This is done by passing sets of similar and dissimilar images to the network so that it can learn to reduce the loss and Euclidean distance between similar images and increase it in dissimilar images. As for VGG 16, it is a pre-trained 16-layer model that is based on CNN, these 16 layers consist of max layer, pooling layers, and many more. CNN is simply a convolutional neural network on which both Siamese and VGG models are based. The performance analysis shows the VGG16 to have best accuracy about 85-90%, Siamese shows 65-70% and CNN shows 65-70% and the Siamese network to have the highest speed in identification.



Techno-Societal 2020 pp 477–487

IoT Enabled Secured Card Less Ration Distribution System

[Shilpa K. Rudrawar](#) , [Kuldeepak Phad](#) & [Prajwal Durugkar](#)

Conference paper | [First Online: 20 May 2021](#)

260 Accesses

Abstract

Proposed paper put light on the automation in distribution of goods by using IOT based ration distribution system which uses the biometric verification and the cloud storage technology. Proposed system looks like an Automated Teller machine (ATM). We can simplify the process by using an interactive approach. Aadhar cards contain details like contact number, residential details, details of bank account and available scheme. Details of customers are stored and maintained as the database in the cloud storage by the government. Here we are storing the customer's data in the cloud using storage technology such as Google Firebase. This database contains the necessary information such as Aadhar details,



Techno-Societal 2020 pp 241–247

Detection of Brain Tumor Using Image Processing and Neural Networks

[Vanshika Dhillon](#) , [Dipti Sakhare](#) & [Shilpa Rudrawar](#)

Conference paper | [First Online: 20 May 2021](#)

260 Accesses

Abstract

Artificial Intelligence (AI) is an umbrella consisting of many small blocks like machine learning, evolution computation, robotics, vision, natural language process and planning, speech processing etc. In the past years AI has developed a lot and given its share to make human life better, easy and compact. The word "technology" is a term which can be defined in many ways. The definition of the word keeps evolving with the continuous development in various fields. Decades ago, it used to take an entire room to accommodate a single computer but now we use the same computer at the ease of our fingertips. With the rapid development in technology mankind's expectations and needs have also increased. Human race demands accurate results in less time with easier



Recent Advances in Manufacturing Modelling and Optimization pp 231–240

Selection of Passenger Car Using TOPSIS Method

[S. Y. Borole](#) , [P. U. Malu](#) & [A. G. Kamble](#)

Conference paper | [First Online: 22 April 2022](#)

152 Accesses

Part of the [Lecture Notes in Mechanical Engineering](#) book series (LNME)

Abstract

The car is one of the basic needs in today's world for transportation of the passengers, and selection of car is a very crucial task for the customer. The quality of the car varies with respect to the attributes. The customers are in search of a car which is best in attributes. The present work gives the selection procedure for selection of best car using multi-attribute decision-making method viz: technique for order of preference by similarity to ideal solution method based upon different attribute. There are five alternatives and five attributes considered like cost, mileage, safety rating, transmission and brake horsepower for the selection of car and the ranks are obtained. The



Recent Advances in Manufacturing Modelling and Optimization pp 829–842

Project Scheduling Using Linear Programming, CPM and Crashing Time Technique

[Takshay V. Sayre](#), [Keshav Kumar](#), [Divyansh A. Waghmare](#),
[Yash S. Deshpande](#) & [Vishal A. Bhosale](#)

Conference paper | [First Online: 22 April 2022](#)

152 Accesses

Part of the [Lecture Notes in Mechanical Engineering](#) book series (LNME)

Abstract

Project scheduling is a method by which we can shorten the duration of the project or crash the duration of a project at the expense of certain added cost to meet the specified project deadline. The project might lag behind the given schedule for many numbers of reasons, and this situation may call for measures like crashing some activities by appointing extra resources. This crashing of activities is generally done by trial-and-error method which is not very productive and incurs extra costs. The crashing of activity is to be done in such a way that the project should be completed



Recent Advances in Manufacturing Modelling and Optimization pp 739–749

Application of Polymer Composite for Weight Reduction in the Automobile Sector Toward a Sustainable Development

[Anand S. Baldota](#), [Vishal J. Dulange](#), [Shahrukh S. Patel](#) & [Manoj W. Bhalwankar](#) 

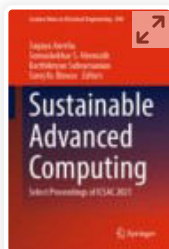
Conference paper | [First Online: 22 April 2022](#)

157 Accesses

Part of the [Lecture Notes in Mechanical Engineering](#) book series (LNME)

Abstract

In recent years, co-relation of sustainable development with the the growth of the industries, these questions have been a hot topic for research. The increasing awareness, greater restrictions on emission control, and its long-term environmental impact have led to an urgent need to develop lightweight and fuel-efficient vehicles in the global automobile industry. Polymer composites due to their lightweight and recyclability have been largely used in the automotive sector. This has led to a constant need to research and develop high-



Sustainable Advanced Computing pp 381–394

Region-Based Stabilized Video Magnification Approach

[Sanket Yadav](#) , [Prajakta Bhalkare](#) & [Usha Verma](#)

Conference paper | [First Online: 31 March 2022](#)

96 Accesses

Part of the [Lecture Notes in Electrical Engineering](#) book series (LNEE, volume 840)

Abstract

Eulerian video magnification (EVM) is used to magnify the imperceptible signals inside the video in the form of color. For this, it requires the jitter-free stable video of the target occupying the major part of the frame. And most of the time, the real-world/real-time videos cannot satisfy the above requirements completely. This is where EVM lacks optimal results. And this thought motivated authors to develop a new region-based stabilized video magnification (RSVM) approach. This preprocesses the input by stabilization of video, then detection–tracking–cropping of ROI, to get the motion-free-modulated input which satisfies requirements of EVM. Further, performance of both methods is

analyzed for different inputs and amplification factor with performance metrics as PSNR, elapsed time, extents of color, and motion magnification. Results reveal that the RSVM approach performs better than EVM to handle motions and also fasten the process.

Keywords

Video stabilization Region of interest

Eulerian video magnification

This is a preview of subscription content, [access via your institution.](#)

▼ Chapter

EUR 24.95

Price excludes VAT (India)

- DOI: 10.1007/978-981-16-9012-9_31
- Chapter length: 14 pages
- Instant PDF download
- Readable on all devices
- Own it forever
- Exclusive offer for individuals only
- Tax calculation will be finalised during checkout

Buy Chapter

> eBook

EUR 128.39

> Hardcover Book

EUR 159.99

[Learn about institutional subscriptions](#)

References

1. Wu H-Y, Rubinstein M, Shih E, Guttag J, Durand F, Freeman W (2012) Eulerian video

magnification for revealing subtle changes in the world. *ACM Trans Graph* 31(4):1–8

2. Liu L, Lu L, Luo J, Zhang J, Chen X (2014) Enhanced Eulerian video magnification. In: 2014 7th international congress on image and signal processing. Dalian, pp 50–54, <https://doi.org/10.1109/CISP.2014.7003748>
-

3. Alzahrani A, Whitehead A (2015) Preprocessing realistic video for contactless heart rate monitoring using video magnification. In: 2015 12th conference on computer and robot vision. Halifax, NS, pp 261–268. <https://doi.org/10.1109/CRV.2015.41>
-

4. Zhang K, Jin X, Wu A (2017) Accelerating Eulerian video magnification using FPGA. In: 2017 19th international conference on advanced communication technology (ICACT). Bongpyeong, pp 554–559, <https://doi.org/10.23919/ICACT.2017.7890151>
-

5. Yu H, Lin H, Zhang E, Li J, Chen G (2017) Region-based euler video amplification algorithm. In: 2017 10th international congress on image and signal processing, BioMedical Engineering and Informatics (CISP-BMEI). Shanghai, pp 1–5, <https://doi.org/10.1109/CISP-BMEI.2017.8302082>
-

6. Wu X, Yang X, Jin J et al (2018) PCA-based magnification method for revealing small signals in video. *SIViP* 12:1293–1299.
<https://doi.org/10.1007/s11760-018-1282-0>
-

7. Al-allaq ZJ, Shahadi HI, Albattat HJ (2019) Powerful and low time phase-based video magnification enhancing technique. In: 2019 4th scientific international conference Najaf (SICN). Al-Najef, Iraq, pp 133–138,
<https://doi.org/10.1109/SICN47020.2019.9019338>
-

8. Moya-Albor E, Brieva J, Ponce H, Martínez-Villaseñor L (2020) A non-contact heart rate estimation method using video magnification and neural networks. *IEEE Instrum Meas Mag* 23(4):56–62.
<https://doi.org/10.1109/MIM.2020.9126072>
-

9. Zhang J, Zhang K, Yang X, Wen C (2020) Heart rate measurement based on video acceleration magnification. In: 2020 Chinese control and decision conference (CCDC). Hefei, China, pp 1179–1182,
<https://doi.org/10.1109/CCDC49329.2020.9164451>
-

10. Zhang Y, Pintea SL, Van Gemert JC (2017) Video acceleration magnification. In: 2017 IEEE conference on computer vision and pattern

recognition (CVPR). Honolulu, HI, pp 502–510,
<https://doi.org/10.1109/CVPR.2017.61>

11. Yadav S, Bhalkare P, Shingde S, Verma U (2020) Performance analysis of video magnification methods. In: 2020 third international conference on smart systems and inventive technology (ICSSIT). Tirunelveli, India, pp 1293–1301,
<https://doi.org/10.1109/ICSSIT48917.2020.9214167>
-

12. Li B, Chen Y, Ren J, Cheng L (2017) A fast video stabilization method based on feature matching and histogram clustering. In: Balas V, Jain L, Zhao X (eds) Information technology and intelligent transportation systems. Advances in intelligent systems and computing, vol 455. Springer, Cham.
https://doi.org/10.1007/978-3-319-38771-0_31
-

13. Viola P, Jones M (2001) Rapid object detection using a boosted cascade of simple features. In: Proceedings of the 2001 IEEE computer society conference on computer vision and pattern recognition. CVPR 2001, Kauai, HI, USA, pp I–I,
<https://doi.org/10.1109/CVPR.2001.990517>
-

14. Tomasi C, Kanade T (1991) Shape and motion from image streams: a factorization method-2. point features in 3D motion. Technical Report

CMU-CS-91–105, Carnegie Mellon University,
Pittsburgh, PA

15. Senigagliesi L, Ricciuti M, Ciattaglia G, Santis AD, Gambi E (2021) Comparison of video and radar contactless heart rate measurements. In: Communications in computer and information science information and communication technologies for ageing well and e-health, pp 96–113. https://doi.org/10.1007/978-3-030-70807-8_6

16. Kassab LY, Law A, Wallace B, Larivière-Chartier J, Goubran R, Knoefel F (2021) Effects of region of interest size on heart rate assessment through video magnification. IEEE Int Symp Med Meas Appl (MeMeA) 2021:1–6. <https://doi.org/10.1109/MeMeA52024.2021.9478596>

17. Sharma P, Kokare PM, Kolekar MH (2019) Performance comparison of KLT and CAMSHIFT algorithms for video object tracking. In: Khare A, Tiwary U, Sethi I, Singh N (eds) Recent trends in communication, computing, and electronics. Lecture notes in electrical engineering, vol 524. Springer, Singapore. https://doi.org/10.1007/978-981-13-2685-1_31

18. Lucas BD, Kanade T (1981) An iterative image

registration technique with an application to stereo vision. In: Proceedings of the 7th international joint conference on artificial intelligence – vol 2 (IJCAI'81). Morgan Kaufmann Publishers Inc., San Francisco, CA, USA, pp 674–679

19. Zhao J, Zhang W, Chai R, Wu H, Chen W (2021) Non-contact physiological parameters detection based on MTCNN and EVM. In: Communications in computer and information science cognitive systems and signal processing, pp 507–516.
https://doi.org/10.1007/978-981-16-2336-3_48
-

20. Coachkriengsak “Steve jobs passion in work,” YouTube, 2 Aug 2011 [Video file]. Available: <https://www.youtube.com/watch?v=PznJqxon4zE>. [Accessed: 15 Jan 2020]
-

Author information

Authors and Affiliations

School of Electrical Engineering, MIT Academy of Engineering, Pune, India

Sanket Yadav, Prajakta Bhalkare & Usha Verma

Corresponding author

Correspondence to [Sanket Yadav](#).

Editor information

Editors and Affiliations

**Department of Computer Science, CHRIST
(Deemed to be University), Bengaluru,
Karnataka, India**

Dr. Sagaya Aurelia

**Department of Mechanical Engineering, Indian
Institute of Technology Madras, Chennai, Tamil
Nadu, India**

Dr. Somashekhar S. Hiremath

**Department of Information Technology,
University of Technology and Applied Science,
Sultanate of Oman, Oman**

Dr. Karthikeyan Subramanian

**Department of Computer Science Engineering,
National Institute of Technology Silchar, Silchar,
Assam, India**

Dr. Saroj Kr. Biswas

Rights and permissions

[Reprints and Permissions](#)

Copyright information

© 2022 The Author(s), under exclusive license to
Springer Nature Singapore Pte Ltd.

About this paper

Cite this paper

Yadav, S., Bhalkare, P., Verma, U. (2022). Region-Based
Stabilized Video Magnification Approach. In: Aurelia, S.,
Hiremath, S.S., Subramanian, K., Biswas, S.K. (eds)

Sustainable Advanced Computing. Lecture Notes in
Electrical Engineering, vol 840. Springer, Singapore.

https://doi.org/10.1007/978-981-16-9012-9_31

[.RIS](#)  [.ENW](#)  [.BIB](#) 

DOI

https://doi.org/10.1007/978-981-16-9012-9_31

Published	Publisher Name	Print ISBN
31 March 2022	Springer, Singapore	978-981-16- 9011-2

Online ISBN	eBook Packages
978-981-16- 9012-9	Intelligent Technologies and Robotics Intelligent Technologies and Robotics (R0)

Not logged in - 43.227.20.34

Not affiliated

SPRINGER NATURE

© 2022 Springer Nature Switzerland AG. Part of [Springer Nature](#).

Conferences > 2022 12th International Confe... ?

Enhancing the Security of Medical Images in Telemedicine Using Region-based Crypto-Watermarking Approach

Publisher: IEEE Cite This PDF

Usha Verma ; Neelam Sharma All Authors

1 Paper Citation

40 Full Text Views

Alerts

View References

Manage Content Alerts

Add to Citation Alerts

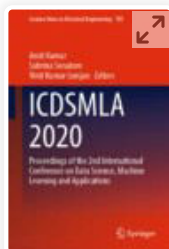
Abstract	<p>Download PDF</p>
Document Sections	
I. Introduction	Abstract: Along with maintaining the confidentiality and privacy of patient information, the preservation and authentication of internal physiological features of tissues and organ... View more
II. Related Work In Literature	
III. Methodology	► Metadata
IV. Implementation and Results	Abstract: Along with maintaining the confidentiality and privacy of patient information, the preservation and authentication of internal physiological features of tissues and organs present in any type of medical images is equally important while transmitting medical images in Telemedicine. To achieve it, this paper presents a region-based approach for Medical Image by integrating cryptography in the digital watermarking. To preserve the internal physiological features, medical image is separated into two regions – Region of Interest (ROI) and Not-a-Region of Interest (NROI). ROI contains the important internal physiological features of human body. Therefore, no information is embedded in ROI to preserve it. Cryptography is integrated only for generation and exchange of the secret key of ROI using Elliptic curve cryptography. Patient information and secret key is embedded into NROI using wavelet-based hybrid watermarking technique. The proposed work is tested on varieties of medical image dataset of MRI, CT scan and X-ray against various intentional and unintentional attacks and evaluated with performance metrics PSNR (Peak signal to Noise Ratio), SSIM (Structural Similarity Index), NC (Normalized Correlation) and BER (Bit Error Ratio). Secret key is matched at receiving end to authenticate the
V. Conclusion	
Authors	
Figures	
References	
Citations	
Keywords	
Metrics	

More Like This

An Image Watermarking Algorithm for Medical Computerized Tomography Images
2019 5th Iranian Conference on Signal Processing and Intelligent Systems (ICSPIS)
Published: 2019

X-ray medical image processing using directional wavelet transform
1996 IEEE International Conference on Acoustics, Speech, and Signal Processing Conference Proceedings
Published: 1996

Show More



ICDSMLA 2020 pp 717–726

Design of Secure Biometric System Using Cancelable Techniques

[Aarti Laxman Gilbile](#)  & [Pramod D. Ganjewar](#)

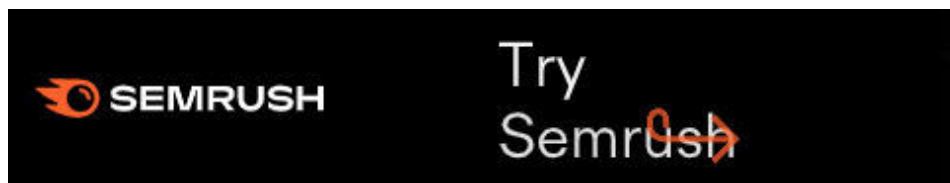
Conference paper | [First Online: 09 November 2021](#)

591 Accesses

Part of the [Lecture Notes in Electrical Engineering](#) book series (LNEE, volume 783)

Abstract

Individual identification can be accurately done by measuring biological parameters termed as biometrics. These have been proved as an unusual tool for identity verification. Recognition of biometrics and applications based on it is increased tremendously, so the privacy protection monitors are raising the privacy concerns. For reducing the privacy threats, the research work has increased to find methods to protect the biometric data. Security of biometric template is that the most challenging aspect of biometric identification system. The biometric data are stored as it is within the database which increases the rate of compromising it. This can also cause serious threat or misuse of



AIP

Conference Proceedings

HOME

BROWSE

MORE ▼

[Home](#) > [AIP Conference Proceedings](#) > [Volume 2417, Issue 1](#) > [10.1063/5.0072779](#)

< PREV

NEXT >



No Access

Published Online: 19 October 2021

CFD analysis of exhaust pipe of a diesel engine

AIP Conference Proceedings **2417**, 060002 (2021); <https://doi.org/10.1063/5.0072779>Pawankumar Yadav^{a)} and Pramod Kothmire^{b)}[View Affiliations](#)[View Contributors](#)

Topics ▼

ABSTRACT



PDF



E-READER

Conferences > 2021 2nd Global Conference fo... ?

Design & Development of Insurance Money Predictor to Claim with Insurance Company

Publisher: IEEE Cite This PDF

Ankita Jadhav ; Mayuri Kulkarni ; Pranav Abute ; Prachi Rajarapolu All Authors

1
Paper
Citation

34
Full
Text Views

Alerts

Manage Content Alerts

Add to Citation Alerts

Abstract

Document Sections

I. Introduction

II. Literature Review

III. Methodology Implemented

IV. System Development

V. Results

Show Full Outline

Authors

Figures

References

Citations

Keywords

Metrics

Download PDF

Abstract:In this pandemic situation of Covid-19, the whole world had suffered a lot. Whatever issues occurred is very uncertain and unexpected. In the life cycle of a human being,... **View more**

► Metadata
Abstract:
In this pandemic situation of Covid-19, the whole world had suffered a lot. Whatever issues occurred is very uncertain and unexpected. In the life cycle of a human being, it is always desirable to be safe and have a secure lifestyle in every aspect. To face sudden, unexpected situation insurance is one of the solutions. Nowadays due to increasing awareness among the society people are more inclined towards taking medical insurance from various companies. As we know there are several companies in ensuring the various diseases, climatic hazards, man-made and natural emergencies. Insurance money is going to support the human in morally and financially. The insurance companies are having their own rules and regulations for giving money/claims to a client. Some hidden calculations are always out of reach to the common man. Day by day accurate insurance calculation and claim for money become a challenging task for society. In this paper, a system has been developed using a machine learning algorithm for accurate claim calculation. Implemented system will help the client to claim monthly or quarterly premiums based on various parameters like the number of family members you want to insure, the total income of the family, the expected amount of insurance, age group of family members, etc. To make the process more user-friendly and fast, we have developed a website.

More Like This

News-EDS: News based Epidemic Disease Surveillance using Machine Learning
2020 14th International Conference on Open Source Systems and Technologies (ICOSST)
Published: 2020

Analysis and design of epidemic disease monitoring cloud platform
2022 IEEE 6th Information Technology and Mechatronics Engineering Conference (ITOEC)
Published: 2022

Show More

Conferences > 2021 2nd Global Conference fo... ?

Crack Detection on Metal Surfaces Using Image Processing Techniques

Publisher: IEEE

Cite This

PDF

Megharaj Sonawane ; Aditya Borse ; Hrishikesh Sonawane ; Aashish Mali ; Prachi Raj...

All Authors

School of Electrical Engineering MIT Academy of Engineering, Pune, India

64 Full Text Views

Alerts

Manage Content Alerts

Add to Citation Alerts

Abstract

Document Sections

I. Introduction

II. Literature Review

III. Methodology Implemented

IV. Algorithm Implemented

V. Result

Show Full Outline

Authors

Figures

References

Keywords

Metrics

More Like This

Download PDF

Abstract:It is impossible to imagine an industry without a machine. Huge number of machines are working together in industry. Many times if the failure occurs in machine it become... [View more](#)

► Metadata

Abstract:

It is impossible to imagine an industry without a machine. Huge number of machines are working together in industry. Many times if the failure occurs in machine it becomes a challenging task to identify it. Fault may occur due to various reasons. Here the main focus is on identifying the fault occurred due to the fine crack on metal body. Faulty spare parts can be easily identified and can be replaced. But finding a fault due to the crack on metal body is becomes difficult to work out. To find out such type of faults machine disassembling is the only option. Disassembling any machine is not that much easy task and hence a system is developed here which will help in identifying the crack on metal body without disassembling any machine. It is possible to detect the exact size, location of the crack. Digital image processing concepts are used to identify the crack on a metal body. Scanning of metal body will be done to identify the crack on metal body, with the help of scanning mechanism (using ultrasonic, xray, gamma rays Radiography). The image of metal body will get captured which will get inputted to the systems for the processing purpose and by using the different algorithms of image processing, image will get processed. Firstly image will get converted into black and white form and then the digitization of image will be done. Based on the digitized data, using the segmentation

More Like This

A Hybrid Fault Diagnosis Approach for Blade Crack Detection using Blade Tip Timing

2020 IEEE International Instrumentation and Measurement Technology Conference (I2MTC)

Published: 2020

An automated thermographic image segmentation method for induction motor fault diagnosis

IECON 2014 - 40th Annual Conference of the IEEE Industrial Electronics Society

Published: 2014

Show More

https://ieeexplore.ieee.org/document/9587516

1/3

Conferences > 2021 International Conference... ?

Lecture Summarization using Video Processing and Automatic Text Summarization

Publisher: IEEE

Cite This

PDF

Janhavi Chadawar ; Vivek Deshmukh ; Sahil Kharade ; Tushar Shelar ; Nilesh Bhandare All Authors

75 Full Text Views

Alerts

Manage Content Alerts

Add to Citation Alerts

Abstract

Document Sections

I. Introduction

II. Literature Survey

III. Methodology

IV. Work/Module Description

V. Proposed Project Design

Show Full Outline

Authors

Figures

References

Keywords

Metrics

More Like This

Download PDF

Abstract:Nowadays machine learning has achieved a lot of success in technical fields. One of these is video processing but text is recognized which is in a computer readable forma... **View more**

► Metadata
Abstract:
Nowadays machine learning has achieved a lot of success in technical fields. One of these is video processing but text is recognized which is in a computer readable format, our paper is focusing on detection of handwritten text and summarizing the document for which we found a better result with some methods which are clearly explained in this paper. This paper is following three modules to achieve the better result as from video selecting keyframes without losing whiteboard data, after selecting keyframes to identify the text which is a difficult task can be achieved. Preparing short notes with more accuracy is required for that this paper shows some ML libraries.These paper will give us a brief idea about which methods are used for modules to achieve a good accuracy.

Published in: 2021 International Conference on Intelligent Technologies (CONIT)

Date of Conference: 25-27 June 2021 **INSPEC Accession Number:** 21467270

More Like This

A BiCMOS continuous-time filter for video signal processing applications
IEEE Journal of Solid-State Circuits
Published: 1998

A single chip video signal processing architecture for image processing, coding, and computer vision
IEEE Transactions on Circuits and Systems for Video Technology
Published: 1995

Show More

Conferences > 2021 International Conference... ?

Surveillance Through Semi-Autonomous Bot

Publisher: IEEE

Cite This

PDF

<< Results

Rohit Kadhane ; Akshit Kumar ; Kushal Bhattad ; Ashish Srivastava

All Authors

22 Full Text Views

Alerts

Manage Content Alerts

Add to Citation Alerts

Abstract

Document Sections

I. Introduction

II. System Design and Implementation

III. Result

IV. Conclusion

Authors

Figures

References

Keywords

Metrics

More Like This

Download PDF

Abstract:This paper consists of the design and implementation of the semi-autonomous surveillance bot. The idea presented in the paper is to monitor a surrounding or unknown area.... **View more**

Metadata

Abstract:
This paper consists of the design and implementation of the semi-autonomous surveillance bot. The idea presented in the paper is to monitor a surrounding or unknown area. This paper carries the different phases of realization such as the motion of the robot, obstacle avoidance, and video capturing and streaming. After the video has been captured the recorded clip is streamed to a remote server which assesses the surrounding. For the implementation of the idea, different tools were required for the execution of the precursor. For building the model, the hardware required was Raspberry Pi, infrared sensors, L293D motor driver. Raspberry Pi consisting of a Raspbian operating system running on python language for video capturing and obstacle sensing was used.

Published in: 2021 International Conference on Design Innovations for 3Cs Compute Communicate Control (ICDI3C)

Date of Conference: 10-11 June 2021 **INSPEC Accession Number:** 21142299

Date Added to IEEE Xplore: 27 September 2021

More Like This

A design of mobile robot based on Network Camera and sound source localization for intelligent surveillance system
2008 International Conference on Control, Automation and Systems
Published: 2008

ERS-210 Mobile Video Surveillance System
2005 portuguese conference on artificial intelligence
Published: 2005

Show More

Conferences > 2021 Innovations in Power and...

?

Comparative Analysis of Nine level T-Type MLI

Publisher: IEEE

Cite This

PDF

<< Results

Vijay Pise ; Gajanan Dhakne ; Vishal Waghmare ; Akash Waghmare ; Mandar Bhalekar

All Authors

11 Full Text Views

Alerts

Manage Content Alerts

Add to Citation Alerts

Abstract

Document Sections

I. Introduction

II. Multilevel Inverter Topology

III. Simulation Result

IV. Comparative Table

V. Conclusion

Authors

Figures

References

Keywords

Metrics

More Like This

Download PDF

Abstract:This paper is a comparison between Traditional Cascaded H-Bridge Multilevel Inverter (MLI) and Modern T-Type MLI. The most suitable topology to be used in Electrical/E-ve... [View more](#)

► Metadata

Abstract:

This paper is a comparison between Traditional Cascaded H-Bridge Multilevel Inverter (MLI) and Modern T-Type MLI. The most suitable topology to be used in Electrical/E-vehicle to get smooth AC for increasing the performance is found based on comparison of the use of the number of power devices, THD values, and FFT analysis. The MATLAB simulation results of both topologies for Nine level AC output are compared and presented systematically.

Published in: 2021 Innovations in Power and Advanced Computing Technologies (i-PACT)

Date of Conference: 27-29 November 2021

INSPEC Accession Number: 21705344

Date Added to IEEE Xplore: 08 February 2022

DOI: 10.1109/i-PACT52855.2021.9696693

► ISBN Information:

Publisher: IEEE

More Like This

Classification Based Method Using Fast Fourier Transform (FFT) and Total Harmonic Distortion (THD) Dedicated to Proton Exchange Membrane Fuel Cell (PEMFC) Diagnosis

2017 IEEE Vehicle Power and Propulsion Conference (VPPC)

Published: 2017

Identification of harmonic loads using fast fourier transform and radial basis Function Neural Network

2017 International Electronics Symposium on Engineering Technology and Applications (IES-ETA)

Published: 2017

Show More

Conferences > 2021 Innovations in Power and... ?

Smart Metering of Electricity

Publisher: IEEE

Cite This

PDF

<< Results

Khushal Babu ; Sainath Meharkar ; Chaitanya Pujari ; Shwetambari Thakare ; Mandar ... All Authors

Back to Results

35 Full Text Views

Alerts

Manage Content Alerts

Add to Citation Alerts

Abstract

Document Sections

I. Introduction

II. System Configuration

III. Block Diagram

IV. Hardware Implementation

V. Methodology

Show Full Outline

Authors

Figures

References

Keywords

Metrics

More Like This

Download PDF

Abstract:As population rises the demand of electricity also increases and energy theft becomes a major issue in countries like India. A large loss is faced by the utility of elect... **View more**

► Metadata
Abstract:
As population rises the demand of electricity also increases and energy theft becomes a major issue in countries like India. A large loss is faced by the utility of electricity every year due to power theft. The automatic meter reading (AMR) system already exists but with potentially reduced reliability and risk of loss of privacy. To collect consumption, diagnostic and status data by visiting consumers' places every time is tedious work. In this paper, an attempt is made based on a microcontroller ESP32 for monitoring, detecting and controlling energy theft remotely. The Internet is used for communication to the central utility system. The consumer will be motivated to use electrical appliances effectively by sharing the real time usage with it.

Published in: 2021 Innovations in Power and Advanced Computing Technologies (i-PACT)

Date of Conference: 27-29 November 2021 **INSPEC Accession Number:** 21562942

More Like This

Hardware Design of Automatic Meter Reading System Based on Internet

2008 IEEE International Symposium on Knowledge Acquisition and Modeling Workshop

Published: 2008

Internet of Things Enabled Power Theft Detection and Smart Meter Monitoring System

2020 International Conference on Communication and Signal Processing (ICCSP)

Published: 2020

Show More

https://ieeexplore.ieee.org/document/9696870

1/2

Conferences > 2021 International Conference... ?

Personalization of Information using Graph Convolutional Network

Publisher: IEEE Cite This PDF

<< Results

Aditi Pandey ; Kaustubh Patil ; Sanskar Sharma ; Mayura Kulkarni All Authors

11 Full Text Views

Alerts

Manage Content Alerts

Add to Citation Alerts

More Like This

Application of an Improved Nearest Neighbor Method

2021 International Applied Computational Electromagnetics Society (ACES-China) Symposium

Published: 2021

Rumour Detection Based on Graph Convolutional Neural Net

IEEE Access

Published: 2021

Show More

Abstract

Document Sections

I. Introduction

II. Related Work

III. Proposed Approach

IV. Implementation

V. Performance Evaluation

Show Full Outline

Authors

Figures

References

Keywords

Metrics

Abstract: There exists several researches that have been done on link-based search engines for instance, Clever and Google. They involve the use of link structure to get precise results. View more

Metadata

Abstract: There exists several researches that have been done on link-based search engines for instance, Clever and Google. They involve the use of link structure to get precise results. Generally, search engines based on link structure give users high-quality results than search engines which are text based. However, those search engines encounter difficulty producing the result fitting to a specific user's profile. Personalization means knowing the user intimately enough to not only meet their needs but also predict them. This paper presents an analogy to a personalized search engine using an already existing GCN (Graph Convolutional Network) architecture on (Cora) the paper citation dataset (similar to web pages) and additionally followed by KNN algorithm to rank the personalized citations in best consonance with a user's profile.

Published in: 2021 International Conference on Advancements in Electrical, Electronics, Communication, Computing and Automation (ICAECA)

Date of Conference: 08-09 October INSPEC Accession Number:

Conferences > 2021 9th International Confer...

Design and Development of Gamification Tool for Teenagers for Selection of Higher Education Path Based on Personality Traits

Publisher: IEEE

Cite This

PDF

<< Results

Deepali Bhalerao ; Dhiraj Bagul ; Nikhil Kesapure ; Deven Bharati ; Rupa Hiremath ; N... All Authors

Back to Results

60 Full Text Views

Alerts

Manage Content Alerts

Add to Citation Alerts

Abstract

Document Sections

I. Introduction

II. Methodology

III. Story Development

IV. System Analysis

V. System Architecture

Show Full Outline

Authors

Figures

References

Keywords

Download PDF

Abstract:Gamification is used as a powerful way to connect and engage player in an effective and enjoyable funny mood. The current research work demonstrates how gamification is d... [View more](#)

Metadata
Abstract: Gamification is used as a powerful way to connect and engage player in an effective and enjoyable funny mood. The current research work demonstrates how gamification is designed and developed in an innovative way to find out different personality traits of the teenagers and recommends the possible career choices available for them based on their personality traits connecting it to the requirements of different professional careers. OCEAN model is used to find out different personalities and gamification concepts like design, elements and storytelling are used to develop gamified system.

Published in: 2021 9th International Conference on Reliability, Infocom Technologies and Optimization (Trends and Future Directions) (ICRITO)

Date of Conference: 03-04 September **INSPEC Accession Number:** 2021 21437139

More Like This

Intelligent Computer-Aided Instruction Modeling and a Method to Optimize Study Strategies for Parallel Robot Instruction
IEEE Transactions on Education
Published: 2013

How to Improve the Quality and Effect of Computer Aided Instruction's Application in Classroom Teaching in Institutes of Higher Learning
2010 Second International Workshop on Education Technology and Computer Science
Published: 2010

Show More



ICCCE 2021 pp 675–680

Efficient Use of Convolutional Neural Networks for Classification of Sugarcane Leaf Diseases

[Swapnil Dadabhau Daphal](#)  & [S. M. Koli](#)

Conference paper | [First Online: 16 May 2022](#)

133 Accesses

Part of the [Lecture Notes in Electrical Engineering](#) book series (LNEE, volume 828)

Abstract

Early identification and diagnosis of plant diseases are more crucial for holistic development of the agriculture sector in India. Farmer's general estimates and observations are time costly, sometimes vague and misjudged. For this purpose, a appropriate deep neural network is proposed for the automatic identification of sugarcane disease. The classification involves 5 types of diseases and 1 healthy class. Experimentation is performed over the manually collected dataset of size 1470 images. Performance estimation of the network is dependent on the choice of optimization. In this paper comparative analysis for different optimizers



ICCCE 2021 pp 859–869

Recent Trends and Techniques of CBIR to Enhance Retrieval Performance

[Prajakta Ugale](#)  & [Suresh Mali](#)

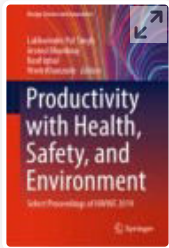
Conference paper | [First Online: 16 May 2022](#)

130 Accesses

Part of the [Lecture Notes in Electrical Engineering](#) book series (LNEE, volume 828)

Abstract

The vast growth in social media platforms such as Twitter, Instagram, Whatsapp, Facebook, etc. leads to the uploading of billions of images on the web. Content-Based Image Retrieval (CBIR) is essential to improve the performance of the data search. Computer vision research community facing research challenges related to the retrieval of relevant images from large databases. Most of the current search engines use text-based search whose performance highly depends on text Annotation and metadata of the images. In this paper, we aim to present an extensive survey of recent work carried out on CBIR based on various

**Productivity with Health, Safety, and Environment** pp 47–54

To Study the Stress Management of Women Police in Pune Urban Area

[Nandini Patole](#), [Shilpi Bora](#), [Mahesh D. Goudar](#) & [Abhijit Malge](#)

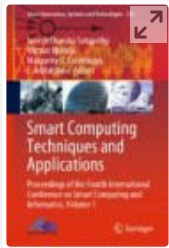
Conference paper | [First Online: 14 May 2022](#)

28 Accesses

Part of the [Design Science and Innovation](#) book series (DSI)

Abstract

Work-related stress and allied physical and psychological well-being issues are not addressed for women police personnel in Indian context with sufficient importance. In this study, the specialist has embraced distinct research structure to explore and examine the given issue. Depictions being made on the bases of logical perceptions are disclosed to be more exact by applying different techniques. The universe of this study is constrained to Pune District. 50 women police were selected randomly. A suitability sampling method (percentage) is used for selecting sample in the study. Majority part of the respondents faces issues



Smart Computing Techniques and Applications pp 525–536

Yield Estimation and Drought Monitoring Through Image Processing Using MATLAB

[Shaikh Akbar Shaikh Rasul](#) , [Jadhav Swamini Narendra](#) & [Dipti Y. Sakhare](#)

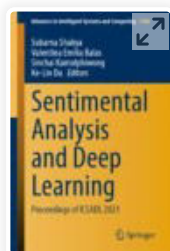
Conference paper | [First Online: 08 July 2021](#)

279 Accesses

Part of the [Smart Innovation, Systems and Technologies](#) book series (SIST, volume 225)


Abstract

This paper elucidates the pre-harvest yield estimation method and technique for cotton crop by image processing. This pixel-based image analysis of image processing is done using the image processing toolbox of the MATLAB 2019b. The images for abovementioned purpose are taken through camera armed drone (quadrotor). Further, there is a need for a better and transparent surveying method to assess the eligibility of a particular farm, for claiming the agricultural insurance. From the findings of proposed research, a suggestion for Agriculture Insurance Companies



Sentimental Analysis and Deep Learning, pp 451–464

Covid-19 Data Analysis to Predict the Level of Hospitalization

[Advet Jadhav](#) , [Maheshwari Satpute](#), [Utkarsh Rai](#),
[Apeksha Wadibhasme](#) & [Usha Verma](#)

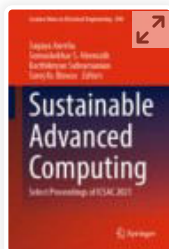
Conference paper | [First Online: 26 October 2021](#)

510 Accesses

Part of the [Advances in Intelligent Systems and Computing](#) book series (AISC, volume 1408)

Abstract

The spread of Coronavirus has resulted in a global pandemic. It has caused a heavy burden on medical facilities world over. The analysis of Covid-19 data presented in the paper may help the medical experts to categorize the patient into four levels of hospitalization based on their age, symptoms, and any previous medical history. Different prediction analysis algorithms are implemented, and results are presented to verify the accuracy of the implemented methods. Naive Bayes algorithm is found useful to categorize the patients with highest accuracy and R square score. Its results are compared with some of the traditional machine



Sustainable Advanced Computing pp 381–394

Region-Based Stabilized Video Magnification Approach

[Sanket Yadav](#) , [Prajakta Bhalkare](#) & [Usha Verma](#)

Conference paper | [First Online: 31 March 2022](#)

96 Accesses

Part of the [Lecture Notes in Electrical Engineering](#) book series (LNEE, volume 840)

Abstract

Eulerian video magnification (EVM) is used to magnify the imperceptible signals inside the video in the form of color. For this, it requires the jitter-free stable video of the target occupying the major part of the frame. And most of the time, the real-world/real-time videos cannot satisfy the above requirements completely. This is where EVM lacks optimal results. And this thought motivated authors to develop a new region-based stabilized video magnification (RSVM) approach. This preprocesses the input by stabilization of video, then detection–tracking–cropping of ROI, to get the motion-free-modulated input which satisfies requirements of EVM. Further, performance of both methods is